Vol. 86, No. 3, June 2013

MAA

MATHEMATICS MAGAZINE

Coffee and Milk (p. 204)

- Two-sided Eulerian numbers via balls in boxes
- Let π be a function
- Feedback, control, and the distribution of Primes

An Official Publication of the **Mathematical Association of America**

EDITORIAL POLICY

Mathematics Magazine aims to provide lively and appealing mathematical exposition. The *Magazine* is not a research journal, so the terse style appropriate for such a journal (lemma-theorem-proof-corollary) is not appropriate for the *Magazine*. Articles should include examples, applications, historical background, and illustrations, where appropriate. They should be attractive and accessible to undergraduates and would, ideally, be helpful in supplementing undergraduate courses or in stimulating student investigations. Manuscripts on history are especially welcome, as are those showing relationships among various branches of mathematics and between mathematics and other disciplines.

A more detailed statement of author guidelines appears in this *Magazine*, Vol. 83, at pages 73–74, and is available at the *Magazine*'s website www.maa.org/pubs/mathmag.html. Manuscripts to be submitted should not be concurrently submitted to, accepted for publication by, or published by another journal or publisher.

Please submit new manuscripts by email directly to the editor at mathmag@maa.org. A brief message containing contact information and with an attached PDF file is preferred. Word-processor and DVI files can also be considered. Alternatively, manuscripts may be mailed to Mathematics Magazine, 132 Bodine Rd., Berwyn, PA 19312-1027. If possible, please include an email address for further correspondence.

Cover image by Annie Stromquist

MATHEMATICS MAGAZINE (ISSN 0025-570X) is published by the Mathematical Association of America at 1529 Eighteenth Street, N.W., Washington, D.C. 20036 and Lancaster, PA, bimonthly except July/August.
The annual subscription price for *MATHEMATICS MAGAZINE* to an individual member of the Association is $131. Student and unemployed members receive a 66% dues discount; emeritus members receive a 50% discount; and new members receive a 20% dues discount for the first two years of membership.)

Subscription correspondence and notice of change of address should be sent to the Membership/Subscriptions Department, Mathematical Association of America, 1529 Eighteenth Street, N.W., Washington, D.C. 20036. Microfilmed issues may be obtained from University Microfilms International, Serials Bid Coordinator, 300 North Zeeb Road, Ann Arbor, MI 48106.

Advertising correspondence should be addressed to

MAA Advertising
1529 Eighteenth St. NW
Washington DC 20036

Phone: (877) 622-2373
E-mail: tmarmor@maa.org

Further advertising information can be found online at www.maa.org

Change of address, missing issue inquiries, and other subscription correspondence:

MAA Service Center, *maahq@maa.org*

All at the address:

The Mathematical Association of America
1529 Eighteenth Street, N.W.
Washington, DC 20036

Periodicals postage paid at Washington, D.C. and additional mailing offices.

Postmaster: Send address changes to Membership/Subscriptions Department, Mathematical Association of America, 1529 Eighteenth Street, N.W., Washington, D.C. 20036-1385.

Printed in the United States of America

Vol. 86, No. 3, June 2013

MAA

MATHEMATICS MAGAZINE

LETTER FROM THE EDITOR

A sequence of n distinct terms—like $1, 2, \ldots, n$—can be rearranged in $n!$ ways. In how many of them does the sequence decrease at exactly k places?

We are asking how many permutations $\pi \in S_n$ have exactly k *descents.* This is a question about *permutation statistics,* and the answer is given by the *Eulerian number* $A_{n,k+1}$. Eulerian numbers are important because they are also the answers to many other questions, in permutation statistics as well as other areas of mathematics. Kyle Peterson's article takes us from the basics of Eulerian numbers to the edge of research. He uses generating functions and elegant counting methods, and finds some appealing identities along the way.

Draw a circle on the ground. What is the ratio of its circumference to its diameter? If you measure distances along the ground, then it matters whether your circle is in Kansas or around the base of Pike's Peak. It is a question of the geometry of surfaces. Justin Schultz and Catherine Stenson use surfaces of revolution to introduce the principles involved, and to display the range of possibilities.

Prime numbers, in isolation, are notoriously hard to predict. But on a larger scale, we know that their density curve is smooth and predictable—like the path of a cool, calm, and collected driver. Susan Marshall and Donald R. Smith infer the presence of a feedback and control mechanism, and they model it with a delay-differential equation. This technique doesn't compete with the most advanced methods of the number theorists. But if you have ever wondered why the prime number theorem is true, this model might provide just the intuition you need, and it also suggests an explanation for Littlewood's remarkable discoveries about the relationship between $\pi(x)$ and $\mathrm{Li}(x)$.

After explaining prime numbers, the "cool, calm, and collected driver" might want to visit the driving school of Antonín Slavík. In his note, Slavík provides the car with a starting point, a constant speed, and a function describing curvature as a function of time, and sets it on its way. The images on page 215 are not much like the ideal paths that Marshall and Smith describe, but they definitely have their own points of interest.

The cover shows a cool, calm, and collected cup of coffee. How cool is it? As you can see on page 204, that depends on how it was collected.

Have you found an integrating factor for your differential equation? That's great! But what if you don't like it? Is it essentially unique, or can you hope to find a better one? That is one of the issues addressed in this issue by Mowaffaq Hajja. His note starts with the peculiar problem of finding integrating factors for an exact differential equation.

I don't often mention the Reviews Column or the Problems Section in this space, because most of our readers know what valuable resources these are. If you are new to the MAGAZINE, take a look! Then you can choose whether to read each issue forwards or backwards.

Walter Stromquist, Editor

ARTICLES

Two-Sided Eulerian Numbers via Balls in Boxes

T. KYLE PETERSEN
DePaul University
Chicago, IL 60614
tpeter21@depaul.edu

> I will shamelessly tell you what my bottom line is. It is placing balls into boxes . . .
>
> —Gian-Carlo Rota, *Indiscrete Thoughts*

Gian-Carlo Rota was a professor at MIT from 1959 until his death in 1999. He is arguably the father of the field known today as algebraic combinatorics. Rota had 50 students (notably Richard Stanley) and, as of this writing, he has 329 mathematical descendants, including many of the top names in the field today. (And me.) If putting balls in boxes was good enough for him, well, it should be good enough for any of us.

In this article we will first give a gentle introduction to permutation statistics and Eulerian numbers, followed by an explanation of how to use the idea of balls in boxes in this setting. Then we will take those ideas and study a perfectly natural (though less well-known) refinement: the "two-sided" Eulerian numbers. We will finish with a discussion of symmetries of the Eulerian numbers and a conjecture of Ira Gessel.

Permutation statistics

The symmetric group S_n is the set of all permutations of length n, i.e., all bijections $w : \{1, 2, \ldots, n\} \to \{1, 2, \ldots, n\}$. We generally write a permutation in one-line notation: $w = w(1)w(2)\cdots w(n)$, so a typical element of S_7 is $w = 5624713$.

For any permutation $w \in S_n$, we define a *descent* to be a position r such that $w(r) > w(r+1)$, and we denote by $\mathbf{des}(w)$ the number of descents of w. For example, if $w = 5624713$, then there are descents in position 2 (since $6 > 2$) and in position 5 (since $7 > 1$). Hence, $\mathbf{des}(w) = 2$. The permutation $12\cdots n$ is the only permutation with no descents, while its reversal, $n\cdots 21$, has the maximal number of descents, with $n-1$.

The function

$$\mathbf{des} : \bigcup_{n\geq 1} S_n \to \{0, 1, 2, 3, \ldots\}$$

is an example of a *permutation statistic*. Any function from the set of permutations to a subset of the integers can fairly be called a permutation statistic. The reader is referred to [**1**] or [**13**] for more about permutation statistics generally.

Math. Mag. **86** (2013) 159–176. doi:10.4169/math.mag.86.3.159.

Another common permutation statistic is the *inversion number*, $\mathbf{inv}(w)$, which is the number of pairs $r < s$ such that $w(r) > w(s)$. Notice the useful fact that w and its inverse permutation must have the same number of inversions: If $r < s$ and $w(r) > w(s)$, then $w(s) < w(r)$ and $w^{-1}(w(s)) = s > r = w^{-1}(w(r))$. For example, with $w = 5624713$, we get $w^{-1} = 6374125$ and we have $\mathbf{inv}(w) = \mathbf{inv}(w^{-1}) = 13$. (Notice that $\mathbf{des}(w) = 2$ while $\mathbf{des}(w^{-1}) = 3$, so descent numbers do not enjoy this property.) Again, the permutation $12\cdots n$ has no inversions, while $n\cdots 21$ has the most, with $\binom{n}{2}$ of them. Here, every pair of indices is an inversion.

We mention **inv** because we can use it to give an alternate definition of **des** as follows. First, recall that the *rth simple transposition*, denoted σ_r, is the permutation that swaps r and $r+1$ for some r and fixes all other elements of $\{1, 2, \ldots, n\}$. There are $n-1$ such elements in S_n, one for each $r = 1, 2, \ldots, n-1$. The simple transpositions are very special because they form a *minimal generating set* for S_n, i.e., every permutation w in S_n can be obtained by applying a sequence of simple transpositions, and no proper subset of them will do the same.

Now consider the permutation obtained by composing a simple transposition with a permutation w:

$$w \circ \sigma_r = w(1)\cdots w(r-1)w(r+1)w(r)w(r+2)\cdots w(n).$$

We see that this action swaps the numbers in positions r and $r+1$ of w. Thus r is a descent position of w if and only if r is *not* a descent position of $w \circ \sigma_r$. Moreover, r is a descent of w if and only if $\mathbf{inv}(w) > \mathbf{inv}(w \circ \sigma_r)$, i.e.,

$$\mathbf{des}(w) = |\{r : \mathbf{inv}(w \circ \sigma_r) < \mathbf{inv}(w)\}|.$$

This identity is certainly not the most useful way to compute the descent number of a permutation, but it suggests that maybe we should consider the action of composition of w with σ_r on the left side as well. Here, we find $\sigma_r \circ w = (w^{-1} \circ \sigma_r)^{-1}$ since $\sigma_r^{-1} = \sigma_r$, and so (remembering that inverses have the same inversion number) we have:

$$\begin{aligned}\mathbf{des}(w^{-1}) &= |\{r : \mathbf{inv}(w^{-1} \circ \sigma_r) < \mathbf{inv}(w^{-1})\}| \\ &= |\{r : \mathbf{inv}(\sigma_r \circ w) < \mathbf{inv}(w)\}|.\end{aligned}$$

Thus we may fairly call $\mathbf{des}(w)$ the number of *right descents* of w, while $\mathbf{des}(w^{-1})$ is the number of *left descents* of w. The left descents are also called *inverse descents* in the literature, and this number is also denoted by $\mathbf{ides}(w)$. See, for example, [**9**, Section 13]. It is not too difficult to compute $\mathbf{ides}(w)$ from one-line notation: It is the number of instances in which r appears to the right of $r+1$. For example, $\mathbf{ides}(5624713) = 3$ since the 1 appears to the right of the 2, the 3 appears to the right of the 4, and the 4 appears to the right of the 5.

In this article we will study both the right descent number on its own, and how left and right descents are related. This leads, respectively, to the Eulerian numbers, and to the "two-sided" Eulerian numbers of the title.

The Eulerian numbers

With a little patience, or a bit of computer programming, we can compute $\mathbf{des}(w)$ for each w in S_n and count how many permutations have no descents, one descent, two descents, and so on. We call this the *distribution* of **des** over S_n. (The term comes from the fact that if we divide our counts by $n!$ we get a probability distribution.) The reader may like to check by hand that in S_3 there is one permutation with no descents,

there are four permutations with one descent, and there is one permutation with two descents. With a little more effort, you can find the distribution for S_4 as well. As this task requires $n!$ things to check for a given n, you may not want to try anything bigger than $n = 4$ by hand.

We write $A_{n,i}$ for the number of permutations w in S_n for which $\mathbf{des}(w) = i - 1$. (This shift in indices is done for historical reasons; primarily, it makes certain formulas come out nicer.) The numbers $A_{n,i}$ are called the *Eulerian numbers*, after Leonhard Euler. In TABLE 1, we see the values of $A_{n,i}$ for $n \leq 8$.

TABLE 1: The Eulerian numbers $A_{n,i}$

$n\backslash i$	1	2	3	4	5	6	7	8
1	1							
2	1	1						
3	1	4	1					
4	1	11	11	1				
5	1	26	66	26	1			
6	1	57	302	302	57	1		
7	1	120	1191	2416	1191	120	1	
8	1	247	4293	15619	15619	4293	247	1

A great deal of mathematical literature is devoted to the distribution of **des**, and we remark that this distribution manifests itself in many other ways. For instance, let $\mathbf{runs}(w)$ denote the number of *increasing runs* of w (maximal increasing subwords), let $\mathbf{asc}(w)$ denote the number of *ascents* of w (positions r with $w(r) < w(r+1)$), and let $\mathbf{exc}(w)$ denote the number of *excedances* of w (positions r with $w(r) > r$). Then, remarkably, we have:

$$\begin{aligned} A_{n,i} &= |\{w \in S_n : \mathbf{des}(w) = i - 1\}|, \\ &= |\{w \in S_n : \mathbf{runs}(w) = i\}|, \\ &= |\{w \in S_n : \mathbf{asc}(w) = i - 1\}|, \\ &= |\{w \in S_n : \mathbf{exc}(w) = i - 1\}|. \end{aligned}$$

The second and third equalities are perhaps straightforward (there is necessarily one descent between each increasing run, and swapping each $w(r)$ for $n + 1 - w(r)$ trades descents for ascents), but that **exc** has the same distribution as **des** is not so obvious.

Euler himself was not interested in permutation statistics, but was rather investigating solutions of certain functional equations in which the numbers $A_{n,i}$ emerged. See the original [**8**, Caput VII, pp. 389–390] (available digitally online) or Leonard Carlitz's survey article [**4**]. Carlitz points to several interesting occurrences of the Eulerian numbers in analysis and number theory in the first half of the 20th century, while in the early 1980s, Anders Björner described the Eulerian numbers in a topological setting; see [**2**]. Suffice it to say, there are a variety of good reasons to study the Eulerian numbers, but for this article we will stick to the combinatorial point of view.

We will now discuss one of the standard tools of enumerative combinatorics, with which we will encode the Eulerian numbers. Given a sequence of numbers $a_0, a_1, a_2, \ldots$, we define the *generating function* for the sequence to be the power series (a polynomial, if the sequence is finite) in which the coefficient of t^i is a_i:

$$\sum_{i \geq 0} a_i t^i = a_0 + a_1 t + a_2 t^2 + \cdots .$$

So, for example, the geometric series

$$\frac{1}{1-t} = 1 + t + t^2 + \cdots$$

is the generating function for the sequence 1, 1, 1, ... Another example that might be familiar comes from the binomial theorem:

$$(1+t)^n = \binom{n}{0} + \binom{n}{1}t + \binom{n}{2}t^2 + \cdots + \binom{n}{n}t^n,$$

so that for fixed n, $(1+t)^n$ is the generating function for the binomial coefficients $\binom{n}{i}$. Whether a generating function has finitely many terms or not, the reader should try not to worry about problems of convergence of the series. (For those who want to worry about it, rest assured that all series mentioned in this paper converge for $|t| < 1$.) The reader should think of a generating function as a "clothesline" on which the sequence hangs.

The generating function for Eulerian numbers, with n fixed, will be denoted

$$A_n(t) = \sum_{i=1}^{n} A_{n,i}t^i = A_{n,1}t + A_{n,2}t^2 + \cdots + A_{n,n}t^n.$$

We call this the *nth Eulerian polynomial*. For example, the fourth Eulerian polynomial is

$$A_4(t) = t + 11t^2 + 11t^3 + t^4.$$

Since $A_{n,i}$ is the number of permutations with $i-1$ descents, we can get the same generating function by summing not on i, but on the set of all permutations in S_n. That is, we give each permutation w a *weight* of $t^{\mathbf{des}(w)+1}$ and compute the weighted sum

$$A_n(t) = \sum_{w \in S_n} t^{\mathbf{des}(w)+1}.$$

Since the number of summands contributing t^i to the sum is precisely the number of permutations with $i-1$ descents, we see the coefficients are indeed the Eulerian numbers.

We will now discuss the "balls in boxes" approach to the Eulerian numbers.

Balls in boxes

We begin with the generating function for the sequence $b_0, b_1, b_2, \ldots$, where b_k is the number of ways of putting n labeled balls into k distinct boxes.

Fix the number of balls, n. We claim that the generating function for all the ways of putting n distinct balls into boxes is

$$b_0 + b_1 t + b_2 t^2 + \cdots = \sum_{k \geq 0} k^n t^k.$$

Indeed, if there are k different boxes, there are a total k^n ways to put n labeled balls into the boxes; we have k choices for each ball. A typical choice with $k = 9$, $n = 6$ might look like this:

We will use a shorthand notation for pictures like the one above, e.g.,

$$||56|2||14|||3$$

Here we draw a vertical bar for the divisions between the boxes, so that the number of boxes is one more than the number of bars. By way of standardization, we list the balls in each box in increasing order. So balls 5 and 6 were placed in the third box, ball 2 in the fourth box, and so on. We call such a diagram for balls in boxes a *barred permutation*.

With this notation, we could say that the generating function for balls in boxes is really the generating function for barred permutations, where we count each barred permutation u with weight $t^{\#\text{of bars in } u+1}$ $(= t^{\#\text{of boxes}})$, i.e.,

$$\sum_{\text{barred perm. } u} t^{\#\text{ of bars in } u+1} = \sum_{k\geq 0} k^n t^k.$$

We get this expression by thinking of fixing the number of bars and inserting the numbers $1, 2, \ldots, n$ between the bars, just like we put distinct balls in boxes.

To make the connection with Eulerian polynomials, we will now compute this generating function in a different way: by first putting down the numbers $\{1, 2, \ldots, n\}$ to form a permutation and then inserting bars to form all barred permutations.

To consider how this must be done, imagine that we have formed a permutation and we'd now like to insert bars to form a valid barred permutation. Since we require numbers to increase within a box, we know that there *must* be a bar in each descent position of a barred permutation (i.e., at the end of every maximal increasing run), but otherwise, we can insert bars into the gaps between the numbers at will. So, for example, the barred permutations corresponding to $w = 562143$ are obtained from the barred permutation

$$56|2|14|3$$

by adding bars arbitrarily in the gaps between the numbers, i.e., there can be any number of bars to the left of 5, any number of bars between the 5 and the 6, at least one bar between the 6 and the 2, at least one bar between the 2 and the 1, and so on.

Given a permutation w in S_n, what is the generating function for the barred permutations corresponding to w? To approach this question, let's consider a special case first.

With the identity permutation, $w = 12\cdots n$, there are $\binom{n+k}{n}$ ways to insert k bars: Have $n + k$ symbols (n numbers and k bars) and we need only decide where to place the n numbers. So on one hand, the generating for barred permutations produced from $12\cdots n$ is

$$\sum_{\substack{\text{barred perm. } u \\ \text{from } 12\cdots n}} t^{\#\text{ of bars in } u+1} = \sum_{k\geq 0} \binom{n+k-1}{n} t^k.$$

On the other hand, forget about fixing k and observe we are free to add any number of bars in each of the gaps between the numbers. The possible weights of the bars in

any one gap are encoded by $1 + t + t^2 + \cdots = 1/(1-t)$, and because there are $n+1$ gaps to be independently filled, we can also express this generating function as:

$$\begin{aligned}\sum_{\substack{\text{barred perm. } u \\ \text{from } 12\cdots n}} t^{\#\text{ of bars in } u+1} &= t \cdot \underbrace{(1 + t + t^2 + \cdots)}_{\text{bars in first gap}} \underbrace{(1 + t + t^2 + \cdots)}_{\text{bars in second gap}} \cdots \\ &= t \cdot \underbrace{(1 + t + t^2 + \cdots)^{n+1}}_{n+1 \text{ gaps}} \\ &= \frac{t}{(1-t)^{n+1}}.\end{aligned}$$

For permutations with descents, we need only multiply this generating function by a power of t to reflect the number of bars required by descent positions:

$$\begin{aligned}\sum_{\substack{\text{barred perm. } u \\ \text{from } w}} t^{\#\text{ of bars in } u+1} &= \frac{t^{\mathbf{des}(w)+1}}{(1-t)^{n+1}} \\ &= t^{\mathbf{des}(w)} \cdot \sum_{k \geq 0} \binom{k+n-1}{n} t^k \\ &= \sum_{k \geq 0} \binom{k+n-1}{n} t^{\mathbf{des}(w)+k} \\ &= \sum_{l \geq 0} \binom{l+n-1-\mathbf{des}(w)}{n} t^l. \qquad (1)\end{aligned}$$

So, returning to the example of $w = 562143$, we get that the generating function for the sequence counting its corresponding barred permutations according to the number of bars is:

$$\frac{t^4}{(1-t)^7} = t^3 \cdot \sum_{k \geq 0} \binom{k+5}{6} t^k = \sum_{l \geq 0} \binom{l+2}{6} t^l.$$

Summing (1) over all permutations w in S_n gives us, on the one hand,

$$\frac{A_n(t)}{(1-t)^{n+1}}.$$

On the other hand, the sum gives the generating function for all barred permutations, which we know to be $\sum_{k \geq 0} k^n t^k$.

In other words, we have the following.

THEOREM 1. (THE GENERATING FUNCTION) *For any $n \geq 1$, we have*

$$\frac{A_n(t)}{(1-t)^{n+1}} = \sum_{k \geq 0} k^n t^k.$$

This theorem is a classic result in enumerative combinatorics, going back at least to the work of MacMahon [**14**, Chapter IV, § 462]. See [**16**, Section 4.5] for a modern treatment and generalizations.

So, for example, the reader can check that the $n = 3$ case gives the generating function for the sequence $1, 8, 27, \ldots$, of cubes:

$$\frac{t + 4t^2 + t^3}{(1-t)^4} = t + 8t^2 + 27t^3 + 64t^4 + 125t^5 + \cdots,$$

and if $n = 4$ we get fourth powers:

$$\frac{t + 11t^2 + 11t^3 + t^4}{(1-t)^5} = t + 16 + 81t^3 + 256t^4 + 625t^5 + \cdots.$$

Worpitzky's identity

Another consequence of the balls in boxes approach is *Worpitzky's identity*, which is explained in Knuth's book [**13**, Section 5.1.3]:

$$k^n = \sum_{1 \le i \le n} A_{n,i} \binom{k+n-i}{n}. \tag{2}$$

This equation shows that Eulerian numbers describe a kind of "change-of-basis" between binomial coefficients and nth powers.

For example, when $n = 4$, $k = 3$,

$$A_{4,1}\binom{6}{4} + A_{4,2}\binom{5}{4} + A_{4,3}\binom{4}{4} + A_{4,4}\binom{3}{4} = 1 \cdot 15 + 11 \cdot 5 + 11 \cdot 1 + 1 \cdot 0 = 81.$$

To obtain Worpitzky's identity, we first recall from Equation (1) that

$$\frac{t^i}{(1-t)^{n+1}} = \sum_{k \ge 0} \binom{k+n-i}{n} t^k.$$

Then, from the left-hand side of Theorem 1, we get:

$$\begin{aligned}
\frac{A_n(t)}{(1-t)^{n+1}} &= \sum_{i=0}^{n} A_{n,i} \left(\frac{t^i}{(1-t)^{n+1}} \right) \\
&= \sum_{i=0}^{n} A_{n,i} \cdot \sum_{k \ge 0} \binom{k+n-i}{n} t^k \\
&= \sum_{k \ge 0} \left(\sum_{i=0}^{n} A_{n,i} \binom{k+n-i}{n} \right) t^k.
\end{aligned}$$

But according to the right-hand side of Theorem 1, the coefficient of t^k for this series is k^n. Hence, (2) follows.

Recurrence relation

Next, we can derive a recurrence for Eulerian polynomials with Theorem 1 and some calculus. Let $F_n(t) = \sum k^n t^k = A_n(t)/(1-t)^{n+1}$, and observe that

$$\begin{aligned} F_n(t) &= \sum_{k\geq 0} k^n t^k \\ &= t \cdot \sum_{k\geq 0} k^{n-1} \cdot k t^{k-1} \\ &= t \cdot F'_{n-1}(t) \\ &= t\left(\frac{n A_{n-1}(t)}{(1-t)^{n+1}} + \frac{A'_{n-1}(t)}{(1-t)^n}\right) \\ &= \frac{nt A_{n-1}(t) + t(1-t)A'_{n-1}(t)}{(1-t)^{n+1}}. \end{aligned}$$

Comparing numerators yields the following well-known identity for Eulerian polynomials:

$$A_n(t) = nt A_{n-1}(t) + t(1-t)A'_{n-1}(t). \tag{3}$$

From this equation, it is possible to deduce that the Eulerian polynomials factor into linear factors over the reals, and moreover, that the roots of $A_n(t)$ are all distinct, non-positive numbers. According to Carlitz [**4**], this fact was first observed by Ferdinand Frobenius.

By comparing the coefficient of t^i on the left and on the right of (3), we also get a handy recurrence for Eulerian numbers:

$$A_{n,i} = i A_{n-1,i} + (n+1-i)A_{n-1,i-1}, \tag{4}$$

which resembles a weighted version of Pascal's recurrence for binomial coefficients.

The reader should check this numeric recurrence against TABLE 1 to see how nicely it works. When drawing the numbers in a triangular array, we don't simply add the two numbers above to get the next entry; we add the appropriately weighted linear combination of the two. For example, the first few rows of such a triangle can be generated by hand as shown in FIGURE 1 (so no need to write out all 120 permutations in S_5 to get the numbers $A_{5,i}$).

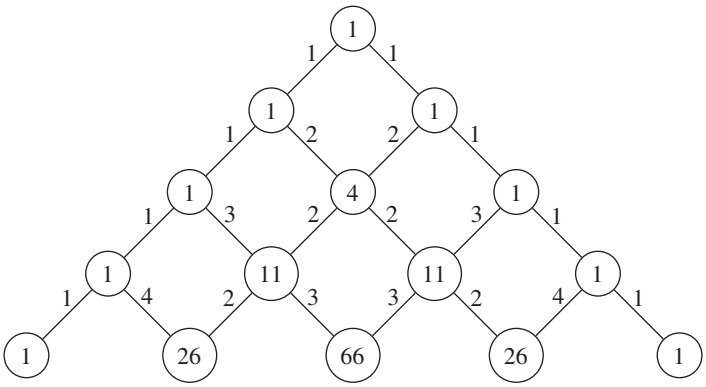

Figure 1 Generating Eulerian numbers via the recurrence relation

There is also a direct combinatorial proof of this recurrence. Imagine inserting the number n into a permutation of S_{n-1}. What happens if you insert it in a descent position? What happens if you insert it in an ascent position? See, for example, [**13**, Section 5.1.3].

There are many, many, more things that could be said at this point about Eulerian numbers. Some of these, including the row symmetry an astute reader may have noticed in TABLE 1, will be discussed at the end of the paper.

Two-sided Eulerian numbers

We are now going to extend the method of balls in boxes to study the "two-sided" Eulerian numbers. Let $A_{n,i,j}$ denote the number of permutations w with $i-1$ left descents and $j-1$ right descents, i.e.,

$$A_{n,i,j} = |\{w \in S_n : \mathbf{des}(w^{-1}) = i-1 \text{ and } \mathbf{des}(w) = j-1\}|.$$

We also define a generating function, the two-sided Eulerian polynomial:

$$A_n(s,t) = \sum_{w \in S_n} s^{\mathbf{des}(w^{-1})+1} t^{\mathbf{des}(w)+1} = \sum_{i,j=1}^{n} A_{n,i,j} s^i t^j.$$

We think of $A_n(s,t)$ as the generating function for the joint distribution of left and right descents. In TABLE 2 we see the two-sided Eulerian numbers for $n \leq 8$.

The two-sided Eulerian numbers were first studied by Carlitz, Roselle, and Scoville in 1966 [**5**], though rather than descents and inverse descents, they looked at the equivalent notion of "jumps" (ascents) and "readings" (inverse ascents). The results we prove here are all presented in [**5**, Section 7], and proved using a mixture of combinatorics and manipulatorics (i.e., manipulation of formulas using binomial identities and such). Here we take the balls in boxes approach to prove:

- an analogue of Theorem 1,
- a Worpitzky-like identity to compare with (2), and
- a recurrence relation that refines (4).

Balls in boxes, revisited

To prove these "two-sided" results, we will put balls in boxes another way. First, we introduce a two-dimensional analogue of barred permutations.

Permutations in S_n can be represented visually as an array of n indistinguishable balls so that no two balls lie in the same column or row. (Some authors like to think of non-attacking rooks on a chessboard.) If $w(i) = j$, we put a ball in column i (from left to right) and row j (from bottom to top). For example, with $w = 562143$, we draw the array in FIGURE 2.

The advantage of such an array is that w^{-1} is easily seen in this picture. Rather than reading the heights of the balls from left to right to get w, we can read the column numbers of the balls from bottom to top to get w^{-1}. So in FIGURE 2, $w^{-1} = 436512$. (Check this! Why is it generally true?)

The analogue of a barred permutation, which we call a *two-sided* barred permutation, is any way of inserting both horizontal and vertical lines into the array of balls, with the requirement that there be at least one vertical line between balls that form

TABLE 2: The two-sided Eulerian numbers $[A_{n,i,j}]_{1\le i,j\le n}$, $n = 1, \ldots, 8$

$n = 1$

$i\backslash j$	1
1	1

$n = 2$

$i\backslash j$	1	2
1	1	0
2	0	1

$n = 3$

$i\backslash j$	1	2	3
1	1	0	0
2	0	4	0
3	0	0	1

$n = 4$

$i\backslash j$	1	2	3	4
1	1	0	0	0
2	0	10	1	0
3	0	1	10	0
4	0	0	0	1

$n = 5$

$i\backslash j$	1	2	3	4	5
1	1	0	0	0	0
2	0	20	6	0	0
3	0	6	54	6	0
4	0	0	6	20	0
5	0	0	0	0	1

$n = 6$

$i\backslash j$	1	2	3	4	5	6
1	1	0	0	0	0	0
2	0	35	21	1	0	0
3	0	21	210	70	1	0
4	0	1	70	210	21	0
5	0	0	1	21	35	0
6	0	0	0	0	0	1

$n = 7$

$i\backslash j$	1	2	3	4	5	6	7
1	1	0	0	0	0	0	0
2	0	56	56	8	0	0	0
3	0	56	659	440	36	0	0
4	0	8	440	1520	440	8	0
5	0	0	36	440	659	56	0
6	0	0	0	8	56	56	0
7	0	0	0	0	0	0	1

$n = 8$

$i\backslash j$	1	2	3	4	5	6	7	8
1	1	0	0	0	0	0	0	0
2	0	84	126	36	1	0	0	0
3	0	126	1773	1980	405	9	0	0
4	0	36	1980	8436	4761	405	1	0
5	0	1	405	4761	8436	1980	36	0
6	0	0	9	405	1980	1773	126	0
7	0	0	0	1	36	126	84	0
8	0	0	0	0	0	0	0	1

a descent in w, and at least one horizontal line between balls that form a descent in w^{-1}. Other horizontal and vertical lines can be added arbitrarily. See FIGURE 3 for an example. This two-sided barred permutation corresponds to two ordinary barred permutations, one for w: ||56|2||14|||3, and one for w^{-1}: |4|3||6|5|12|.

Now fix an arrangement of balls corresponding to a permutation w. We will give a two-sided barred permutation the weight

$$s^{(\#\text{of horizontal bars}+1)}\, t^{(\#\text{of vertical bars}+1)},$$

so the example seen in FIGURE 3 would contribute s^8t^9. Since the horizontal and vertical bars can be inserted independently of one another, we see that the generating function for the number of two-sided barred permutations corresponding to a fixed

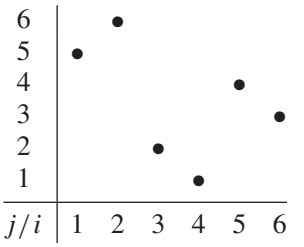

Figure 2 Another model for a permutation

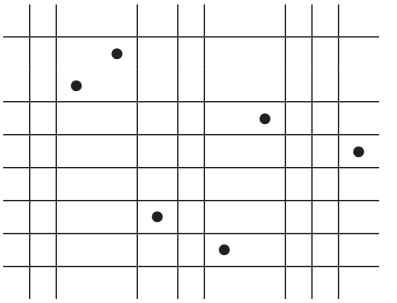

Figure 3 A two-sided barred permutation

permutation w in S_n is the product of the generating function for barred permutations for w^{-1} (in the variable s) with the generating function for barred permutations of w (in the variable t). Thus (1) gives:

$$\frac{s^{\mathbf{des}(w^{-1})+1}\, t^{\mathbf{des}(w)+1}}{(1-s)^{n+1}(1-t)^{n+1}}. \tag{5}$$

Adding up (5) over all permutations in S_n we get the generating function for all two-sided barred permutations is

$$\frac{A_n(s,t)}{(1-s)^{n+1}(1-t)^{n+1}}. \tag{6}$$

Now consider forming two-sided barred permutations with the bars first. Given $k-1$ vertical bars and $l-1$ horizontal bars, we get a k-by-l grid of boxes in which to place our balls, with the convention that if more than one ball goes into a particular row or column, then we arrange the balls diagonally from bottom left to top right. For example, FIGURE 4 shows an arrangement of 7 balls in a 5×4 grid of boxes and its corresponding two-sided barred permutation (with underlying permutation 1723465).

With n unlabeled balls and kl distinct boxes, this means there are a total of

$$\binom{kl+n-1}{n}$$

two-sided barred permutations with $k-1$ vertical lines and $l-1$ horizontal lines. (We are essentially choosing n of the kl boxes, with repetition allowed.) The generating function for the number of *all* two-sided barred permutations is thus

$$\sum_{k,l\geq 0} \binom{kl+n-1}{n} s^k t^l,$$

and comparing with (6) yields the following.

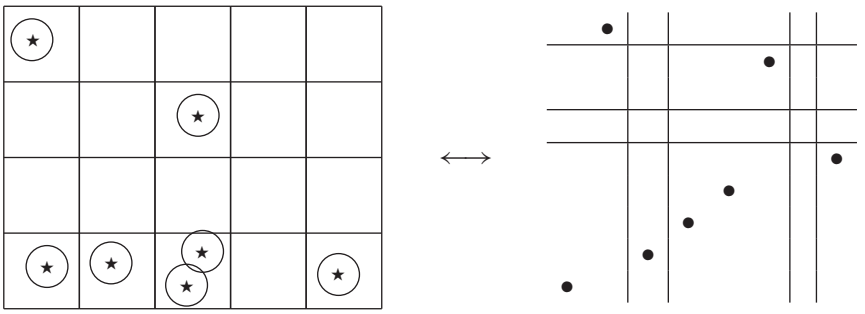

Figure 4 The correspondence between balls in an array of boxes and a two-sided barred permutation

THEOREM 2. (THE TWO-SIDED GENERATING FUNCTION) *For $n \geq 1$, we have*

$$\frac{A_n(s,t)}{(1-s)^{n+1}(1-t)^{n+1}} = \sum_{k,l\geq 0} \binom{kl+n-1}{n} s^k t^l.$$

Worpitzky's identity (two-sided)

Just as Worpitzky's identity can be derived from Theorem 1 and Equation (1), Theorem 2 and Equation (1) yields the following "Worpitzky-like" identity of binomial coefficients,

$$\binom{kl+n-1}{n} = \sum_{i,j=1}^{n} A_{n,i,j} \binom{k+n-i}{n} \binom{l+n-j}{n}. \tag{7}$$

To get (7), we use (1) and (5) to see that for any permutation $w \in S_n$ with $\mathbf{des}(w^{-1}) = i-1$, $\mathbf{des}(w) = j-1$, the generating function for its barred permutations is

$$\begin{aligned}\frac{s^i t^j}{(1-s)^{n+1}(1-t)^{n+1}} &= \sum_{k\geq 0} \binom{k+n-i}{n} s^k \cdot \sum_{l\geq 0} \binom{l+n-j}{n} t^l \\ &= \sum_{k,l\geq 0} \binom{k+n-i}{n} \binom{l+n-j}{n} s^k t^l.\end{aligned}$$

There are $A_{n,i,j}$ such permutations, so summing over $w \in S_n$ yields

$$\begin{aligned}\frac{A_n(s,t)}{(1-s)^{n+1}(1-t)^{n+1}} &= \sum_{i,j=1}^{n} A_{n,i,j} \left(\frac{s^i t^j}{(1-s)^{n+1}(1-t)^{n+1}} \right) \\ &= \sum_{i,j=1}^{n} A_{n,i,j} \cdot \sum_{k,l\geq 0} \binom{k+n-i}{n} \binom{l+n-j}{n} s^k t^l \\ &= \sum_{k,l\geq 0} \left(\sum_{i,j=1}^{n} A_{n,i,j} \binom{k+n-i}{n} \binom{l+n-j}{n} \right) s^k t^l\end{aligned}$$

as the generating function for all two-sided barred permutations for S_n. But we already know there are $\binom{kl+n-1}{n}$ two-sided barred permutations of weight $s^k t^l$, and so we have (7), as desired.

We remark that this Worpitzky-like identity can also be proved (and considerably generalized) using the method of bipartite P-partitions, as follows from [**12**, Corollary 10].

Recurrence relation (two-sided)

Now from Theorem 2 we obtain a recurrence relation akin to (3), which makes for easy computation of the two-sided Eulerian polynomials (see [**5**, Equation 7.8]). We have:

$$\begin{aligned} nA_n(s,t) &= \big(n^2st + (n-1)(1-s)(1-t)\big)A_{n-1}(s,t) \\ &\quad + nst(1-s)\frac{\partial}{\partial s}A_{n-1}(s,t) + nst(1-t)\frac{\partial}{\partial t}A_{n-1}(s,t) \\ &\quad + st(1-s)(1-t)\frac{\partial^2}{\partial s\,\partial t}A_{n-1}(s,t). \end{aligned} \tag{8}$$

To obtain (8), we let $F_n(s,t) = A_n(s,t)/(1-s)^{n+1}(1-t)^{n+1}$, and note the following identity of binomial coefficients that we will need:

$$\begin{aligned} n\binom{kl+n-1}{n} &= \frac{n\cdot(kl+n-1)!}{n!\,(kl-1)!} \\ &= (kl+n-1)\cdot\frac{(kl+n-2)!}{(n-1)!\,(kl-1)!} \\ &= kl\binom{kl+n-2}{n-1} + (n-1)\binom{kl+n-2}{n-1}. \end{aligned}$$

Thus, we can see that

$$\begin{aligned} nF_n(s,t) &= \sum_{k,l\geq 0} n\binom{kl+n-1}{n}s^k t^l \\ &= \sum_{k,l\geq 0} kl\binom{kl+n-2}{n-1}s^k t^l + \sum_{k,l\geq 0}(n-1)\binom{kl+n-2}{n-1}s^k t^l \\ &= st\frac{\partial^2}{\partial s\,\partial t}F_{n-1}(s,t) + (n-1)F_{n-1}(s,t). \end{aligned} \tag{9}$$

Now, with a little calculus, we have

$$\begin{aligned} \frac{\partial^2}{\partial s\,\partial t}F_{n-1}(s,t) &= \frac{\partial}{\partial s}\left[\frac{nA_{n-1}(s,t)}{(1-s)^n(1-t)^{n+1}} + \frac{\frac{\partial}{\partial t}A_{n-1}(s,t)}{(1-s)^n(1-t)^n}\right] \\ &= \frac{n^2A_{n-1}(s,t)}{(1-s)^{n+1}(1-t)^{n+1}} + \frac{n\frac{\partial}{\partial s}A_{n-1}(s,t)}{(1-s)^n(1-t)^{n+1}} \\ &\quad + \frac{n\frac{\partial}{\partial t}A_{n-1}(s,t)}{(1-s)^{n+1}(1-t)^n} + \frac{\frac{\partial^2}{\partial s\,\partial t}A_{n-1}(s,t)}{(1-s)^n(1-t)^n}. \end{aligned}$$

After giving each term a common denominator, we compare numerators in (9) to get (8), as desired.

By comparing coefficients on both sides of (8), we also get the following four-term numeric recurrence:

$$\begin{aligned} nA_{n,i,j} = (ij + n - 1)A_{n-1,i,j} \\ + [1 - n + j(n + 1 - i)]A_{n-1,i-1,j} + [1 - n + i(n + 1 - j)]A_{n-1,i,j-1} \\ + [n - 1 + (n + 1 - i)(n + 1 - j)]A_{n-1,i-1,j-1}. \end{aligned} \tag{10}$$

The reader is invited to use this recurrence to obtain the first few arrays in TABLE 2. Is there a nice visual way to understand this recurrence?

Valley-hopping and γ-nonnegativity

So far we've used models of balls in boxes to explore some of the basic facts about one- and two-sided Eulerian numbers. In this section we will get rid of the boxes altogether and let those same balls roam free, to play a game called "valley-hopping." The goal is to explain a property called "γ-nonnegativity" for the Eulerian numbers. We will then present a conjecture due to Ira Gessel that proposes a two-sided version of γ-nonnegativity.

Now, a sharp-eyed reader may have already noticed the well-known fact that the Eulerian numbers are *symmetric* for fixed n:

$$A_{n,i} = A_{n,n+1-i},$$

or in terms of Eulerian polynomials, $A_n(t) = t^{n+1}A_n(1/t)$. This symmetry can be explained by observing that if w has i descents, then it has $n - 1 - i$ ascents.

Similarly, we can find the following symmetries for two-sided Eulerian numbers in TABLE 2:

$$A_{n,i,j} = A_{n,j,i}, \quad \text{or} \quad A_n(s,t) = A_n(t,s), \tag{11}$$

$$A_{n,i,j} = A_{n,n+1-i,n+1-j}, \quad \text{or} \quad A_n(s,t) = (st)^{n+1}A_n(1/s, 1/t), \tag{12}$$

and

$$A_{n,i,j} = A_{n,n+1-j,n+1-i}, \quad \text{or} \quad A_n(s,t) = (st)^{n+1}A_n(1/t, 1/s). \tag{13}$$

It is a fun exercise to come up with combinatorial arguments to verify symmetries (11) and (12). (Hint: how does flipping a permutation array upside-down affect descents and inverse descents?) Symmetry (13) follows from the first two.

Another property exhibited by the Eulerian polynomials is *unimodality*, i.e., the Eulerian numbers in a given row increase up to a certain maximum and then decrease:

$$A_{n,1} \le A_{n,2} \le \cdots \le A_{n,\lceil n/2 \rceil} \ge \cdots \ge A_{n,n-1} \ge A_{n,n}.$$

Most good distributions satisfy this property of having the bulk of the mass in the middle, with the rest spread out symmetrically. The canonical example is the binomial distribution, $\binom{n}{i}$ with fixed n. Similarly, the two-sided Eulerian numbers appear to increase in the direction of the middle of the main diagonal, with a maximum at $A_{n,\lceil n/2 \rceil,\lceil n/2 \rceil}$. However, things are somewhat delicate. See TABLE 2.

Both the symmetry and unimodality of the Eulerian polynomials follow from a stronger result, first proved in 1970 by Foata and Schützenberger [**10**, Théorème 5.6]. See also Carlitz and Scoville [**6**].

THEOREM 3. *For $n \geq 1$, there exist nonnegative integers $\gamma_{n,i}$, $i = 1, \ldots, \lceil n/2 \rceil$, such that*

$$A_n(t) = \sum_{1 \leq i \leq \lceil n/2 \rceil} \gamma_{n,i} t^i (1+t)^{n+1-2i}.$$

For example, when $n = 4, 5$ we have:

$$\begin{aligned} A_4(t) &= t + 11t^2 + 11t^3 + t^4 \\ &= t(1+t)^3 + 8t^2(1+t), \\ A_5(t) &= t + 26t^2 + 66t^3 + 26t^4 + t^5 \\ &= t(1+t)^4 + 22t^2(1+t)^2 + 16t^3. \end{aligned}$$

In other words, the polynomials $A_n(t)$ can be expressed as a positive sum of symmetric binomial terms with the same center of symmetry. Since the binomial distribution is symmetric and unimodal, so is the Eulerian distribution. We might say that the Eulerian distribution is "super binomial." Gessel has conjectured a similar expansion for two-sided Eulerian numbers that we will discuss shortly.

First, we explain how Foata and Schützenberger's result can be given a wonderfully visual proof via an action called *valley-hopping*. The argument here has its roots in the work of Foata and Strehl [**11**] from 1974, was re-discovered by Shapiro, Woan, and Getu [**15**] in 1983, and was dusted off more recently (and applied in a wonderful variety of ways) by Brändén [**3**] in 2008.

We define the valley-hopping action on permutations as follows. We visualize permutations as arrays of balls again, but now we connect the dots to form a kind of mountain range. Some balls sit at peaks, others sit in valleys, and the rest are somewhere in between. If a ball is not at a peak or in a valley, then it is free to jump straight across a valley to the nearest point on a slope at the same height.

Valley hopping naturally partitions S_n into equivalence classes, according to whether one permutation can be obtained from another through a sequence of hops. For example, the permutation $w = 863247159$ would be drawn as shown in FIGURE 5. There are 2^6 permutations in its equivalence class, formed by choosing which of the six free balls will be on the left sides of their respective valleys and which will be on the right. Write $u \sim w$ if u can be obtained from w through valley-hopping. Notice that when a free ball is on the right side of a valley, it is *not* in a descent position, while if it is on the left side of a valley, it *is* in a descent position. (This is why we labeled the arcs in the picture with $t + 1$.) Moreover, this property holds true regardless of the positions of the other free balls.

As for the non-free balls, we know that peaks are *always* in descent positions while valleys are *never* in descent positions. If a permutation has $i - 1$ peaks, then it must have i valleys, and the remaining $n + 1 - 2i$ balls are free. Thus, we can conclude that for a fixed w in S_n with $i - 1$ peaks,

$$\sum_{u \sim w} t^{\mathbf{des}(u)+1} = t^i (1+t)^{n+1-2i}.$$

For example, the equivalence class for $w = 863247159$ would contribute

$$t^2(1+t)^6.$$

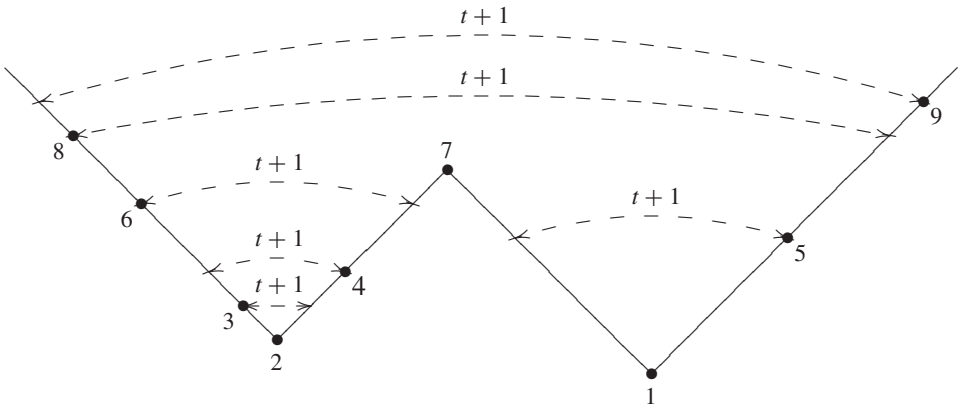

Figure 5 Valley-hopping for the permutation $w = 863247159$

Since the union of all equivalence classes is S_n, we see that the Eulerian polynomial is a sum of terms of the form $t^i(1+t)^{n+1-2i}$, proving Theorem 3. Moreover, the coefficient $\gamma_{n,i}$ equals the number of distinct equivalence classes with $i-1$ peaks.

We now turn to the two-sided case.

It is possible to show that any polynomial in two variables (of degree n in each) satisfying symmetries (11) and (12) can be written uniquely in the basis

$$\{(st)^i(s+t)^j(1+st)^{n+1-j-2i}\}_{0\le j+2i\le n+1}.$$

Thus, the two-sided Eulerian polynomials can be expressed in this basis, and Gessel has conjectured that such an expression has nonnegative coefficients. See [**3**, Conjecture 10.2].

GESSEL'S CONJECTURE. *For $n \ge 1$, there exist nonnegative integers $\gamma_{n,i,j}$, $0 \le i-1$, j, $j+2i \le n+1$, such that*

$$A_n(s,t) = \sum_{i,j} \gamma_{n,i,j}(st)^i(s+t)^j(1+st)^{n+1-j-2i}.$$

For example, when $n = 4, 5$, we have

$$\begin{aligned} A_4(s,t) &= st + 10(st)^2 + 10(st)^3 + (st)^4 + s^2t^3 + s^3t^2 \\ &= st(1+st)^3 + 7(st)^2(1+st) + (st)^2(s+t) \\ A_5(s,t) &= st + 20(st)^2 + 54(st)^3 + 20(st)^4 + (st)^5 + 6s^2t^3 + 6s^3t^2 + 6s^3t^4 + 6s^4t^3 \\ &= st(1+st)^4 + 16(st)^2(1+st)^2 + 16(st)^3 + 6(st)^2(s+t)(1+st) \end{aligned}$$

In terms of the arrays $[A_{n,i,j}]$, we see:

$$\begin{bmatrix} 1 & 0 & 0 & 0 \\ 0 & 10 & 1 & 0 \\ 0 & 1 & 10 & 0 \\ 0 & 0 & 0 & 1 \end{bmatrix} = \begin{bmatrix} 1 & 0 & 0 & 0 \\ 0 & 3 & 0 & 0 \\ 0 & 0 & 3 & 0 \\ 0 & 0 & 0 & 1 \end{bmatrix} + 7 \cdot \begin{bmatrix} 0 & 0 & 0 & 0 \\ 0 & 1 & 0 & 0 \\ 0 & 0 & 1 & 0 \\ 0 & 0 & 0 & 0 \end{bmatrix} + \begin{bmatrix} 0 & 0 & 0 & 0 \\ 0 & 0 & 1 & 0 \\ 0 & 1 & 0 & 0 \\ 0 & 0 & 0 & 0 \end{bmatrix}$$

and

$$\begin{bmatrix} 1 & 0 & 0 & 0 & 0 \\ 0 & 20 & 6 & 0 & 0 \\ 0 & 6 & 54 & 6 & 0 \\ 0 & 0 & 6 & 20 & 0 \\ 0 & 0 & 0 & 0 & 1 \end{bmatrix} = \begin{bmatrix} 1 & 0 & 0 & 0 & 0 \\ 0 & 4 & 0 & 0 & 0 \\ 0 & 0 & 6 & 0 & 0 \\ 0 & 0 & 0 & 4 & 0 \\ 0 & 0 & 0 & 0 & 1 \end{bmatrix} + 16 \cdot \begin{bmatrix} 0 & 0 & 0 & 0 & 0 \\ 0 & 1 & 0 & 0 & 0 \\ 0 & 0 & 2 & 0 & 0 \\ 0 & 0 & 0 & 1 & 0 \\ 0 & 0 & 0 & 0 & 0 \end{bmatrix}$$

$$+ 16 \cdot \begin{bmatrix} 0 & 0 & 0 & 0 & 0 \\ 0 & 0 & 0 & 0 & 0 \\ 0 & 0 & 1 & 0 & 0 \\ 0 & 0 & 0 & 0 & 0 \\ 0 & 0 & 0 & 0 & 0 \end{bmatrix} + 6 \cdot \begin{bmatrix} 0 & 0 & 0 & 0 & 0 \\ 0 & 0 & 1 & 0 & 0 \\ 0 & 1 & 0 & 1 & 0 \\ 0 & 0 & 1 & 0 & 0 \\ 0 & 0 & 0 & 0 & 0 \end{bmatrix}$$

It may be possible to use a "manipulatorics" approach to prove Gessel's Conjecture. (Perhaps an inductive proof using the recurrence in (8)?) However, a more satisfying proof might be one that generalizes the valley-hopping proof of Theorem 3.

If we look at both descents and inverse descents for the valley-hopping equivalence class of $w = 12\cdots n$ (i.e., the class with no peaks), we get a distribution of $st(1+st)^{n-1}$. This is encouraging, but for the class of $w = 863247159$ shown in FIGURE 5, we get

$$\sum_{u \sim w} s^{\mathbf{des}(u^{-1})+1} t^{\mathbf{des}(u)+1} = s^3t^2(1+t)^2(1+st)^4,$$

which is not even symmetric in s and t. So valley-hopping as presently done does not immediately give us a way to prove Gessel's conjecture.

How should we partition S_n so that we get groupings whose distribution of descents and inverse descents is given by $(st)^i(s+t)^j(1+st)^{n+1-j-2i}$?

Generalization

We finish by remarking that S_n is an example of a *finite reflection group*, or *Coxeter group*. The notion of a descent can be generalized to any Coxeter group, and there is a "Coxeter-Eulerian" polynomial that enjoys many of the same properties of the classical Eulerian polynomial, including an analogue of Theorem 3. Moreover, this polynomial has topological meaning, as the "h-polynomial" of something called the Coxeter complex (see [**2, 7, 17**]).

The two-sided Eulerian polynomial generalizes to Coxeter groups as well, and seems to enjoy many of the same properties of $A_n(s,t)$. In particular, the analogue of Gessel's Conjecture appears to hold in any finite Coxeter group. It would be interesting to have a general approach to the problem.

Acknowledgment I would like to thank Ira Gessel for teaching me how to put balls in boxes and for sharing his conjecture.

REFERENCES

1. M. Bóna, *Combinatorics of Permutations*, Discrete Mathematics and Its Applications (Boca Raton), Chapman & Hall/CRC, Boca Raton, FL, 2004.
2. A. Björner and F. Brenti, *Combinatorics of Coxeter Groups*, Graduate Texts in Mathematics, 231, Springer-Verlag, New York, 2005. http://dx.doi.org/10.1007/3-540-27596-7
3. P. Brändén, Actions on permutations and unimodality of descent polynomials, *European J. Combin.* **29** (2008) 514–531. http://dx.doi.org/10.1016/j.ejc.2006.12.010

4. L. Carlitz, Eulerian numbers and polynomials, *Math. Mag.* **32** (1958/1959) 247–260. http://dx.doi.org/10.2307/3029225
5. L. Carlitz, D. P. Roselle, and R. A. Scoville, Permutations and sequences with repetitions by number of increases, *J. Combinatorial Theory* **1** (1966) 350–374. http://dx.doi.org/10.1016/S0021-9800(66)80057-1
6. L. Carlitz and R. A. Scoville, Generalized Eulerian numbers: combinatorial applications, *J. Reine Angew. Math.* **265** (1974) 110–137.
7. K. Dilks, T. K. Petersen, and J. R. Stembridge, Affine descents and the Steinberg torus, *Adv. in Appl. Math.* **42** (2009) 423–444. http://dx.doi.org/10.1016/j.aam.2008.11.002
8. L. Euler, *Institutiones Calculi Differentialis cum Eius Usu in Analysi Finitorum ac Doctrina Serierum*, Ticini: in typographeo Petri Galeatii, 1787.
9. D. Foata and G.-N. Han, The q-series in combinatorics; permutation statistics (lecture notes), preliminary version, 2004. Available online at http://www-irma.u-strasbg.fr/~foata/paper/qseriescom.pdf.
10. D. Foata and M.-P. Schützenberger, *Théorie Géométrique des Polynômes Eulériens* (in French), Lecture Notes in Mathematics, Vol. 138, Springer-Verlag, Berlin, 1970. http://dx.doi.org/10.1007/BFb0060799
11. D. Foata and V. Strehl, Rearrangements of the symmetric group and enumerative properties of the tangent and secant numbers, *Math. Z.* **137** (1974) 257–264. http://dx.doi.org/10.1007/BF01237393
12. I. M. Gessel, Multipartite P-partitions and inner products of skew Schur functions, Combinatorics and algebra (Boulder, Colo., 1983), 289–317, *Contemp. Math.* **34**, Amer. Math. Soc., Providence, RI, 1984. http://dx.doi.org/10.1090/conm/034/777705
13. D. E. Knuth, *The Art of Computer Programming, Vol. 3: Sorting and Searching*, Addison-Wesley, Reading, MA, 1973.
14. P. A. MacMahon, *Combinatory Analysis*, two volumes bound as one, Chelsea, New York, 1960.
15. L. Shapiro, W.-J. Woan, and S. Getu, Runs, slides, and moments, *SIAM J. Algebraic Discrete Methods* **4** (1983) 459–466. http://dx.doi.org/10.1137/0604046
16. R. P. Stanley, *Enumerative Combinatorics*, Vol. 1, Cambridge Studies in Advanced Mathematics, 49, Cambridge University Press, Cambridge, 1997.
17. J. R. Stembridge, Coxeter cones and their h-vectors, *Adv. Math.* **217** (2008) 1935–1961. http://dx.doi.org/10.1016/j.aim.2007.09.002

Summary The Eulerian numbers count permutations according to the number of descents. The two-sided Eulerian numbers count permutations according to number of descents and the number of descents in the inverse permutation. Here we derive some results for Eulerian and two-sided Eulerian numbers using an elementary "balls-in-boxes" approach. We also discuss an open conjecture of Ira Gessel about the two-sided Eulerian numbers.

KYLE PETERSEN earned an A.B. in mathematics from Washington University in St. Louis in 2001 and a Ph.D. in mathematics from Brandeis University in 2006, where his advisor was Ira Gessel. After a wonderful three years with the University of Michigan, he joined the faculty at DePaul University, where he has been teaching since 2009. Apart from teaching, he enjoys working with the math club and on summer research projects with undergraduates. His research is in algebraic, enumerative, and topological combinatorics. Outside of the mathematics department, he enjoys running and spending time with his wife and their three children.

Let π Be a Function

JUSTIN T. SCHULTZ
University of Rochester
Rochester, NY 14627-0186
j.t.schultz@rochester.edu

CATHERINE STENSON
Juniata College
Huntingdon, PA 16652
stenson@juniata.edu

Does π have to be 3.14159...? In their article "Let π be 3," Andersen, Stumpf, and Tiller [**1**] find a circle with a circumference-to-diameter ratio of 3. The trick? This circle is on a sphere, and the diameter is measured along the sphere, rather than in the plane of the circle. When π is calculated in this way, it is a function of the radius r of the circle. Here we call the function $\Pi(r)$. Anderson et al. show that $\Pi(r) = \pi \sin(r)/r$, which takes on the value 3 when $r = \pi/6$ as shown in FIGURE 1. They also show that $\Pi(r) = \pi \sinh(r)/r$ on a pseudosphere, where there are circles with Π greater than π.

In this article, we will consider Π on other surfaces. We will also look at the inverse problem—given a specific function $\Pi(r)$, we will find a corresponding surface, or at least a corresponding Riemannian manifold.

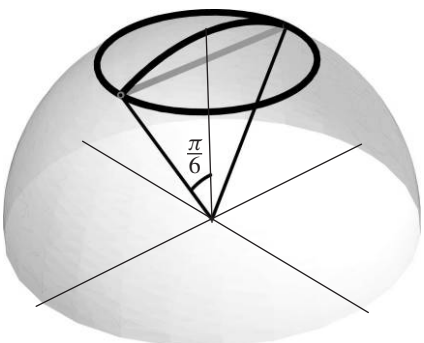

Figure 1 When it is measured along the unit sphere, the diameter of this circle is $\pi/3$. The circumference is $\pi(2\sin(\pi/6)) = \pi$, so the circumference-to-diameter ratio is $\Pi = 3$.

First, what do we mean by a circle on a surface? A circle in the plane is the set of all points that are a distance r from a center point. We can find a point on the circle by starting at the center, choosing a direction, and walking a distance r along a straight line in that direction. We would like to apply this definition on any surface, but what does it mean to "walk along a straight line" on a surface?

When we walk in a straight line on the plane, the unit tangent vector to our path does not change. If we imagine that we are walking along a parameterized curve $\vec{\gamma}(t)$ on a surface and that we are small enough that the tangent plane appears to us to be a good approximation of the surface, we will feel as though we are walking in a straight line if $\vec{T}(t) = \vec{\gamma}'(t)/\|\vec{\gamma}'(t)\|$, the unit tangent to our curve, does not change in the tangent plane. Formally, this means that $\vec{T}'(t)$ should be orthogonal to the tangent

Math. Mag. **86** (2013) 177–188. doi:10.4169/math.mag.86.3.177.

plane of the surface. Curves satisfying this condition are called *geodesics*. Students of multivariable calculus may be familiar with $\vec{T}'(t)/\|\vec{T}'(t)\|$, the *normal vector* of the curve, and may remember that it is perpendicular to $\vec{T}(t)$. In this paper we will always call $\vec{T}'(t)/\|\vec{T}'(t)\|$ the *curve normal vector* to distinguish it from a surface normal vector, and we will always assume that $\|\vec{\gamma}'(t)\|$ is nonzero.

By the above definition, a straight line in $\mathbb{R}^3$ is a geodesic on any surface that contains it, since $\vec{T}'(t)$ is the zero vector and therefore orthogonal to the tangent plane. For example, the lines extending from the point of a cone are geodesics. On a sphere, the geodesics are the great circles. To see this, note that at any point on the sphere, the inward choice of surface normal points toward the center of the sphere. At any point on a circle, the curve normal vector points toward the center of the circle. Thus a circle on a sphere is a geodesic precisely when the center of the circle is also the center of the sphere—that is, when the circle is a great circle (FIGURE 2). It takes a bit more work [**6**, Exercise 3.2.c] to show that great circles are the only geodesics on a sphere. In general, if a surface is sufficiently smooth, it has a unique geodesic in any direction from a given point. Furthermore, just as a straight line is the shortest path between two points in the plane, a geodesic is locally the shortest path between two points. Henderson's text [**6**] contains a further discussion of the idea of straightness on a surface.

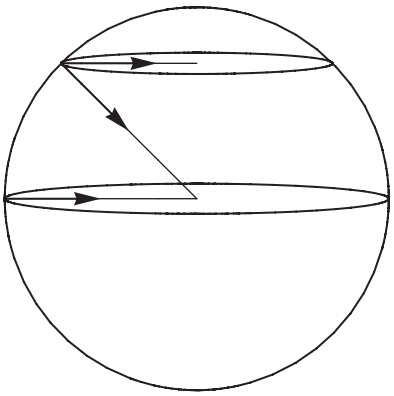

Figure 2 On a sphere, the equator is a geodesic, since the curve normal vector is in the same direction as the inward surface normal. The latitude circle is not a geodesic, since the curve normal vector points to the center of the circle, while the inward surface normal points to the center of the sphere.

Because a geodesic is the analog of a straight line on a surface, we can say that a circle on a surface, or *geodesic circle*, comes from picking a center and then finding all points that are a distance r from the center as measured along geodesics. On all the surfaces we consider, it will be clear that a geodesic circle is itself a curve with a well-defined length. For a geodesic circle, we define the *radius* to be the distance r measured on the surface, the *diameter* to be $2r$, and Π to be the ratio of the circumference to the diameter. We use π to indicate the usual value of $3.14159\ldots$.

For example, we can generate a cone by rotating the line $y = x$ about the x-axis, as illustrated in FIGURE 3. On the cone, the circle at $x = 1$ is centered at the origin. Using the Pythagorean Theorem, we see that it has radius $\sqrt{2}$ on the cone. Its circumference is 2π, so $\Pi = \pi/\sqrt{2}$. This makes sense, because if we cut the cone along the line $y = x$ and then unroll it, we get a sector of the plane with angle $2(\pi/\sqrt{2})$. More generally, the cone generated by $y = ax$, where $a > 0$, has $\Pi = \pi a/\sqrt{1 + a^2}$. As a gets larger, the line $y = ax$ becomes closer to a vertical line, the cone becomes closer

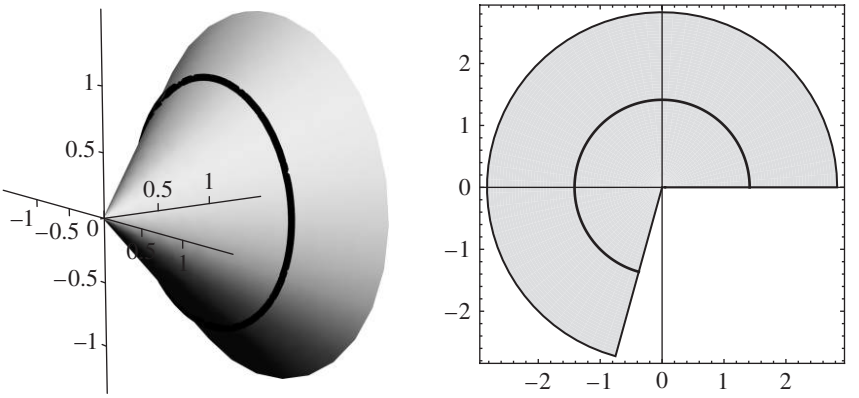

Figure 3 On the left is the cone generated by rotating the line $y = x$ about the x-axis. The circle at $x = 1$ is shown in black. On the right is the cone unrolled into a sector of the plane with angle $2(\pi/\sqrt{2})$. The black curve with radius $\sqrt{2}$ corresponds to the circle at $x = 1$ on the cone.

to a plane, and Π approaches π, as we would expect. For any cone, Π is independent of radius for circles centered at the vertex, just as it is in the plane. As we will see, this is not true for analogous circles on other surfaces of revolution.

Surfaces of revolution

We start by examining Π on surfaces of revolution because their symmetry makes it easy to find the geodesics we need. We can rotate a curve given by the graph of a function $y = f(x)$ about the x-axis to get a surface parameterized by $\vec{S}(x, \theta) = (x, f(x)\cos(\theta), f(x)\sin(\theta))$. We place some conditions on f:

(1) $f(0) = 0$, so that the surface contains the origin, which will be the center of our circles;

(2) The domain of f is of the form $[0, a)$, $[0, a]$, or $[0, \infty)$;

(3) f is twice differentiable, except possibly for a vertical tangent at the origin, so that geodesics exist everywhere on the surface; and

(4) $f(x) \geq 0$ for any $x > 0$ in the domain.

We want to create circles centered at $(0, 0, 0)$. The geodesics through this point are simply the curves with a constant value of θ, say $\theta = \theta_0$. To see this, we first notice that the surface is symmetric about the plane $\theta = \theta_0$, so that a surface normal along the curve $\vec{\gamma}(t) = (t, f(t)\cos(\theta_0), f(t)\sin(\theta_0))$ must lie in the plane $\theta = \theta_0$. Since $\vec{\gamma}(t)$ is a plane curve, its curve normal vector also lies in this plane. Furthermore, a surface normal must be perpendicular to the unit tangent vector $\vec{T}(t)$, since $\vec{T}(t)$ is tangent to the surface as well as to $\vec{\gamma}(t)$. The curve normal vector of $\vec{\gamma}(t)$ is also perpendicular to $\vec{T}(t)$. Thus the curve normal vector of $\vec{\gamma}(t)$ and any choice of surface normal lie in the plane $\theta = \theta_0$ and are perpendicular to the same nonzero vector within that plane, which means one is a scalar multiple of the other (FIGURE 4). Therefore, $\vec{\gamma}(t)$ is a geodesic for any choice of θ_0. (The truly enthusiastic multivariable calculus student can verify this by directly computing

$$\vec{T}'(t) = \frac{f''(t)}{(1 + (f'(t))^2)^{3/2}}(-f'(t), \cos(\theta_0), \sin(\theta_0))$$

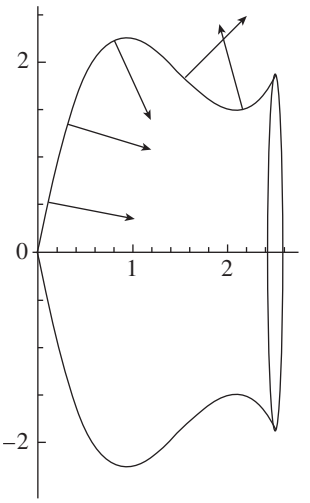

Figure 4 The curve normal vector $\vec{T}'(t)/\|\vec{T}'(t)\|$ at five different points along the curve $\theta = 0$ on the surface of revolution generated by $f(x) = (x - 1.5)^3 - (x - 1.5^3)$. At each point, the curve normal vector is perpendicular to the tangent plane of the surface.

and showing that it is normal to the surface.) Henderson [**6**, Problems 1.7 and 3.4] gives a lovely argument that these curves are geodesics, provided that $T(t)$ exists and is continuous, even if $T'(t)$ fails to exist at some points.

Now that we have our family of geodesics, if we start at the origin and follow each one for a fixed distance, we get a circle of points with the same x-coordinate, say $x = x_0$. The circumference of this circle is $2\pi f(x_0)$, since $f(x_0)$ is the radius of this circle regarded as a curve in $\mathbb{R}^3$. The radius of this circle, measured along the surface, is given by the arc length integral $\int_0^{x_0} \sqrt{1 + f'(u)^2}du$. Thinking of Π (for the time being) as a function of the x-coordinate of our circle, we have

$$\Pi(x) = \frac{\pi f(x)}{\int_0^x \sqrt{1 + f'(u)^2}\, du}. \tag{1}$$

We now show that the value of Π on a cone gives an upper bound on Π for other surfaces of revolution.

PROPOSITION. *Let f be a function satisfying conditions* (1)–(4) *with $f(x_0) = y_0$ for some $x_0 > 0$. Then*

$$\Pi(x_0) \leq \frac{\pi y_0/x_0}{\sqrt{1 + (y_0/x_0)^2}}.$$

Proof. We fix x_0 and y_0 and consider all functions f that satisfy the conditions (1)–(4) with $f(x_0) = y_0$. The circumference of the circle at $x = x_0$ is $2\pi y_0$, but the diameter depends on f. The shorter the diameter, the larger the value of $\Pi(x_0)$. The shortest path from the origin to (x_0, y_0) is the line $g(x) = (y_0/x_0)x$. Thus if $f(x_0) = y_0$, we have

$$\Pi(x_0) \leq \frac{\pi y_0/x_0}{\sqrt{1 + (y_0/x_0)^2}}. \qquad \blacksquare$$

In particular, the Proposition means that $\Pi \leq \pi$. It is possible to have Π greater than π on other surfaces, or even at points other than the origin on surfaces of revolution.

For example, Andersen et al. [**1**] show that Π is greater than π on a pseudosphere. Although the pseudosphere is a surface of revolution, its generating curve does not go through the origin, so our upper bound does not apply.

To see how $\Pi(x)$ can behave between the bounds of 0 and π, we consider functions of the form $f(x) = x^n$, where $n > 0$. Cases with $n = 2$ and $n = 1/2$ are illustrated in FIGURE 5. First, we examine the behavior of $\Pi(x)$ near the origin. We have

$$\lim_{x\to 0} \Pi(x) = \lim_{x\to 0} \frac{\pi x^n}{\int_0^x \sqrt{1 + (nu^{n-1})^2}\, du}.$$

Both the numerator and the denominator approach zero as x approaches zero. Therefore, we can apply L'Hôpital's Rule and the second part of the Fundamental Theorem of Calculus to get

$$\lim_{x\to 0} \Pi(x) = \lim_{x\to 0} \frac{\pi n x^{n-1}}{\sqrt{1 + (nx^{n-1})^2}}.$$

If $n > 1$, then the numerator approaches 0 and the denominator approaches 1, so the limit is 0. If $0 < n < 1$, we can rewrite the limit as $\lim_{x\to 0} \pi/\sqrt{(1/(nx^{n-1})^2) + 1}$. The denominator approaches 1, so the limit is π. If $n = 1$, we simply have the cone described previously with $a = 1$, and the limit is $\pi/\sqrt{2}$.

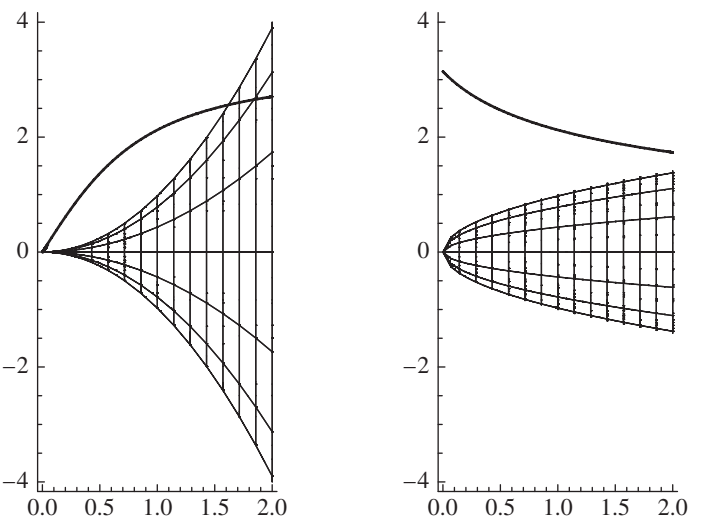

Figure 5 On the left is the surface of revolution generated by $f(x) = x^2$. The dark curve is its pi function $\Pi(x)$. On the right is the surface of revolution generated by $f(x) = x^{1/2}$. The dark curve is its pi function $\Pi(x)$.

Geometrically, this result makes sense. If $0 < n < 1$, then x^n has a vertical tangent at $x = 0$, and the surface of revolution has a tangent plane at the origin. In a small neighborhood of the origin, the surface is well-approximated by the tangent plane, and the value of $\Pi(x)$ should be close to the planar value π. If $n > 1$, then x^n has a horizontal tangent at $x = 0$ and the surface of revolution comes to a sharp point at the origin. The circumference of a circle near the origin is quite small in comparison to the radius on the surface, and we expect the value of $\Pi(x)$ to be near 0.

A similar analysis gives us the behavior of $\Pi(x)$ for large values of x. We have

$$\lim_{x\to\infty} \Pi(x) = \lim_{x\to\infty} \frac{\pi x^n}{\int_0^x \sqrt{1+(nu^{n-1})^2}\,du}.$$

Again we apply L'Hôpital's Rule and the second part of the Fundamental Theorem of Calculus to get $\lim_{x\to\infty} \Pi(x) = 0$ for $0 < n < 1$ and $\lim_{x\to\infty} \Pi(x) = \pi$ for $n > 1$. If $n = 1$, the limit is again $\pi/\sqrt{2}$.

For a general $f(x)$ satisfying conditions (1)–(4) and with $f'(0)$ defined, the same application of L'Hôpital's Rule gives $\lim_{x\to 0} \Pi(x) = \pi f'(0)/\sqrt{1+f'(0)^2}$. This is the value of $\Pi(x)$ on a cone generated by a line of slope $f'(0)$, the tangent line at the origin. Similarly, for large values of x the behavior of $\Pi(x)$ depends on the behavior of $f'(x)$.

The inverse problem and parameterization by arc length

Given a surface, we know how to find Π. What about the inverse problem? Given a function P, can we find a surface for which $\Pi = P$?

To address this problem in the setting of the previous section, we would need to solve for f in terms of Π in equation (1), but this is painful. We will move to a setting where the computations are much cleaner. Instead of beginning with a curve given by a function, we will start with a parametric curve. This will allow us to express Π as a function of the radius r, as Andersen et al. [**1**] do for the sphere.

A curve $\vec{\gamma}(r)$ is parameterized by arc length if $\|\vec{\gamma}'(r)\| = 1$. (Usually arc length is called s, but we use r, since it is also our radius.) If we think of a person walking along the curve at a constant (unit) speed, this is a natural way to parameterize the curve. For a plane curve $\vec{\gamma}(r) = (x(r), y(r))$, this means that $(x'(r))^2 + (y'(r))^2 = 1$. The surface of revolution obtained by revolving $\vec{\gamma}$ around the x-axis is parameterized by $\vec{S}(r,\theta) = (x(r), y(r)\cos(\theta), y(r)\sin(\theta))$. The functions $x(r)$ and $y(r)$ should satisfy the following conditions, analogous to the restrictions on f in the previous section:

(1′) $(x(0), y(0)) = (0, 0)$, so that the surface contains the origin;

(2′) The domain of x and y is of the form $[0, a)$, $[0, a]$, or $[0, \infty)$;

(3′) $x(r)$ and $y(r)$ are twice differentiable, except possibly at 0, so that geodesics will exist everywhere on the surface; and

(4′) $y(r) \geq 0$ for any $r > 0$ in the domain.

In this setting, we have $\Pi(r) = \pi y(r)/r$. As in the previous section, $\Pi(r) \leq \pi$, since a line is still the shortest path between $(0, 0)$ and (x_0, y_0). Also as in the previous section, the curves with a constant value of θ are geodesics.

For example, the semicircle $\vec{\gamma}(r) = (1 - \cos(r), \sin(r))$, $0 \leq r \leq \pi$, generates the sphere $\vec{S}(r,\theta) = (1 - \cos(r), \sin(r)\cos(\theta), \sin(r)\sin(\theta))$. This sphere is centered at $(1, 0, 0)$ and has radius 1. The curves with a constant value of θ are great circles and hence geodesics, as expected. We have $\Pi(r) = \pi \sin(r)/r$, matching the result in [**1**]. In fact, Andersen et al. allow r to be any real number and find that $\pi \sin(r)/r$ is still the right expression for $\Pi(r)$, even when the value is negative.

Now we can solve the inverse problem.

THEOREM 1. *Given a nonnegative twice-differentiable function $P(r)$ with domain as in (2′) satisfying $|\frac{d}{dr} r P(r)| \leq \pi$, there exists a surface of revolution with $\Pi(r) = P(r)$ for $r > 0$.*

Proof. We will define a curve $\gamma(r) = (x(r), y(r))$ that is parameterized by arc length and generates a surface of revolution with $\Pi(r) = P(r)$. Since $\Pi(r) = \pi y(r)/r$ for surfaces of revolution in this setting, we define $y(r) = rP(r)/\pi$. We note that $y(0) = 0$. The restriction $|\frac{d}{dr} rP(r)| \leq \pi$ tells us that $|y'(r)| \leq 1$, which is necessary for a curve parameterized by arc length, since $(x'(r))^2 + (y'(r))^2 = 1$. Solving for x' gives

$$x'(r) = \pm\sqrt{1 - (y'(r))^2} = \pm\sqrt{1 - \left(\frac{1}{\pi}(P(r) + rP'(r))\right)^2}.$$

If we choose the nonnegative square root and the initial condition $x(0) = 0$, we have

$$x(r) = \int_0^r \sqrt{1 - \left(\frac{1}{\pi}(P(u) + uP'(u))\right)^2}\, du.$$

Then $\gamma(r) = (x(r), y(r))$ is the desired curve. ∎

For example, if we choose $\Pi(r) = \sin(r)$, $0 \leq r \leq \pi$, we get the teardrop-shaped surface in FIGURE 6.

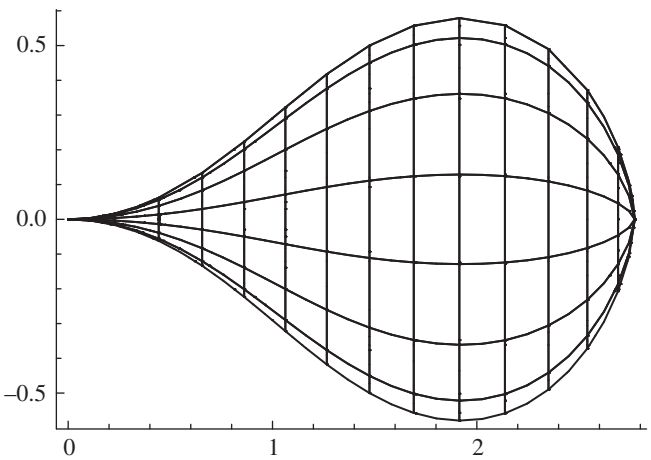

Figure 6 A surface of revolution with $\Pi(r) = \sin(r)$

The curve $\vec{\gamma}(r)$ does not have to be a function graph, so we have a broader class of surfaces of revolution. The vertical line $\vec{\gamma}(r) = (0, r)$, $r \geq 0$ generates a plane, and $\Pi(r) = \pi$, as expected. The clothoid

$$\vec{\gamma}(r) = \left(\int_0^r \cos(u^2/2)\, du, \int_0^r \sin(u^2/2)\, du\right)$$

generates a lovely surface of revolution that curls in on itself. It has

$$\Pi(r) = \frac{\pi}{r} \int_0^r \sin(u^2/2)\, du,$$

which approaches 0 as r gets large. We can see this in FIGURE 7, since there is an upper bound on $y(r)$ but no upper bound on r. The sharp-eyed reader will notice that $x'(r)$ is

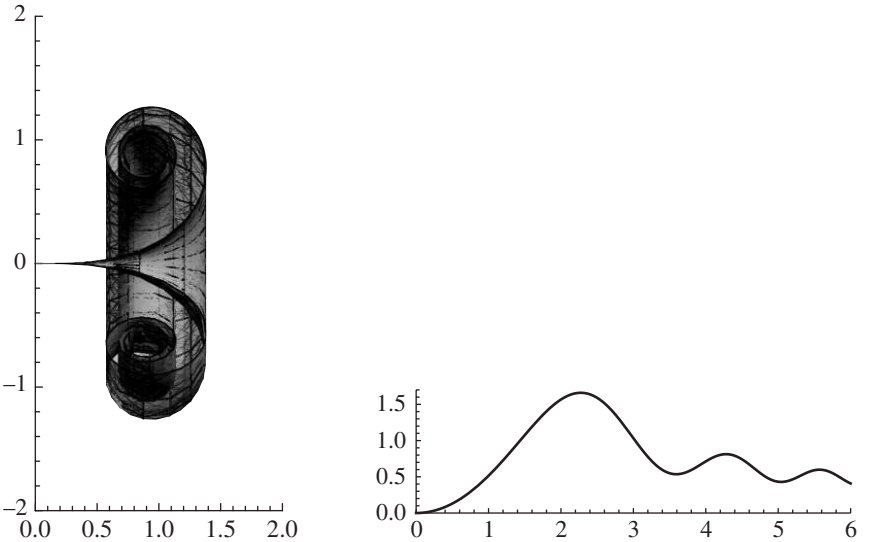

Figure 7 On the left is a cutaway view of the surface of revolution generated by a clothoid (the thick black spiral). On the right is the corresponding pi function $\Pi(r)$. In both figures r goes from 0 to 6.

not always nonnegative for the clothoid. While we chose the nonnegative square root in the proof of Theorem 1, that is not the only possible choice. The clothoid results from alternating between the positive and negative square roots, changing whenever $x'(r) = 0$.

The condition $|\frac{d}{dr} r P(r)| \leq \pi$ in Theorem 1 has a nice geometric interpretation. We can rewrite it as $|\frac{d}{dr} 2r P(r)| \leq 2\pi = \frac{d}{dr} 2\pi r$. This says that the circumference of a circle on the surface cannot grow faster than the circumference of a circle in the plane as a function of r.

Geodesic polar coordinates, Riemannian manifolds, and the inverse problem

We would like to extend our exploration of Π to surfaces that are not surfaces of revolution.

When we looked at circles on a surface of revolution, we were really setting up a version of polar coordinates on the surface. In principle, we can parameterize any surface in this way, at least locally, if we can find a point with geodesics in all directions. We let that point be the origin and choose a fixed direction v as a reference direction. We define $\vec{S}(r, \theta)$ to be the point found by starting at the origin and walking a distance r along the geodesic in the direction that is an angle of θ from v. These are *geodesic polar coordinates*. Banchoff and Lovett [**2**] give a formal definition. It is easy to imagine laying out this coordinate system if you are standing on the surface. In practice, it is hard to find a nice expression for geodesics on an arbitrary surface.

On a surface $\vec{S}(r, \theta) = (x(r, \theta), y(r, \theta), z(r, \theta))$ parameterized in geodesic polar coordinates, the circle of fixed radius r_0 centered at the origin is

$$\vec{\gamma}(\theta) = (x(r_0, \theta), y(r_0, \theta), z(r_0, \theta)).$$

Its circumference is given by the familiar arc length integral

$$\int_0^{2\pi} \|\vec{\gamma}'(\theta)\|\,d\theta = \int_0^{2\pi} \sqrt{\left(\frac{\partial}{\partial\theta}x(r_0,\theta)\right)^2 + \left(\frac{\partial}{\partial\theta}y(r_0,\theta)\right)^2 + \left(\frac{\partial}{\partial\theta}z(r_0,\theta)\right)^2}\,d\theta$$
$$= \int_0^{2\pi} \sqrt{\frac{\partial}{\partial\theta}\vec{S}(r_0,\theta)\cdot\frac{\partial}{\partial\theta}\vec{S}(r_0,\theta)}\,d\theta.$$

Letting r vary and defining $\vec{S}_\theta(r,\theta) = \frac{\partial}{\partial\theta}\vec{S}(r,\theta)$, we can write the circumference of a circle of radius r as

$$\int_0^{2\pi} \sqrt{\vec{S}_\theta(r,\theta)\cdot\vec{S}_\theta(r,\theta)}\,d\theta.$$

This gives

$$\Pi(r) = \frac{1}{2r}\int_0^{2\pi} \sqrt{\vec{S}_\theta(r,\theta)\cdot\vec{S}_\theta(r,\theta)}\,d\theta.$$

If $\|\vec{S}_\theta(r,\theta)\| > 1$ for $0 \le \theta \le 2\pi$, then $\Pi(r) > \pi$, which cannot happen in our original surface of revolution setting. Also, on surfaces of revolution, the circles centered at the origin are circles in $\mathbb{R}^3$, while on an arbitrary surface, it may be that they are only circles in the context of the surface. Thought of as curves in $\mathbb{R}^3$, they may be quite wavy, like the edge of a potato chip.

In geodesic polar coordinates, if we know the dot product $\vec{S}_\theta(r,\theta)\cdot\vec{S}_\theta(r,\theta)$ for all r and θ, we actually know how to measure arc length on the surface, as seen in the following lemma.

LEMMA. *Let $\vec{S}(r,\theta)$ be a twice-differentiable surface parameterized in geodesic polar coordinates and let $\vec{\gamma}(t) = S(\rho(t),\tau(t))$ be a curve on the surface with $\rho(t)$ and $\tau(t)$ both twice-differentiable. Then the arc length of $\vec{\gamma}(t)$ from $t = a$ to $t = b$ is*

$$\int_a^b \sqrt{(\rho'(t))^2 + (\vec{S}_\theta(\rho(t),\tau(t))\cdot\vec{S}_\theta(\rho(t),\tau(t)))(\tau'(t))^2}\,dt.$$

Proof. To measure the length of the curve $\vec{\gamma}(t) = S(\rho(t),\tau(t))$, we need to integrate $\|\vec{\gamma}'(t)\| = \|\vec{S}_r(\rho(t),\tau(t))\rho'(t) + \vec{S}_\theta(\rho(t),\tau(t))\tau'(t)\|$, where $\vec{S}_r(r,\theta) = \frac{\partial}{\partial r}\vec{S}(r,\theta)$. We have

$$\|\vec{\gamma}'(t)\|^2 = \vec{S}_r(\rho(t),\tau(t))\cdot\vec{S}_r(\rho(t),\tau(t))(\rho'(t))^2$$
$$+ 2\vec{S}_r(\rho(t),\tau(t))\cdot\vec{S}_\theta(\rho(t),\tau(t))\rho'(t)\tau'(t)$$
$$+ \vec{S}_\theta(\rho(t),\tau(t))\cdot\vec{S}_\theta(\rho(t),\tau(t))(\tau'(t))^2.$$

Since the θ and r directions are perpendicular to each other in geodesic polar coordinates, just as they are in polar coordinates in the plane, we have $\vec{S}_r(\rho(t),\tau(t))\cdot\vec{S}_\theta(\rho(t),\tau(t)) = 0$. Since r measures distance on the surface in geodesic polar coordinates, a curve with constant θ is parameterized by arc length, so $\vec{S}_r(\rho(t),\tau(t))\cdot\vec{S}_r(\rho(t),\tau(t)) = 1$. Thus the arc length of $\vec{\gamma}(t)$ from $t = a$ to $t = b$ is

$$\int_a^b \sqrt{(\rho'(t))^2 + (\vec{S}_\theta(\rho(t),\tau(t))\cdot\vec{S}_\theta(\rho(t),\tau(t)))(\tau'(t))^2}\,dt.$$ ∎

In the special case of a circle with $\rho(t) = r_0$, where r_0 is constant, and $\tau(t) = t$, this integral reduces to our previous calculation of the circumference of a circle of radius r_0.

Thus, to measure distance on a surface $\vec{S}(r, \theta)$ in geodesic polar coordinates, we do not need to know $\vec{S}(r, \theta)$; we just need to know $\vec{S}_\theta(r, \theta) \cdot \vec{S}_\theta(r, \theta)$. This fundamental quantity deserves a shorter name, so we will follow many differential geometry texts and let $G(r, \theta) = \vec{S}_\theta(r, \theta) \cdot \vec{S}_\theta(r, \theta)$. (Other texts use g_{22}, or, if θ is the first variable rather than the second, g_{11}. For further information about this quantity, see the section on the *first fundamental form* in any standard differential geometry text, such as [**2**],[**4**], [**6**], or [**9**].)

If we do not need $\vec{S}(r, \theta)$ to measure distance, perhaps we can dispense with the surface altogether. We can stay in the (r, θ)-plane and choose a function $G(r, \theta)$ to define the way we measure distance. Specifically, we define the distance along the curve $\vec{\gamma}(t) = (\rho(t), \tau(t))$ between the points $\vec{\gamma}(a)$ and $\vec{\gamma}(b)$ to be

$$\int_a^b \sqrt{(\rho'(t))^2 + G(\rho(t), \tau(t))(\tau'(t))^2}\, dt.$$

If we take this bold step, we have created a *Riemannian manifold of dimension 2*, which we may think of as a two-dimensional space with a *metric*—a rule for measuring arc length. For technical details, see DoCarmo [**4**, Section 5-10].

We will start with a simple example by letting $G(r, \theta) = r^2$. The distance along the curve $\vec{\gamma}(t) = (t, 0)$ from $\vec{\gamma}(0) = (0, 0)$ to $\vec{\gamma}(3) = (3, 0)$ is $\int_0^3 \sqrt{1^2 + t^2 0^2}\, dt = 3$. We seem not to have done anything new yet, since the distance from $(0, 0)$ to $(3, 0)$ along this curve in the Euclidean plane is also 3. But the distance along the curve $\vec{\gamma}(t) = (3, t)$ from $\vec{\gamma}(0) = (3, 0)$ to $\vec{\gamma}(2\pi) = (3, 2\pi)$ is $\int_0^{2\pi} \sqrt{0^2 + 3^2 1^2}\, dt = 6\pi$. In contrast, in the Euclidean plane, the distance from $(3, 0)$ to $(3, 2\pi)$ along this curve is only 2π. In general, if $G(r, \theta) = r^2$, we measure distance along $\gamma(t)$ with $\int_a^b \sqrt{(\rho'(t))^2 + (\rho(t))^2(\tau'(t))^2}\, dt$. This is exactly the arc length integral for curves in polar coordinates in the plane. (Most calculus texts give this integral only in the special case $\vec{\gamma}(t) = (\rho(t), t)$.) If we think of the plane in polar coordinates as the surface $\vec{S}(r, \theta) = (r\cos(\theta), r\sin(\theta), 0)$, we do get $\vec{S}_\theta(r, \theta) \cdot \vec{S}_\theta(r, \theta) = r^2$.

Now we can try $G(r, \theta) = \sin^2(r)$ with $\vec{\gamma}(t) = (\rho, t)$, where ρ is constant and $0 < \rho < \pi$. Then the distance along $\vec{\gamma}$ from $\vec{\gamma}(0) = (\rho, 0)$ to $\vec{\gamma}(2\pi) = (\rho, 2\pi)$ is $\int_0^{2\pi} \sqrt{0^2 + \sin^2(\rho) 1^2}\, dt = 2\pi \sin(\rho)$. If we allow $\rho = \pi$, we get a strange result: The distance is 0. To make sense of this, notice that $G(r, \theta)$ is $\vec{S}_\theta(r, \theta) \cdot \vec{S}_\theta(r, \theta)$ for $\vec{S}(r, \theta) = (1 - \cos(r), \sin(r)\cos(\theta), \sin(r)\sin(\theta))$, the parameterization of the unit sphere given before Theorem 1, and that $2\pi \sin(\rho)$ is the circumference of a circle of radius ρ on this sphere. By introducing $G(r, \theta) = \sin^2(r)$, we can stay in (r, θ)-space and yet measure distance as if we were on a sphere in $\mathbb{R}^3$.

These two examples correspond to familiar surfaces, but we need not restrict ourselves to what we already know. We can choose, say, $G(r, \theta) = 4r^2$ and measure whatever distances we like in this Riemannian manifold without thinking about a corresponding surface in $\mathbb{R}^3$. As we saw in the previous example, the analog of the circumference of a circle with radius ρ is the length of the curve $\vec{\gamma}(t) = (\rho, t)$ from $\vec{\gamma}(0)$ to $\vec{\gamma}(2\pi)$. In this case, the curve length is $\int_0^{2\pi} \sqrt{4\rho^2}\, dt = 4\pi\rho$, which is twice the circumference of a circle with radius ρ in the Euclidean plane.

Once we move to Riemannian manifolds, the inverse problem of starting with a pi function and creating a corresponding manifold becomes much easier. We define $\Pi(r) = (\frac{1}{2r}) \int_0^{2\pi} \sqrt{G(r, \theta)}\, d\theta$ for $r > 0$, where $\int_0^{2\pi} \sqrt{G(r, \theta)}\, d\theta$ is the Riemannian manifold version of circumference. If we want the analog of a surface of revolu-

tion, we can require $G(r, \theta)$ to depend only on r and not on θ. In this case, we have $\int_0^{2\pi} \sqrt{G(r)}\, d\theta = \sqrt{G(r)} \int_0^{2\pi} d\theta = 2\pi\sqrt{G(r)}$. Thus, if we choose any positive differentiable function $\Pi(r)$, we can find the corresponding $G(r) = (r\Pi(r)/\pi)^2$. This gives us the following theorem.

THEOREM 2. *Given any positive differentiable function $g(r)$ defined for $r \geq 0$, the Riemannian manifold of dimension 2 given by $G(r) = (rg(r)/\pi)^2$ satisfies $\Pi(r) = g(r)$ for $r > 0$.*

As we have noted, we can define a Riemannian manifold without worrying about whether it corresponds to a surface in $\mathbb{R}^3$. Still, it would be nice to know when a Riemannian manifold does correspond to a surface in $\mathbb{R}^3$. Theorem 1 says that if $g(r)$ is also twice differentiable and satisfies $|\frac{d}{dr} rg(r)| \leq \pi$, then the Riemannian manifold in Theorem 2 does correspond to a surface of revolution. Furthermore, under slightly more restrictive conditions, this becomes an if-and-only-if statement. A straightforward application of a theorem stated in [**5**] and proved more generally in [**7**, Proposition 2.3] tells us the following:

THEOREM 3. *If, in addition, $g(r)$ is twice differentiable and the second derivative is continuous, the Riemannian manifold defined above corresponds to a surface in $\mathbb{R}^3$ if and only if $|\frac{d}{dr} rg(r)| \leq \pi$.*

Thus, the condition that tells us if our Riemannian manifold corresponds to a surface is exactly the condition that allows us to construct the surface of revolution in Theorem 1.

Area and future work

In the Euclidean plane, the circumference of a circle is $2\pi r$. The area of a circle is $\int_0^r 2\pi u\, du = \pi r^2$. What happens when we look at area on surfaces of revolution and on Riemannian manifolds? Is the area of a circle $\Pi(r)r^2$?

On surfaces of revolution generated by curves parameterized by arc length, the area of a circle of radius r centered at the origin is $2\pi \int_0^r y(u)\, du$. Now $\Pi(r)r^2 = \pi y(r)r$, so we want to know if $2\pi \int_0^r y(u)\, du = \pi y(r)r$. By differentiating both sides and canceling the π, we get $2y(r) = y'(r)r + y(r)$, which gives us the differential equation $y(r) = y'(r)r$. By using separation of variables and the restrictions $y(r) \geq 0$ and $|y'(r)| \leq 1$, we get $y(r) = ar$ for an arbitrary constant $0 \leq a \leq 1$. This means that our curve is a line and our surface of revolution is a cone ($a < 1$) or a plane ($a = 1$).

Thus, it is not generally true that the area of a circle on a surface of revolution is $\Pi(r)r^2$. So we define Π_A to be the ratio of the area enclosed by a circle on a surface and the square of its radius as measured on the surface. That is,

$$\Pi_A(r) = 2\pi \frac{\int_0^r y(u)\, du}{r^2}.$$

To understand the relationship between Π_A and Π, we consider their ratio

$$\frac{\Pi_A(r)}{\Pi(r)} = 2\frac{\int_0^r y(u)\, du}{ry(r)}.$$

Notice that $ry(r)$ is the crude one-rectangle Riemann sum approximation of the integral $\int_0^r y(u)\, du$. This means that $\Pi_A(r) \geq \Pi(r)$ if and only if the area $\int_0^r y(u)\, du$ is at least half the area of this rectangle.

The function $\Pi_A(r)$ has some of the same properties as $\Pi(r)$, and the reader may wish to explore further. Beckenbach [**3**] shows that on surfaces of non-positive Gaussian curvature, $\Pi(r) \geq \pi$ and $\Pi_A(r) \geq \pi$, while on surfaces of non-negative Gaussian curvature, $\Pi(r) \leq \pi$ and $\Pi_A(r) \leq \pi$. We would particularly like to know more about how the relationship between $\Pi(r)$ and $\Pi_A(r)$ changes if we consider manifolds with density, as described in [**8**].

Acknowledgments Thanks to Paul Zorn, Steve Lovett, and David Henderson for their advice on earlier versions of this paper. Thanks to the anonymous referees, particularly the one who introduced us to references [**3**] and [**5**] and proposed Theorem 3. These and other suggestions significantly improved this article.

REFERENCES

1. Robert N. Andersen, Justin Stumpf, and Julie Tiller, Let π be 3, *Math. Mag.* **76** (2003) 225–231. http://dx.doi.org/10.2307/3219328
2. Thomas Banchoff and Stephen Lovett, *Differential Geometry of Curves and Surfaces*, A. K. Peters, Natick, MA, 2010.
3. E. F. Beckenbach, Some convexity properties of surfaces of negative curvature, *Amer. Math. Monthly* **55** (1948) 285–301. http://dx.doi.org/10.2307/2305479
4. Manfredo P. DoCarmo, *Differential Geometry of Curves and Surfaces*, Prentice Hall, Englewood Cliffs, NJ, 1976.
5. Martin Engman, A note on isometric embeddings of surfaces of revolution, *Amer. Math. Monthly* **111** (2004) 251–255. http://dx.doi.org/10.2307/4145134
6. David Henderson, *Differential Geometry: A Geometric Introduction*, Prentice Hall, Upper Saddle River, NJ, 1998.
7. Andrew D. Hwang, A symplectic look at surfaces of revolution, *Enseign. Math.* **49** (2003) 157–172.
8. Frank Morgan, Manifolds with density and Perelman's proof of the Poincaré conjecture, *Amer. Math. Monthly* **116** (2009) 134–142. http://dx.doi.org/10.4169/193009709X469896
9. Dirk J. Struik, *Differential Geometry*, Addison-Wesley, Reading, MA, 1961.

Summary In the plane, the ratio of the circumference of a circle to its diameter is always π. On a sphere, however, this ratio (which we denote Π) takes on other values, provided the diameter is measured along a great circle on the sphere. In this article, we explore Π as a function of radius on surfaces of revolution. We also consider the inverse problem—we begin with a function and, under certain conditions, find a surface or Riemannian manifold with Π equal to that function.

JUSTIN T. SCHULTZ is a graduate student in the Institute of Optics at the University of Rochester, and is supported by an NSF Graduate Research Fellowship. He received his Bachelors in 2008 from Juniata College in Physics and Mathematics. As a Fulbright Scholar at the Australian National University, he studied Bose-Einstein condensates (BECs)—a quantum state of matter close to absolute zero. He currently studies quantum optics and topological spin textures in spinor BECs. A feline aficionado, Justin's interests include long-distance cycling, lasers, Scotch, and irrational numbers.

CATHERINE STENSON is professor of mathematics at Juniata College, where she has advised many undergraduate research students. She received her Ph.D. from Cornell University under the direction of Louis J. Billera. She enjoys gardening, choral music, and traveling with her family.

Feedback, Control, and the Distribution of Prime Numbers

SUSAN H. MARSHALL
Monmouth University
West Long Branch, NJ 07764-1898
smarshal@monmouth.edu

DONALD R. SMITH
Monmouth University
West Long Branch, NJ 07764-1898

We explore the system of prime numbers from an unusual viewpoint, that of an applied mathematician employing mathematical modeling to study a natural phenomenon. We liken the prime numbers to a physical system that can be empirically observed and, based on our observations, we derive a mathematical model in the form of a differential equation to describe the system:

$$f'(x) = \frac{-f(x)f(\sqrt{x})}{2x}, \tag{1}$$

where $f(x)$ represents the "density of primes at x." The model predicts well-known results concerning the distribution of prime numbers and has been discovered at least twice previously. The model seems to have been forgotten by the number theory community, but the distribution of primes is mentioned as an application in the differential equation literature. (See, for example, [**7**, p. 237] or [**16**].) We endeavor to contribute a deeper understanding of the connection between equation (1) and number theory using the framework of feedback and control, a field within engineering.

Lord Cherwell, a prominent British physicist and scientific advisor to Churchill during World War II, discovered equation (1) in the context of prime numbers in about 1942. Cherwell did not publish his finding, but shared it with British mathematician and number theorist E. M. Wright. This led Wright to study a class of differential equations related to (1) in a series of papers spanning a decade [**19, 20, 21, 22, 23, 24**]. In the final paper of this series, Wright credits Cherwell with introducing him to the equations but does not explain how they are derived from number-theoretic concerns [**24**, p. 66].

Another discovery was made by G. Hoffman de Visme, a British electrical engineer, who published his work in a 1961 note in the *Mathematical Gazette* [**12**]. Somewhat fortuitously, this note was sent to Wright to referee, and in the next volume of the *Gazette* appears a note by Wright [**25**] discussing Cherwell's contribution as well as some of Wright's own work on the differential equation. Wright also recounts the story in his 1988 retrospective of his friendship and collaboration with Cherwell [**26**].

The repeated discoveries—all by applied mathematicians with a side interest in number theory—reveal that there is something quite natural about this approach, given the right perspective. The system of prime numbers exhibits randomness combined with deep structure. We propose that this can be understood by viewing the primes as a feedback and control system. We do not know whether Cherwell or Hoffman de Visme viewed the primes in this way; however, their derivation of equation (1) is essentially the same as ours.

Math. Mag. **86** (2013) 189–203. doi:10.4169/math.mag.86.3.189.

Both Cherwell and Hoffman de Visme sought to use the model to explain why the prime number theorem holds. Wright's technical work on the differential equation is instrumental in seeing how the model predicts this famous theorem. Using Wright's work, we are also able to show that the model predicts a surprising result due to Littlewood. Both of these results require sophisticated techniques of proof. The model provides insight into why they follow from simple observations of the system of primes.

On the other hand, the model has limitations. As in any modeling process, we make simplifying assumptions about our system. For example, although the prime numbers are clearly a discrete phenomenon, we assume a smooth version of their density function so that we can use the tools of calculus. Moreover, the element of randomness within the system of prime numbers is not directly incorporated into our model. (Instead we consider "perturbed" solutions, a technique borrowed from physics.) The model does not capture all aspects of the system; for example, some implications of the model are in conflict with the Riemann Hypothesis. We explore these limitations further in the final section of this paper. Despite these limitations, the model appears to give at least a first-order understanding of the system of primes.

Feedback and control systems

A system that uses measurements of its own behavior to adjust its future behavior is a *feedback and control system*.

For example, consider the system of a car and driver. As the driver notices that she is too far to the right, she steers left, in an attempt to keep the car on track. The driver is constantly encountering small "perturbations" (such as a pebble in the road) and we can imagine different reactions as the driver attempts to steer back to the ideal path:

- **Cool, calm, and collected:** This driver gets closer and closer to the line without actually crossing it.
- **Whimsical:** This driver crosses the line before she is able to steer back, and then repeatedly crosses the line in such a way that the distance from the line in successive crossings becomes smaller and smaller.
- **Panicky and Overreacting:** This driver also crosses the line before she is able to steer back, but then overreacts and yanks the wheel back and forth successively more violently. The successive crossings go farther and farther from the line.

Other reactions of the driver are possible, but the reactions listed above represent some typical behaviors of feedback and control systems. For example, a well-designed and maintained car suspension hitting a bump in the road behaves like our cool, calm, and collected driver, while a car with worn shocks resembles our whimsical driver. The panicky and overreacting driver is represented in examples such as the Tacoma Narrows Bridge that collapsed in 1940, or the audio feedback we hear when a microphone gets too close to a speaker.

In our examples, we focused on the reaction of a driver to a single perturbation, even though an actual car is constantly bombarded by random, small changes. Despite the unpredictability of these perturbations, we claim that knowledge of the reaction to just one perturbation is enough to predict at least large-scale behavior of the system. For some systems, like the cool, calm, and collected driver or the whimsical driver, perturbations tend to die out, so that only the most recent perturbations affect the path and their cumulative effect is bounded. For other systems, such as the panicky and overreacting driver, perturbations result in explosively growing behavior that eventually

overwhelms other factors. Wild oscillations are inevitable, even if we cannot predict their exact magnitude or when they will occur.

Mathematically, feedback and control systems are often modeled as differential equations, sometimes involving delay (when time is needed to incorporate the feedback into the system). The solutions of the differential equations tell us about the nature of the system. For example, a solution might be of the form $f(t) = e^{\lambda t}$, where $\lambda = a + bi$ is a complex number and t is a real variable. This function can be written as

$$f(t) = e^{\lambda t} = e^{at}(\cos bt + i \sin bt).$$

When λ is real (that is, $b = 0$), the complex exponential degenerates to a real exponential. If b is nonzero, then the trigonometric functions lead to oscillatory behavior. Various choices for a and b lead to the typical behaviors for our car and driver, where we view $f(t) = 0$ as the ideal path. FIGURE 1 shows these behaviors.

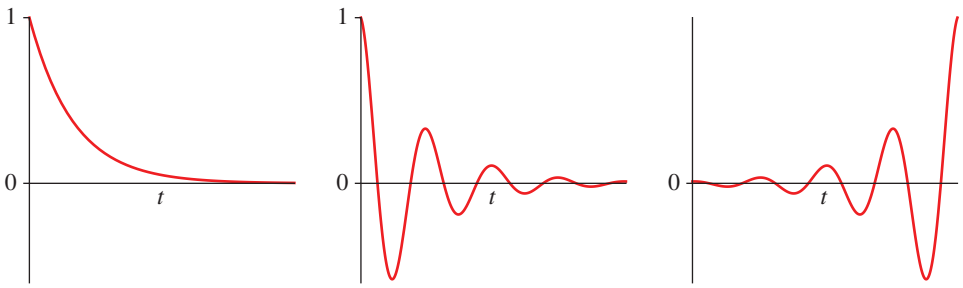

(a) $a < 0, b = 0$
Cool, calm, and collected

(b) $a < 0, b \neq 0$
Whimsical

(c) $a > 0, b \neq 0$
Panicky and overreacting

Figure 1 Typical solutions to feedback and control systems

Primes as a feedback and control system

Why would we suspect the primes of being a feedback and control system? Systems that are subject to randomness do not stay on track without some kind of feedback and control mechanism. When a car stays on the road despite many random perturbations, it is reasonable to infer that there is a driver making corrections.

The distribution of the prime numbers appears to have an element of randomness. Yet, the primes do "stay on track" in a very specific way. Gauss observed around 1792 that the density of primes appears to be inversely proportional to the natural logarithm (see, for example, [**8**, pp. 2–3] or [**18**]). The evidence is quite striking. Gauss tabulated the number of primes in intervals of length 1000, called *chiliads*, and if we plot the average density of the primes in successive chiliads, a beautiful logarithmic shape emerges. In FIGURE 2, the data points are connected and graphed against the function $1/\ln x$. We can see the feedback and control, as the actual density of primes in these intervals jumps above and below the ideal path line of $1/\ln x$.

Gauss's estimate for the density of primes can be used to obtain an approximation for the total number of primes less than or equal to x, traditionally denoted $\pi(x)$. A first approximation is found by simply multiplying by x and comparing $\pi(x)$ to $x/\ln x$. A more sophisticated approximation is found by integrating to obtain the *logarithmic integral*,

$$\mathrm{Li}(x) := \int_2^x \frac{1}{\ln t}\, dt.$$

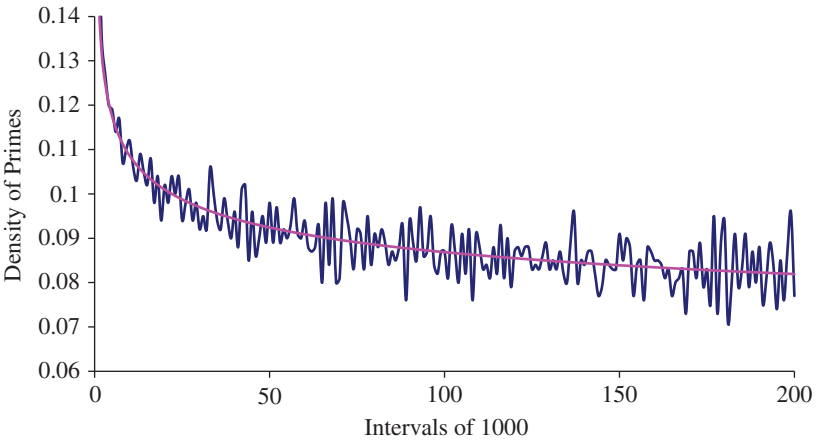

Figure 2 Average density of primes in successive chiliads versus $1/\ln x$

As seen in TABLE 1, these estimates compare favorably to the actual number of primes, with $\mathrm{Li}(x)$ faring a bit better.

TABLE 1: The total number of primes compared to Gauss's estimates

x	$\pi(x)$	$x/\ln x$	$\mathrm{Li}(x)$
10	4	4.3	6.2
10^2	25	21.7	30.1
10^3	168	144.8	177.6
10^4	1 229	1 085.7	1 246.1
10^5	9 592	8 685.9	9 629.8
10^6	78 498	72 382.4	78 627.6
10^7	664 579	620 420.7	664 918.4
10^8	5 761 455	5 428 681.0	5 762 209.4
10^9	50 847 534	48 254 942.4	50 849 235.0
10^{10}	455 052 511	434 294 481.9	455 055 614.6

A century after Gauss's observations, it was shown that both of these estimates are "good" in the sense that their relative errors,

$$\frac{\pi(x) - x/\ln x}{\pi(x)} \quad \text{and} \quad \frac{\pi(x) - \mathrm{Li}(x)}{\pi(x)},$$

both tend to 0 as $x \to \infty$. This relationship is described by saying that these functions are *asymptotic* to one another, written symbolically as $\pi(x) \sim x/\ln x \sim \mathrm{Li}(x)$. This connection between the primes and the natural logarithm is known as the *prime number theorem*. We prefer to state the theorem in terms of the density of primes. The

relationship $\pi(x) \sim x/\ln x$ implies that the average density $\pi(x)/x$ is asymptotic to $1/\ln x$.

THE PRIME NUMBER THEOREM. *Let $x > 0$ be a real number. The average density of primes less than x is asymptotic to $1/\ln x$.*

The absolute error, $\pi(x) - \mathrm{Li}(x)$, behaves rather differently than the relative error. Despite numerical evidence showing $\mathrm{Li}(x)$ as an overestimate for $\pi(x)$, Littlewood [**15**] proved in 1914 that the difference between $\pi(x)$ and $\mathrm{Li}(x)$ changes sign infinitely often. (In fact, all current numerical evidence shows $\mathrm{Li}(x)$ as an overestimate [**14**].) More precisely, he showed the existence of a positive constant k such that we can find arbitrarily large values of x that satisfy

$$\pi(x) - \mathrm{Li}(x) > \frac{k\sqrt{x}\,\ln\ln\ln x}{\ln x} \tag{2}$$

and arbitrarily large values of x that satisfy

$$\pi(x) - \mathrm{Li}(x) < \frac{-k\sqrt{x}\,\ln\ln\ln x}{\ln x}. \tag{3}$$

The function on the right side of (2) is increasing (slowly) for all sufficiently large positive values of x. Thus, Littlewood's theorem tells us not only that the difference changes sign infinitely often, but it also indicates that there are arbitrarily large oscillations between the values of the two functions.

LITTLEWOOD'S THEOREM. *The absolute value of $\pi(x) - \mathrm{Li}(x)$ is unbounded and the sign of $\pi(x) - \mathrm{Li}(x)$ changes infinitely often.*

The apparent randomness of the primes, coupled with the strong structure implied by both the prime number theorem and Littlewood's theorem, suggest a feedback and control mechanism at work. Furthermore, the behavior of the primes fits the pattern of typical feedback and control systems, reinforcing the idea that the primes are governed by feedback and control. The density of primes behaves like the driver who gets successively closer to the ideal path line $1/\ln x$. However, when we consider the difference between the total number of primes and *its* ideal path line $\mathrm{Li}(x)$, Littlewood's theorem is reminiscent of our panicky and overreacting driver.

Modeling the feedback

We would like to understand how the feedback and control mechanism of the primes works, in order to model it. What is it about the system of prime numbers that seems to notice that the density of primes is "off-track" and steers it back? The essential idea is this: "*Too many" primes in one interval tend to decrease the likelihood of primes in higher intervals while "too few" increase the likelihood of future primes*.

The *sieve of Eratosthenes* illustrates this intuitive idea of feedback. The sieve is a tool for finding prime numbers less than a given number. It begins with a list of candidate primes, $\{2, 3, 4, \ldots\}$. At each iteration, the smallest number p on the list that is not yet marked prime must be prime, since it cannot be written as a multiple of numbers smaller than it. We mark p as prime. Then, we remove all larger multiples of p from the list, and move on to the next iteration.

When we begin the sieving process, we consider all numbers as potentially prime. When we remove the multiples of a prime p, we decrease the density of potential primes. Since this process removes $1/p$ of the remaining potential primes, it changes

the density by a factor of $1 - 1/p$. For example, sieving by $p = 2$ removes the even composite numbers and decreases the density of potential primes by $1/2$, and then sieving by $p = 3$ reduces the density by an additional $1/3$. Furthermore, a prime p only begins to affect the density of primes after its square, since smaller multiples of p have been removed at earlier iterations of the sieve.

Armed with these observations, we are now ready to derive a differential equation to model the density of primes at x. Let $f(x)$ be a differentiable function that approximates the density of primes, in the sense that it satisfies the properties we discovered from the sieve of Eratosthenes. The function $f(x)$ should be interpreted as a point density rather than an average density—that is, it approximates the density of primes in the immediate neighborhood of x, not the cumulative density in the interval from 2 to x.

To derive the differential equation, we will estimate the change in our density function over a certain interval in two different ways. One of the key facts we learned from the sieve of Eratosthenes is that a prime begins to affect the density only after its square. Thus, we consider the following two intervals.

- **Interval A** is the interval on the real line given by endpoints x and $x + \mathrm{d}x$.
- **Interval B** is the square of Interval A, and thus has endpoints x^2 and $(x + \mathrm{d}x)^2$.

As usual, the quantity $\mathrm{d}x$ is meant to be an infinitesimal quantity, or at least very small compared to x. We will estimate the change in density on Interval B; that is, we will approximate the quantity $f\big((x + \mathrm{d}x)^2\big) - f(x^2)$.

We consider only the effect of primes from Interval A on the density along Interval B. Each prime in Interval A changes the density on Interval B by a factor of approximately $1 - 1/x$, since all primes in the small Interval A are roughly of size x. Thus, each prime subtracts $f(x^2)/x$ from the density. There are about $f(x)\mathrm{d}x$ primes in Interval A, and so our first approximation of the change in density on Interval B is

$$f\big((x + \mathrm{d}x)^2\big) - f(x^2) \approx \frac{-f(x^2)f(x)\mathrm{d}x}{x}. \tag{4}$$

We can also estimate the change in density on Interval B using derivatives. The change in density is approximately the derivative of f at x^2 multiplied by the length of Interval B. The length of the interval is $(x + \mathrm{d}x)^2 - x^2 = 2x\,\mathrm{d}x + (\mathrm{d}x)^2$. We may safely ignore the second-order term, and our second approximation of the change in density on Interval B is

$$f\big((x + \mathrm{d}x)^2\big) - f(x^2) \approx f'(x^2) \cdot 2x\,\mathrm{d}x. \tag{5}$$

We equate the right-hand sides of (4) and (5), and solve for the derivative to find

$$f'(x^2) = \frac{-f(x^2)f(x)}{2x^2}.$$

Changing variables so that our equation is in terms of x, we recover equation (1) from the introduction:

$$f'(x) = \frac{-f(x)f(\sqrt{x})}{2x}.$$

This equation is our model of the system of primes. The function $f(x)$ represents the density of primes at x and we clearly see the dependence of the change in density on the density at x, the density at $\sqrt{x}$, and on x itself.

As mentioned in the introduction, a previous derivation of the above differential equation was given by G. Hoffman de Visme in 1961 [**12**]. Mathematically, his derivation is essentially the same as ours, yet his is often described as "probabilistic" in the literature. The term probabilistic arises because we can think of the density correction factor $1 - 1/p$ as a probability, namely the probability that a number is not divisible by the prime p.

The prime number theorem

> *Proofs of the prime number theorem are extremely hard to follow, and leave the impression, at least among amateurs, that the essential property of prime numbers, namely their primeness, plays very little part in the argument.*
>
> —G. Hoffman de Visme (1961)

An intuitive justification of the prime number theorem was the motivation for Hoffman de Visme's work. His thoughts are summarized in the first sentence of his *Gazette* article (quoted above) and Wright attributes this motivation to Cherwell's work as well [**25**]. The original proofs of the prime number theorem, independently given by Hadamard and de la Vallée-Poussin in 1896, were inspired by Riemann's famous memoir of 1859 and involved complex analysis and the Riemann zeta-function. Even among nonamateurs, the complex-analytic proofs of this theorem were unsatisfying and an "elementary" (not to be confused with easy) proof was sought. Success came with the work of Erdős [**9**] and Selberg [**17**], who gave independent elementary proofs in 1949. (For an historical survey of these achievements, see [**1, 10**].) Our modeling approach illuminates the prime number theorem from yet another angle.

The prime number theorem tells us that the average density of primes less than x is asymptotic to the function $1/\ln x$. The relationship $\pi(x) \sim \mathrm{Li}(x)$ suggests that the density *at* x is also asymptotic to $1/\ln x$. (The computations with Gauss's chiliads illustrated in FIGURE 2 further support this assertion.) Thus, we expect $f(x) = 1/\ln x$ to be a solution to our differential equation (1). A quick computation shows, in fact, that it is.

To fully validate our model against the prime number theorem, however, we need to go a bit further. We do not expect that the true density of primes is *equal* to $1/\ln x$—rather, we expect $1/\ln x$ to be the *ideal path* of the true density. If this density gets off-track, we want to know that the feedback and control mechanism brings it back on course. From a differential equation point of view, we must show that the solution $1/\ln x$ is stable under perturbations.

In the system of prime numbers, a perturbation is the random appearance (or nonappearance) of a prime that may cause the density to deviate from $1/\ln x$. We want to understand what happens after this perturbation—does our model predict that the density will return to $1/\ln x$? To analyze this mathematically, we consider "perturbed solutions" of our model differential equation (1). That is, we consider a function $f(x)$ that satisfies $f(x) = 1/\ln x$ initially, up to some value $x = x_0$, and then jumps arbitrarily to some other value $f(x_0) \neq 1/\ln(x_0)$ as the result of a single perturbation. Afterward, for $x > x_0$, the behavior of $f(x)$ is governed by (1). If $f(x)$ returns to its path as x increases—that is, if the relative error between $f(x)$ and $1/\ln x$ is eventually negligible—then the solution $1/\ln x$ is said to be *stable under perturbations*.

Since the true density of primes is represented by a perturbed solution $f(x)$, the stability of $1/\ln x$ will also predict the prime number theorem and validate our model against empirical evidence. Relying on Wright, we will compute the limit of the

relative error,

$$\lim_{x\to\infty} \frac{f(x) - 1/\ln x}{1/\ln x}, \tag{6}$$

and show that the limit is equal to zero.

To compute the limit in (6), we first make an advantageous change of variables by letting $x = e^{2^u}$ and defining $g(u) = f(e^{2^u})$. This change of variables will have the convenience of relating $g'(u)$ to the value of g at u and $u - 1$, rather than the relation of $f'(x)$ to the value of f at x and $\sqrt{x}$. We provide a roadmap for the computations involved in the change of variables. The only tools required are calculus and algebra (and a pencil and paper), but the details can be safely skipped on a first reading.

Change of variables Let $x = e^{2^u}$ and $g(u) = f(e^{2^u})$. Applying the chain rule to $g(u)$ (twice), we find that

$$g'(u) = (\ln 2)2^u e^{2^u} f'(e^{2^u}). \tag{7}$$

Substituting for the derivative $f'(e^{2^u})$ in (7) using equation (1) and converting back to g-notation, we find a differential equation for g:

$$g'(u) = -(\ln 2)2^{u-1} g(u-1)g(u). \tag{8}$$

Under the change of variables, our ideal solution $1/\ln x$ becomes 2^{-u}, so that the limit (6) we seek to compute transforms as

$$\lim_{u\to\infty} \frac{g(u) - 2^{-u}}{2^{-u}} = 2^u\, g(u) - 1, \tag{9}$$

where $g(u)$ represents a perturbed solution of (8).

The relative error function We let $h(u)$ represent the relative error function appearing in (9), so that

$$h(u) = 2^u g(u) - 1. \tag{10}$$

Our main tool in computing the limit of $h(u)$ as $u \to \infty$ is a differential-delay equation for $h(u)$. To find it, we first differentiate (10) using the product rule,

$$h'(u) = 2^u g'(u) + (\ln 2)2^u g(u). \tag{11}$$

We then substitute for $g'(u)$ in (11) using equation (8) to find

$$\begin{aligned} h'(u) &= -2^u(\ln 2)2^{u-1} g(u-1)g(u) + (\ln 2)2^u g(u) \\ &= -(\ln 2)2^u g(u)\big(2^{u-1} g(u-1) - 1\big). \end{aligned}$$

Converting back to h-notation, we find our differential-delay equation for the relative error:

$$h'(u) = -(\ln 2)\big(h(u) + 1\big)h(u-1). \tag{12}$$

Equation (12) is a particular member in a family of differential-difference equations studied by Wright in his 1955 paper [**24**]. This family of equations bears his name in deference to his contribution to their study.

Computing the limit We now return to our goal of computing the limit (6) of the relative error between a perturbed solution $f(x)$ and our ideal solution $1/\ln x$. In terms of our new variables, we must compute the limit of the relative error function, $h(u)$, given in (10). We assume $h(u) = 0$ initially, up to some value $u = u_0$, and then jumps arbitrarily to a nonzero value $h(u_0)$ as the result of a single perturbation. Afterward, for $u > u_0$, the behavior of $h(u)$ is governed by (12). To show that $1/\ln x$ is stable under perturbations, we must show that the relative error eventually returns to 0; that is, we must show that the limit of $h(u)$ as $u \to \infty$ is 0.

Equation (12) severely restricts the possible values of the limit of $h(u)$ as $u \to \infty$. If $h(u) \to \ell$ for some $\ell \in \mathbb{R}$, then the derivative must be 0 for large u and thus, equation (12) tells us that

$$-(\ln 2)\ell(\ell + 1) = 0.$$

Hence, ℓ must equal either 0 or -1. Given reasonable initial conditions on the interval $-1 \le u \le 0$, Wright shows that equation (12) has a unique, continuous solution [**24**, Thm 1 (i), p. 66] and that the limiting value of h is determined by the value of $h(0)$. If $h(0)$ exceeds -1, then the limit is 0 [**24**, Thm 3, p. 67]. In our change of variables, $x = e^{2^u}$ and so $u = 0$ corresponds to $x = e$. The value $h(0) = -1$ corresponds to $f(e) = 0$. Since $f(x)$ represents a density function, we are in the situation where $h(0) > -1$ and Wright tells us that $h(u) \to 0$ as $u \to \infty$.

Thus, the solution $1/\ln x$ is stable under perturbations. This tells us that the density of prime numbers reacts to a single perturbation like the cool, calm, and collected driver, or like the whimsical driver—smoothly adjusting to the bump in the road and getting back on track to $1/\ln x$. The model predicts the prime number theorem!

Solutions of $h'(u) = -(\ln 2)\big(h(u) + 1\big)h(u - 1)$

Before we turn our attention to Littlewood's theorem, it will be useful to have more information about the unique solution of (12) guaranteed by Wright. Equation (12) is a nonlinear differential-delay equation, and such equations are difficult to solve explicitly. However, we can get the information we need using numerical and asymptotic methods. We have already seen that any solution to (12) eventually tends to 0, but here we will see exactly *how* the solution goes to 0.

Numerical solutions We use a tangent line approximation to obtain a numerical solution to (12). The tangent line approximation at $u = u_0$ is given by

$$\begin{aligned} h(u) &\approx h(u_0) + h'(u_0)(u - u_0) \\ &= h(u_0) - (\ln 2)\big(h(u_0) + 1\big)h(u_0 - 1)(u - u_0), \end{aligned} \tag{13}$$

where we substitute for the derivative $h'(u_0)$ using (12). Knowledge of the values of $h(u)$ on an interval of length one combined with (13) allow us to compute the values of $h(u)$ on the next such interval. In particular, observe that if $h(u) = 0$ on an interval of length one, then (13) tells us that the value will remain 0 on the next such interval. Since $h(u)$ represents the relative error between $f(x)$ and $1/\ln x$, this tells us that once the system is on track, it stays on track!

When the system is perturbed, however, we expect nonzero values for $h(u)$, and thus use a nonzero initial condition to represent a perturbation. We assume that $h(u) = 0$ for $u < -1$ and set $h(-1) = 1$. (Equation (12) is invariant under translations, which means that a perturbation at any value u_0 has the same effect as at any other value of u_0,

just displaced along the u-axis. Therefore, we lose no generality in taking $u_0 = -1$ in what follows.) Tracing back through our change of variables, this represents perturbing $1/\ln x$ by a factor of 2. We then use (13) to determine values of h when $u > -1$. Note that $h(u) = 1$ on the entire interval $-1 \le u \le 0$, since (12) tells us that $h'(u) = 0$ on that interval. FIGURE 3 shows the approximation on the interval $0 \le u \le 9$. (Recall that a u-value of 9 corresponds to an x-value of $e^{2^9} \approx 2.28 \times 10^{222}$.) From the graph in FIGURE 3, we not only see that $h(u) \to 0$ as $u \to \infty$, but we also see *how* $h(u)$ is tending to zero. It looks like our old friend, the whimsical driver! Different initial conditions with $h(0) > -1$ lead to similar approximations.

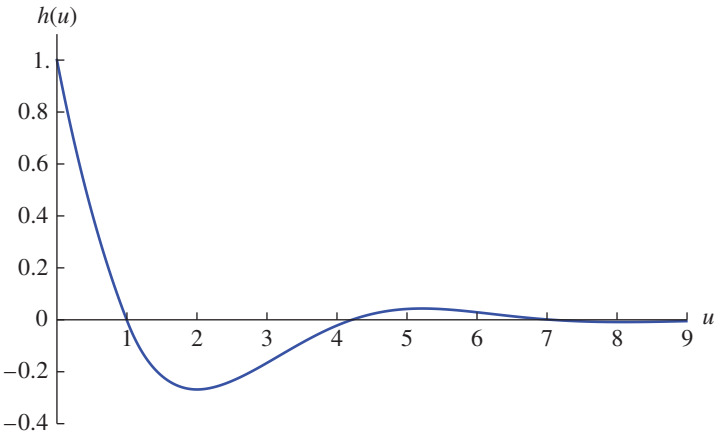

Figure 3 Numerical solution to $h'(u) = -(\ln 2)\big(h(u) + 1\big)h(u - 1)$

Asymptotic solutions Because $h(u) \to 0$ as $u \to \infty$, we expect solutions of (12) will be well approximated, when u is large, by solutions of the associated *linear* differential-delay equation, found by removing the quadratic term of equation (12):

$$h'(u) = -(\ln 2)\, h(u - 1). \tag{14}$$

We have much more hope of finding an explicit solution in the linear case. Indeed, we can find solutions to (14) using a common technique in differential equations. We set $h(u) = Ae^{\omega u}$, where $\omega = a + bi$ is a complex number and substitute this form into (14). Simplifying, we find that solutions of

$$\omega e^{\omega} = -\ln 2 \tag{15}$$

give rise to solutions of (14). Equations such as (15) arise in many applications and have been studied extensively. In particular, Wright studied them in conjunction with equation (12). There are countably many solutions to (15) occurring in conjugate pairs, all of which have negative real part. (See, for example, [**24**, Theorem 5, p. 72].) This is encouraging; the negative real part of ω leads to an exponentially-damped oscillatory solution, matching our numerical data. The solution with the least negative real part is $\omega = -0.5716236091 \pm 1.086461157i$. (This numerical solution was found using the multi-valued complex-valued function, Lambert-W, implemented in Maple. For a nice overview of this function and its many uses, see [**6**].) The corresponding solution to (14) is the most dominant asymptotically, and so we expect that the relative error will resemble this solution in the long run. Indeed, Wright *proved* that any solution to (12) is asymptotic to

$$Ae^{-0.5716236091u} \sin(1.086461157u + B) \tag{16}$$

for appropriate constants A and B (provided $h(0) > -1$) [**24**, Thm 7 and Eqn (6.7) on p. 77 combined with Thm 8 on p. 78]. Equation (16) is graphed in FIGURE 4, with A and B chosen so that $h(0) = 1$, matching the initial condition of the numerical approximation in FIGURE 3.

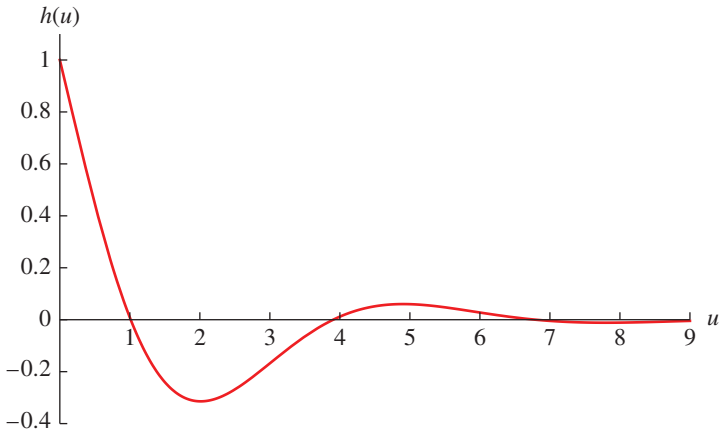

Figure 4 Asymptotic solution to $h'(u) = -(\ln 2)\big(h(u) + 1\big)h(u-1)$

Littlewood's theorem

Armed with more specific information about the relative error $h(u)$, we turn our attention to Littlewood's theorem. In particular, Littlewood's theorem tells us that the difference between $\pi(x)$ and its approximation $\mathrm{Li}(x)$ changes sign infinitely often. The function $\mathrm{Li}(x)$ is defined by integrating $1/\ln x$. The function $\pi(x)$ can similarly be represented as an integral using our model. A solution $f(x)$ to (1) represents the density of primes at x and so $\pi(x)$ is approximated by integrating $f(x)$. Thus,

$$\pi(x) - \mathrm{Li}(x) \approx \int_2^x \big(f(t) - 1/\ln t\big)\,\mathrm{d}t. \tag{17}$$

To study this integral, we apply the previously-used change of variables ($t = e^{2^s}$) and rewrite the integrand in terms of h using equation (10):

$$\begin{aligned}\big(f(t) - 1/\ln t\big)\mathrm{d}t &= (\ln 2)2^s e^{2^s}\big(g(s) - 2^{-s}\big)\,\mathrm{d}s \\ &= (\ln 2)e^{2^s} h(s)\,\mathrm{d}s. \end{aligned}\tag{18}$$

Since h is asymptotic to an exponentially-damped trigonometric function, our approximation to $\pi(x) - \mathrm{Li}(x)$ is (eventually) found by integrating an exponentially-growing trigonometric function. (The double-exponential appearing in (18) will eventually dominate the exponential appearing in (16)). The peaks and troughs of such a function become successively more pronounced, like our overreacting and panicky driver in FIGURE 1c. Now imagine integrating such a function. When we integrate, the negative area of a trough is canceled by a portion of the positive area of the next peak, and vice-versa. Thus, each zero of the integrand will give rise to a sign change of the integral function. The infinitely many zeros of (16) predict infinitely many sign changes of $\pi(x) - \mathrm{Li}(x)$!

Limitations of the model

Thus far, we have seen that our model predicts the prime number theorem and the infinite crossings of Littlewood's theorem. The model agrees with empirical data, at least regarding gross behavior of the system. However, this section will illustrate the need for caution in using the model to predict the finer details of the distribution of primes.

In the last section, we saw that each zero of $h(u)$ gives rise to a zero of $\pi(x) - \mathrm{Li}(x)$. The asymptotic form of $h(u)$ given in (16) tells us that there are infinitely many such zeros. The specific frequency and period of the trigonometric function in (16) allow us to deduce more precise information. For example, the specific frequency, along with a change back to the variable x, predicts that the number of sign changes of $\pi(x) - \mathrm{Li}(x)$ on the interval $(2, x)$ is at least

$$\frac{1.086461157u}{\pi} = \frac{1.086461157 \ln\ln x}{\pi \ln 2} \approx \frac{1}{2} \ln\ln x. \tag{19}$$

We expect (19) to be a lower bound for the number of sign changes, as the random nature of the system may lead to several sign changes in the area of a single sign change predicted by the continuous model. Indeed, Kaczorowski [**13**] proved in 1985 that, for x sufficiently large, the number of sign changes of $\pi(x) - \mathrm{Li}(x)$ on $(2, x)$ is at least $c \ln x$, for some positive constant c. Thus, our model is predicting fewer sign changes than what is currently known. Despite knowing that there are infinitely many sign changes between $\pi(x)$ and $\mathrm{Li}(x)$, no one yet knows where the first one occurs. (Currently, the best result is that the first sign change occurs for some $x < 1.39 \times 10^{316}$ [**2, 4**].) Without numerical data regarding actual sign changes, we cannot confirm that the discrepancy between our bound and that of Kaczorowski can be explained by random sign changes clustered about a single sign change predicted by the model.

Littlewood's theorem includes more information than just the infinitely many sign changes of $\pi(x) - \mathrm{Li}(x)$. Littlewood gave precise information concerning how much $\pi(x) - \mathrm{Li}(x)$ differs from zero, in the form of functional bounds found in inequalities (2) and (3). Our model gives a similar result. Using the exact form of the solution to $h(u)$ in (16), we can estimate the integral in (17) at specific x-values, which in turn allows us to estimate $\pi(x) - \mathrm{Li}(x)$. For arbitrarily small $\epsilon > 0$, the model predicts the existence of a positive constant k_ϵ such that we can find arbitrarily large values of x that satisfy

$$\pi(x) - \mathrm{Li}(x) > k_\epsilon x^{2^{-\epsilon}} (\ln x)^{-0.825}, \tag{20}$$

and arbitrarily large values of x that satisfy

$$\pi(x) - \mathrm{Li}(x) < -k_\epsilon x^{2^{-\epsilon}} (\ln x)^{-0.825}. \tag{21}$$

Both Littlewood's theorem and our model suggest that the total number of primes $\pi(x)$ behaves like our panicky and overreacting driver with respect to the ideal path of $\mathrm{Li}(x)$. The functions in (20) and (21), however, predict more volatile oscillations than Littlewood's theorem. This result warrants skepticism, though, because it is in conflict with the Riemann hypothesis, perhaps the most famous open conjecture in mathematics today.

The Riemann hypothesis is a conjecture about the placement of the zeros of the Riemann zeta function, a function of a complex variable with deep connections to the distribution of primes. Indeed, the Riemann hypothesis implies that the prime number theorem and the proofs of Hadamard and de la Vallée-Poussin from 1896 rely on partial

information about the location of the zeros, rather than the precise placement predicted by Riemann in 1859. An equivalent version of the Riemann hypothesis gives bounds on the absolute error between $\pi(x)$ and its approximation $\mathrm{Li}(x)$, the quantity we are interested in. This is the version we state.

RIEMANN HYPOTHESIS. *For all $\epsilon > 0$, there exists a positive constant C_ϵ such that*

$$\left|\pi(x) - \mathrm{Li}(x)\right| \leq C_\epsilon x^{\frac{1}{2}+\epsilon}.$$

Littlewood's theorem tells us that the value of $\pi(x) - \mathrm{Li}(x)$ jumps above and below the solid curve in FIGURE 5 while the Riemann hypothesis predicts the value stays *within* the dotted curve. Our model predicts the value jumps above and below a curve that vastly exceeds the dotted line in FIGURE 5, giving rise to the conflict. The Riemann hypothesis is an open conjecture, not a proved theorem, yet a large amount of supporting evidence exists. Thus, we should view our model's prediction with caution, at the very least. (For more information about the Riemann hypothesis, a good starting point is Bombieri's article [**3**], which can be found on the Clay Mathematics Institute's website [**5**], along with other interesting resources.)

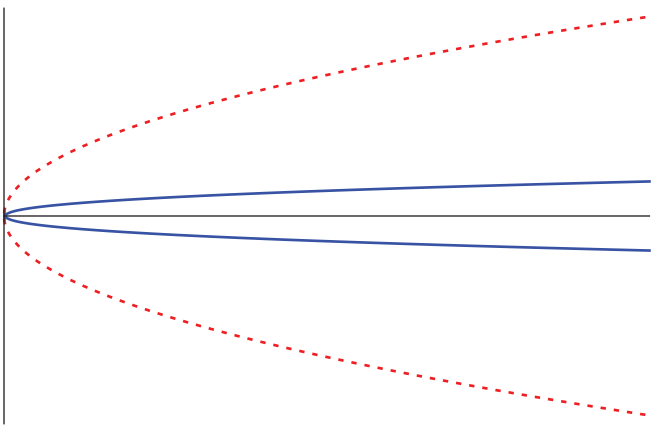

Figure 5 Comparison of bounds for $\pi(x) - \mathrm{Li}(x)$; Littlewood (solid) and Riemann Hypothesis (dotted).

A natural next step in any modeling process is to fine-tune the model based on what we've learned about it. We based our derivation of equation (1) on the Sieve of Eratosthenes, considering the effect of a prime x on the density at x^2. A finer analysis—for example, incorporating the effect of a prime x on the density at powers of x beyond 2—might improve the situation. However, there may be a limit to how well we can describe the system using this approach. By multiplying the density correction factors together, the Sieve of Eratosthenes provides an approximation for the density of primes less than x:

$$\prod_{p \leq \sqrt{x}} \left(1 - \frac{1}{p}\right). \tag{22}$$

The product in (22) is known to be asymptotic to

$$\frac{2e^{-\gamma}}{\ln x},$$

where γ is the Euler-Mascheroni constant given by

$$\gamma := \lim_{n\to\infty}\left(1+\frac{1}{2}+\frac{1}{3}+\cdots+\frac{1}{n}-\ln n\right).$$

Unfortunately, this does not quite give the correct answer, as $2e^{-\gamma}$ is about $1.12292\ldots$ rather than 1 as expected from the prime number theorem. (For more about this approximation, see [**11**, p. 13].) The use of more sophisticated tools from number theory may lead to a model with better predictive power. However, this may be at the expense of the intuitive insight that this model brings to the table.

Acknowledgment The authors would like to thank Alexander Perlis and the anonymous referees for their helpful suggestions on both the style and substance of earlier versions of this article.

REFERENCES

1. Paul T. Bateman and Harold G. Diamond, A hundred years of prime numbers, *Amer. Math. Monthly* **103** (1996) 729–741.
2. Carter Bays and Richard H. Hudson, A new bound for the smallest x with $\pi(x) > \mathrm{li}(x)$, *Math. Comp.* **69** (2000) no. 231, 1285–1296 (electronic).
3. Enrico Bombieri, The Riemann hypothesis, in *The Millennium Prize Problems,* Clay Mathematics Institute, Cambridge, MA, 2006, 107–124.
4. Kuok Fai Chao and Roger Plymen, A new bound for the smallest x with $\pi(x) > \mathrm{li}(x)$, *Int. J. Number Theory* **6** (2010) 681–690.
5. Clay Mathematics Institute, "Millennium problems—Riemann hypothesis," http://www.claymath.org/millennium/Riemann_Hypothesis/, 2011.
6. R. M. Corless, G. H. Gonnet, D. E. G. Hare, D. J. Jeffrey, and D. E. Knuth, On the Lambert W function, *Adv. Comput. Math.* **5** (1996) 329–359.
7. R. D. Driver, *Ordinary and Delay Differential Equations,* Springer-Verlag, New York, 1977. http://dx.doi.org/10.1007/978-1-4684-9467-9
8. H. M. Edwards, *Riemann's Zeta Function,* Academic Press, New York, 1974.
9. P. Erdős, On a new method in elementary number theory which leads to an elementary proof of the prime number theorem, *Proc. Nat. Acad. Sci. USA* **35** (1949) 374–384.
10. L. J. Goldstein, A history of the prime number theorem, *Amer. Math. Monthly* **80** (1973) 599–615.
11. Andrew Granville, Harald Cramér and the distribution of prime numbers, *Scand. Actuar. J.* (Harald Cramér Symposium, Stockholm, 1993) (1995) 12–28.
12. G. Hoffman de Visme, The density of prime numbers, *Math. Gaz.* **45** (1961) 13–14.
13. J. Kaczorowski, On sign-changes in the remainder-term of the prime-number formula, II, *Acta Arith.* **45** (1985) 65–74.
14. Tadej Kotnik, The prime-counting function and its analytic approximations: $\pi(x)$ and its approximations, *Adv. Comput. Math.* **29** (2008) 55–70.
15. J. E. Littlewood, Sur la distribution des nombres premiers, *C. R. Acad. Sci. Paris* **158** (1914) 1869–1875.
16. Eduardo Liz, Gonzalo Robledo, and Sergei Trofimchuk, Wright's conjecture: between the distribution of primes and population growth, *Cubo Mat. Educ.* **3** (2001) 89–107.
17. Atle Selberg, An elementary proof of the prime-number theorem, *Ann. of Math.* (2) **50** (1949) 305–313.
18. Yuri Tschinkel, About the cover: on the distribution of primes—Gauss' tables, *Bull. Amer. Math. Soc.* (N.S.) **43** (2006) 89–91.
19. E. M. Wright, The non-linear difference-differential equation, *Quart. J. Math.,* Oxford Ser. **17** (1946) 245–252.
20. ———, The linear difference-differential equation with asymptotically constant coefficients, *Amer. J. Math.* **70** (1948) 221–238.
21. ———, Linear difference-differential equations, *Proc. Cambridge Philos. Soc.* **44** (1948) 179–185.
22. ———, The linear difference-differential equation with constant coefficients, *Proc. Roy. Soc. Edinburgh. Sect. A.* **62** (1949) 387–393.
23. ———, The stability of solutions of non-linear difference-differential equations, *Proc. Roy. Soc. Edinburgh. Sect. A.* **63** (1950) 18–26.
24. ———, A non-linear difference-differential equation, *J. Reine Angew. Math.* **194** (1955) 66–87.
25. ———, A functional equation in the heuristic theory of primes, *Math. Gaz.* **44** (1960) 15–16.
26. ———, Number theory and other reminiscences of Viscount Cherwell, *Notes and Records Roy. Soc. London* **42**(2) (1988) 197–204.

Summary A differential-difference equation modeling the density of primes has been independently discovered several times by applied mathematicians with an interest in number theory, including Lord Cherwell. In this article, we use the framework of feedback and control to explain the natural connection between this equation and the distribution of prime numbers. Building on work of E. M. Wright, who learned of the equation from Cherwell and studied it for over a decade, we explain how the model predicts both the prime number theorem and a theorem of Littlewood. We close with known limitations of the model.

SUSAN H. MARSHALL teaches mathematics at Monmouth University, located on the Jersey Shore. Her primary research area is number theory, and in particular she finds the interplay between number theory and other mathematical subjects (such as geometry) fascinating. As an undergraduate at Wake Forest University, she had a particular fondness for differential equations, but was lured to arithmetic geometry as a graduate student at the University of Arizona. This project exposed her to somewhat unexpected connections between number theory and the fields of differential equations and mathematical modeling.

DONALD R. SMITH is Associate Professor of Management and Decision Sciences at the Leon Hess Business School of Monmouth University. He originally intended to major in mathematics, but transitioned to physics while an undergraduate at Cornell University, and then to operations research for his graduate work, earning a Masters degree from Columbia University and a Ph.D. from the University of California at Berkeley. His primary research interests have been in modeling stochastic systems. He has always been fascinated by the distribution of primes, and found this work fun because it put an operations research modeling perspective on this captivating topic.

Maybe We're All the Same at Heart

I can tell that 41 and 107 are different integers, because they have different digits.

But if I multiply both of them by 3,

$$41 \times 3 = 123 \qquad 107 \times 3 = 321$$

then the results have the same digits! Only their order distinguishes them.

Let's say that two positive integers m and n are *really the same at heart* if there is a positive integer c such that the products mc and nc have the same digits. Let's be more precise: We insist that the decimal representations of mc and nc have the same number of 1's, the same number of 2's, and so on up to the same number of 9's. We ignore 0's, because mc and nc can each have as many leading zeros as we like.

Then 41 and 107 are really the same at heart, because we can choose $c = 3$. (And if we don't like $c = 3$, we can try $c = 9006$.)

Which pairs m and n are really the same at heart?

Fair warning: This might not be easy. The answer will be in the solutions to this year's USA Mathematical Olympiad, in our October issue. The problem was proposed by Richard Stong.

NOTES

Cooling Coffee without Solving Differential Equations

ROBERT ISRAEL
University of British Columbia
Vancouver, Canada
israel@math.ubc.ca

PETER SALTZMAN
Berkeley, California
saltzman.pwa@gmail.com

STAN WAGON
Macalester College
St. Paul, Minnesota
wagon@macalester.edu

"A mathematician is a device for turning coffee into theorems."

—A. Rényi [**3**, p. 731]

Almost all differential equations texts and many calculus texts have the following exercise: Assuming Newton's law of cooling, which strategy will yield a colder drink?

Be impatient: Add milk to hot coffee and wait five minutes.

Be patient: Wait five minutes, then add the cold milk.

Newton's law is that temperature $Y(t)$ obeys the differential equation

$$Y'(t) = -k(Y(t) - A),$$

where A is room temperature. Students can find the explicit exponential solution and prove that the patient strategy is best. Of course, there are assumptions: The milk is kept cold during the time period, the mixing of the liquids is instantaneous, and the temperature of the mixed liquid becomes the weighted average of the temperatures of the constituents. We will say that the patient strategy *wins* when it yields a drink that is colder than (or the same temperature as) the result of the impatient strategy.

But for several reasons, Newton's law is not an especially good model. First, it is not an ironclad description of pure conduction. Over large temperature intervals, conduction is not necessarily governed by a simple linear rate law; models such as $Y^{5/4}$ (Lorentz law) or Y^p for other values of $p > 1$ have been proposed in other contexts. There appears to be no simple law of heat conduction that is generally applicable. More important for the coffee-and-milk problem are the other mechanisms of heat loss, such as radiation and evaporation. Experiments show that the loss through evaporation is

Math. Mag. **86** (2013) 204–210. doi:10.4169/math.mag.86.3.204.

quite large for hot water. The trick of coating the liquid with oil will entirely remove evaporation, and so we can compare the effects experimentally as in FIGURE 1 (data generated by Macalester College students D. Nizam and R. Onkal).

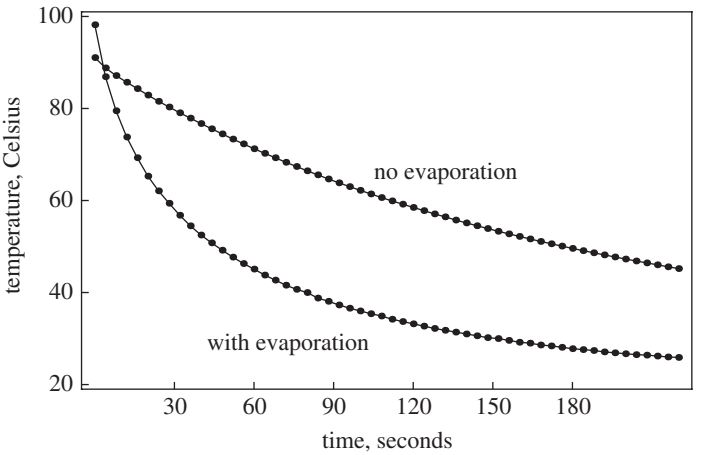

Figure 1 Cooling water, where a coat of oil was used to suppress evaporation

It is natural to ask whether the problem of cooling coffee can be settled without having to set up and solve a differential equation. Thus we want to find physically realistic conditions on $f(Y)$ that allow a mathematical proof that the patient strategy is best when heat loss is governed by the differential equation $Y' = -f(Y)$. We will prove here that the patient strategy wins for all parameter values if and only if $f(Y)$ "looks convex from the origin." This is a weaker variant of the property of convexity, and we formalize it in the next section.

There are physical reasons why the patient strategy is best. If the milk were not kept cold but simply sat beside the coffee in an open container, then there should be no difference in the two methods. The change of temperature is roughly (not exactly: different heat coefficient, different evaporation effect) the same for both liquids and the result of mixing them is therefore roughly independent of the time at which they are mixed. But by staying cold until it is added, the milk is exempt from any heat absorption while the coffee cools; this exemption makes it seem reasonable that the patient strategy leads to a cooler mixed liquid.

However, as observed by Rees and Viney [**2**], there are two effects at work.

- Arguing for patience: The coffee loses heat more quickly at the beginning, since under any reasonable model of heat loss, the loss is greater when the temperature difference is greater.
- Arguing for impatience: If the cold milk is added to hot coffee, then the mixing reduces the temperature by more than if the milk is added to cooler coffee.

The interplay between the two mechanisms can be delicate. Consider the model $Y' = -\sqrt{Y}$, where the ambient temperature is zero, the coffee starts at temperature $+1$, the milk is kept cold at -0.1, and the relative amount of coffee is 0.95. FIGURE 2 shows the two temperature profiles, with the patient drinker adding milk at time 1. The impatient strategy yields the cooler coffee in this case.

Other functions that arise in models of cooling are $Y' = A^4 - Y^4$ from the Stefan law of radiation (in the Kelvin scale), and an exponential function from an ODE approximation of evaporation. The Clausius–Clapeyron equation [**1**] can be used to get

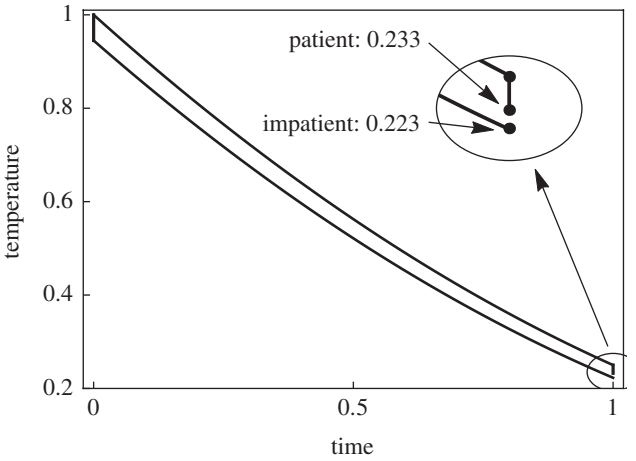

Figure 2 The impatient strategy leads to colder coffee when heat loss follows a square root law.

such a model. It has the form (Kelvin scale): $Y' = c_0\left(e^{-c_1/Y} - 0.3e^{-c_1/A}\right)$, where 0.3 is a typical relative humidity, A is the ambient temperature (293 K), and c_1 is derived from physical considerations such as the latent heat of evaporation and is about 4900. Modeling real data, using fine measurements of the mass lost to evaporation, led to a value for c_0 of 19000.

These various models are shown in FIGURE 3, where all functions have been rescaled to run from $(0, 0)$ to $(1, 1)$. The rescaling is for convenience, not for direct comparison. For hot coffee, the evaporative loss is greater than the losses from conduction or radiation. The figure includes a scaled version of

$$f(Y) = Y(\pi + 4\arctan(Y - 1)),$$

an interesting example that will be discussed later: The scaled version of this function is nonconvex for $Y \geq 2/3$. There is a subtlety regarding evaporation, since that process continues and heat is lost even when the liquid is at the ambient temperature. As can be easily verified with two thermometers and a glass of water, the equilibrium temperature of water in a constant-temperature room is a little below room temperature.

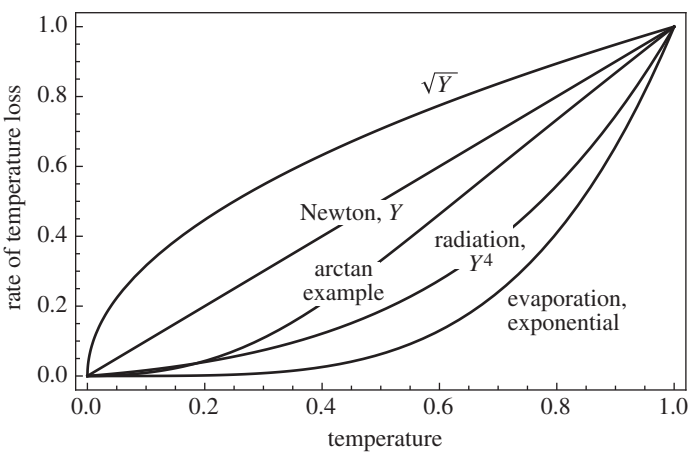

Figure 3 Various functions that arise in the study of cooling

In the next section, we show that a certain convexity assumption on $f(Y)$ is the exact condition needed for the patient strategy to win.

When patience wins

Keeping to a scale where the equilibrium temperature is zero, it is clear that the temperature of real coffee must be nonincreasing, so we want $f(Y) \geq 0$ when $Y \geq 0$. The key to a general result about the patient strategy is the imposition of a weak form of convexity on $f(Y)$.

We focus here on continuously differentiable functions $f(Y)$ defined on $\mathbb{R}$, or possibly on $[0, \infty)$, with $f(0) = 0$ and $f(Y)$ positive when Y is positive and negative when Y is negative. Such a function is called a *cooling law*.

We define a cooling law to be *V-convex* if $f(Y)/Y$ is nondecreasing for all $Y > 0$, and *V-concave* if $F(Y)/Y$ is nonincreasing for all $Y > 0$. The "V" stands for *visually*, since, viewed from the origin, the graph is rising just as a convex function would. The physical interpretation of V-convexity is that the relative rate of heat loss is nondecreasing.

A convex function—that is, a function with $f''(Y) \geq 0$ for all $Y > 0$—is always V-convex. (The proof is an exercise using $f(0) = 0$ and three applications of the mean value theorem.) The models in FIGURE 3, except for the arctan example and the square root function, are all convex, and therefore also V-convex. Powers such as $\sqrt{Y}$ or $Y^{2/3}$ (with exponents less than 1) are concave and therefore not V-convex. But the notion of V-convexity is weaker than convexity. The arctan example in FIGURE 3 illustrates this; as we have seen, this function is not convex on all of $(0, \infty)$, but it is V-convex.

In what follows, C is the initial (positive) temperature of the coffee, M is the temperature of the milk (a negative constant), α (between 0 and 1) is the relative proportion of coffee, and $\beta = 1 - \alpha$. We will always take the equilibrium temperature to be zero. (We may think of this as room temperature, but as we have noted, evaporation may make the equilibrium slightly below room temperature.) We will always assume C to be positive, M to be negative, and α to be between 0 and 1. Then impatient mixing gives the new temperature $\alpha C + \beta M$. We assume that the cooling process follows an unspecified differential equation $Y'(t) = -f(Y)$, where $Y(t)$ is the temperature of the liquid at time t.

Introduce F, the temperature function, by $F(t, x) = Y(t)$, where Y obeys the differential equation with initial temperature is $Y(0) = x$. We assume that f is continuously differentiable, so that the initial-value problem has a unique solution for all x and $F(t, x)$ is well defined. We will study in detail the cooling system $R_t(x)$, where $R_t(x) = F(t, x)$; it is often understood that t is fixed and then the subscript will be suppressed. It is a standard result that f being continuously differentiable implies the same for R. Now, the assertion that patience wins is

$$F(t, \alpha C + \beta M) \geq \alpha F(t, C) + \beta M.$$

We will show that this is always the case when $f(Y)$ is V-convex, meaning that patience always wins whatever our choices for α, C, M, and t. We will show that the converse holds as well, in this sense: When f is not V-convex, we can find values of α, C, M, and t for which impatience yields the cooler drink.

LEMMA 1. *A function $f(Y)$ is V-convex if and only if $f'(Y) \geq f(Y)/Y$ for all $Y > 0$, and $f(Y)$ is V-concave if and only if $f'(Y) \leq f(Y)/Y$ for all $Y > 0$.*

Proof. Apply the quotient rule. ∎

LEMMA 2. *For $t \geq 0$, $R_t'(x) = f(R_t(x))/f(x)$.*

Proof. Because $f(0) = 0$, $Y = 0$ is an equilibrium point of the differential equation, and it follows that $R_t(x) \geq 0$ whenever $x \geq 0$. Standard separation of variables yields $\int \big(-1/f(Y)\big)\, dY = t + c$ to get $g'(Y) = -1/f(Y)$; then $t + c = g(y)$. Now assume initial temperature x and let $t = 0$ to obtain $c = g(x)$ and $t + g(x) = g(F(t, x))$. Let h be a local inverse of g. Then $F(t, x) = h(t + g(x))$ and

$$\frac{\partial}{\partial x} F(t, x) = \frac{g'(x)}{g'[h(t + g(x))]} = \frac{g'(x)}{g'[F(t, x)]} = \frac{f(F(t, x))}{f(x)}. \qquad \blacksquare$$

The next lemma shows how V-convexity flips between the cooling law and the temperature function.

LEMMA 3. *Let $f(Y)$ be a cooling law. Then $f(Y)$ is V-convex if and only if for all $t \geq 0$, $R_t(x)$ is a V-concave function of x.*

Proof. A function f is V-convex if and only if for all $t \geq 0$, letting $R = R_t$, we have $f(x)/x \geq f(R(x))/R(x)$ for all nonnegative x (because $R(x) \leq x$ and $\lim_{x \to 0} R(x) = 0$). By Lemma 2, this is equivalent to $R(x)/x \geq f(R(x))/f(x) = R'(x)$, and Lemma 1 then concludes the proof. $\blacksquare$

The next two theorems show that V-convexity of $f(Y)$ is equivalent to the patient strategy winning for all values of α, C, M, and t.

THEOREM 1. *If a cooling law $f(Y)$ is V-convex, then the patient strategy always wins.*

Proof. We may assume that α is large enough that $Y_0 = \alpha C + \beta M \geq 0$. For if it is not, then it is easy to see that the patient strategy wins. If α is such that Y_0 is negative, then the impatient temperature will only rise from Y_0, while the mix for the patient drinker at time t yields temperature $\alpha Y(t) + \beta M \leq Y_0$.

Fix t and use R for R_t. Let $h(Y) = (R(\alpha C + y) - R(\alpha C))/y$ and define r to be $h(\beta M)$. The goal is to show that $R(\alpha C + \beta M) > \alpha R(C) + \beta M$. But the definitions of h and r mean that $R(\alpha C + \beta M) = R(\alpha C) + r\beta M$ and so it suffices to show that (a) $R(\alpha C) \geq \alpha R(C)$, and (b) $r < 1$. But $\alpha C < C$, so lemma 3 gives $R(\alpha C)/(\alpha C) \geq R(C)/C$, which yields (a). By the mean value theorem and lemmas 1 and 3, there is a $y \in [\alpha C + \beta M, \alpha C]$ such that $r = R'(y) \leq R(y)/y$. This last expression is less than 1, since temperature is strictly decreasing when it is positive, proving (b). $\blacksquare$

THEOREM 2. *If a cooling law $f(Y)$ is not V-convex, then there are values of α, C, M, and t for which the patient strategy loses.*

Proof. From the hypothesis, there exist C and C_1 such that $0 < C_1 < C$ and $f(C)/C < f(C_1)/C_1$. Because the temperature decreases to 0, there is $t > 0$ such that $R_t(C) = C_1$; fix this value of t. Then $f(C)/C < f(R(C))/R(C)$, or $R(C)/C < f(R(C))/f(C) = R'(C)$ by lemma 2. But $R(C)/C < R'(C)$ implies that there exists $y < C$ with $R(y)/y < R(C)/C$ (choosing $y < C$ such that $\frac{R(C)-R(y)}{C-y} > \frac{R(C)}{C}$ works); letting $\alpha = y/C$, we then have $R(\alpha C)/(\alpha C) < R(C)/C$, or $R(\alpha C) < \alpha R(C)$. Now, as M approaches 0 from the left, $R(\alpha C + \beta M) - \beta M \to R(\alpha C) < \alpha R(C)$, so we can find $M < 0$ such that $R(\alpha C + \beta M) - \beta M < \alpha R(C)$. For these values of α, C, M, and t, the impatient strategy wins. $\blacksquare$

To summarize, the cooling laws f for which patience wins are exactly those that arise by taking a C^1 function g that is defined on some interval of reals containing $[0, b)$, is nowhere negative, and is nondecreasing for nonnegative reals, and letting $f(Y) = Yg(y)$. Newton's law is the case that g is constant.

Even when Theorem 2 applies, there can be values of the parameters for which the patient strategy wins. For example, if $f(Y) = \sqrt{Y}$ and t is the final time, it is easy to solve the differential equation algebraically and work out that the patient strategy wins whenever $16M \leq (1-\alpha)t^2 + 8\alpha t - 16\alpha$. This condition is illustrated in FIGURE 4.

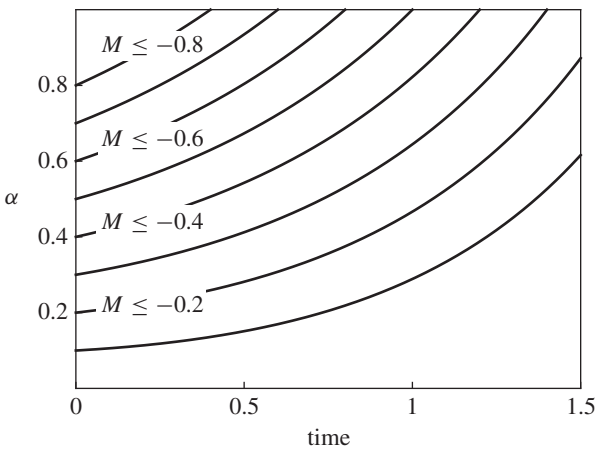

Figure 4 Upper bound on the milk temperature that allows the patient strategy to win for a square-root cooling law

Temperature half-life

The preceding mathematical results are satisfying, but can we use physics to justify the requirement that a cooling law be V-convex? One approach is to consider the concept of the half-life of the temperature, that is, the amount of time needed for the temperature to drop to half its value. The half-life for a given starting value x is the time τ such that $F(x, \tau) = x/2$. A related concept in the context of insulation of buildings is the *time constant*, that is, the time needed for the temperature to drop to $1/e$ of its value relative to ambient temperature. The common generalization of both of these concepts is the *ρ-life*, for any ρ satisfying $0 < \rho < 1$; the ρ-life is the time τ such that $F(x, \tau) = \rho x$. For Newton's law, the half-life is constant, as is the ρ-life for any ρ, but for more general cooling laws the half-life and the ρ-life depend on x.

It seems plausible that for any cooling law for water, the half-life should be a nonincreasing function of x, and similarly for the ρ-life. It turns out that the more general concept is equivalent to V-convexity. This is not surprising, given that V-convexity is an assertion about relative loss of heat.

THEOREM 3. *A function has nonincreasing ρ-life for all ρ if and only if it is V-convex.*

Proof. Using separation of variables, we find that the ρ-life is $\int_{\rho x}^{x} (1/f(Y))\, dY$. This being nonincreasing in x for $x > 0$ is equivalent to the derivative of the integral with respect to x being nonpositive: $\frac{1}{f(x)} - \frac{\rho}{f(\rho x)} \leq 0$, or $f(\rho x) \leq \rho f(x)$. This last being true for all $x > 0$ and $0 < \rho < 1$ is equivalent to $f(x)/x$ being nondecreasing for $x > 0$, the definition of V-convexity. ∎

So all the models in FIGURE 3, except the square root, yield temperatures with decreasing ρ-life.

Final thoughts

Our result assumed a first-order equation $Y'(t) = -f(Y)$ for heat loss and showed that for a surprisingly wide class of cooling laws, patience always pays.

A more exact treatment of heat transfer would assume that the temperature varies with position as well as time, thus leading to a partial differential equation. A PDE would also be relevant to a careful analysis of evaporation, since the humidity above the container would vary in a layered way. In some cases, such PDEs might be well approximable by a first-order ODE, but that will not always be the case, especially for short time intervals. Thus we have the open problem of generalizing the results here to a PDE model of heat transfer.

Our work assumes that coffee obeys the same cooling law with or without milk. This might not be entirely realistic. Regarding radiation, Rees and Viney [**2**] use Newton's law but with different coefficients for white and black coffee. Also, the addition of milk changes the mass, and therefore the time required for a one-degree drop in temperature. Perhaps the ideas discussed here could be extended to such two-model situations.

We gave a heuristic justification for V-convexity, but wonder whether there is a thermodynamic justification of this behavior for cooling liquids. It is tricky, since there are certain situations (e.g., the dropping of a red-hot metal block into cool water) where the cooling effect is not at all like cooling coffee: Steam insulation can cause the cooling of the block to start off slowly, and later increase.

Acknowledgment We are grateful to Ian Cave, Michael Elgersma, James Heyman, and Antonin Slavik for helpful comments.

REFERENCES

1. R. Portmann and S. Wagon, How quickly does hot water cool?, *Mathematica in Education and Research* **10**(3) (July 2005) 1–9. Available at http://stanwagon.com/public/EvaporationPortmannWagonMiER.pdf
2. W. G. Rees and C. Viney, On cooling tea and coffee, *Amer. J. Physics* **56**(5) (May 1988) 434–437. http://dx.doi.org/10.1119/1.15572
3. J. Suzuki, *A History of Mathematics*, Pearson, Upper Saddle River, NJ, 2002.

Summary A classic textbook problem is to show, assuming Newton's law of cooling, that if cold milk is added to coffee that has been cooling down, the result will be colder than if the milk was added at an earlier time. We formulate and prove a theorem that shows this holds when the linear function of Newton's law is replaced by any function satisfying a certain weak convexity condition. This is relevant to the real-world problem, since Newton's law is not an adequate model for cooling liquids; it ignores the large amount of heat loss due to evaporation, as well as the smaller loss due to radiation.

Intrinsically Defined Curves and Special Functions

ANTONÍN SLAVÍK
Charles University, Faculty of Mathematics and Physics
Prague, Czech Republic
slavik@karlin.mff.cuni.cz

The curvature of a plane curve measures the rate of rotation of the unit tangent vector as we move along the curve. In particular, the curvature of a unit speed curve at a given point equals the instantaneous angular velocity of the tangent vector; positive curvature corresponds to a counterclockwise rotation, and negative to a clockwise rotation. Conversely, the curvature function contains enough information to recover the original curve up to translation and rotation. In this case, the curve is said to be defined intrinsically.

In the present article, we show that even for the simplest curvature functions (power functions and the sine function), the problem of reconstructing the curve leads to integrals that cannot be evaluated in terms of elementary functions. Still, it is possible to study both qualitative and quantitative properties of the corresponding curves.

Preliminaries

We start by recalling some basic facts from differential geometry. (See, for example, Pressley's text [**9**].) A plane curve is a differentiable mapping $\boldsymbol{c} : I \to \mathbb{R}^2$, where I is an interval on the real line. We restrict our attention to unit speed curves, for which $\|\boldsymbol{c}'(s)\| = 1$ for every $s \in I$. The unit tangent vector is defined as $\boldsymbol{T}(s) = \boldsymbol{c}'(s)$. Let $\alpha : I \to \mathbb{R}$ be a continuous function such that $\boldsymbol{T}(s) = (\cos\alpha(s), \sin\alpha(s))$ for every $s \in I$ (in other words, $\alpha(s)$ measures the oriented angle between $\boldsymbol{T}(s)$ and the horizontal axis). Then the curvature κ of $\boldsymbol{c}$ satisfies $\kappa(s) = \alpha'(s)$ for every $s \in I$. (This formula can even serve as the definition of curvature.)

Given a continuous function $\kappa : I \to \mathbb{R}$, how do we find a unit speed curve $\boldsymbol{c} : I \to \mathbb{R}^2$ whose curvature at $\boldsymbol{c}(s)$ is $\kappa(s)$? Let $\boldsymbol{c}(s) = (x(s), y(s))$, so that $x(s)$, $y(s)$ are the components of the unknown function $\boldsymbol{c}$. Combining the relations $\alpha'(s) = \kappa(s)$ and $\boldsymbol{T}(s) = (\cos\alpha(s), \sin\alpha(s))$, we obtain the following system of differential equations:

$$\alpha'(s) = \kappa(s), \quad x'(s) = \cos\alpha(s), \quad y'(s) = \sin\alpha(s).$$

The solution

$$\alpha(s) = \int \kappa(s)\,\mathrm{d}s, \quad x(s) = \int \cos\alpha(s)\,\mathrm{d}s, \quad y(s) = \int \sin\alpha(s)\,\mathrm{d}s,$$

depends on the choice of integration constants, which correspond to translation and rotation of the curve. Throughout this paper we will assume the initial conditions $x(0) = y(0) = \alpha(0) = 0$. With these conditions,

$$\alpha(s) = \int_0^s \kappa(u)\,\mathrm{d}u, \quad x(s) = \int_0^s \cos\alpha(u)\,\mathrm{d}u, \quad y(s) = \int_0^s \sin\alpha(u)\,\mathrm{d}u.$$

Math. Mag. **86** (2013) 211–219. doi:10.4169/math.mag.86.3.211.

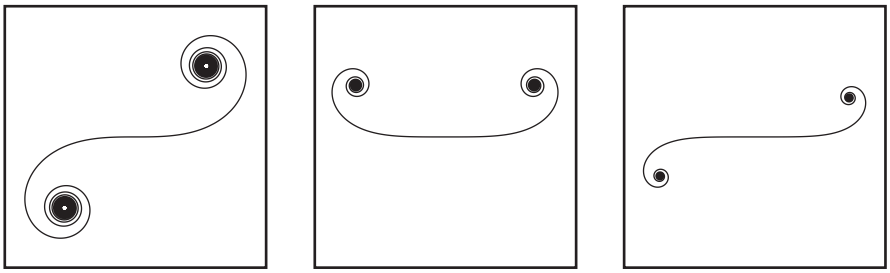

Figure 1 Curves with curvature $\kappa(s) = s^n$, $n \in \{1, 2, 3\}$

Power functions

With the formulas for recovering a curve from its curvature at hand, we can start experimenting with various choices of the function κ. An obvious first choice to try is $\kappa(s) = s^n$, where n is a nonnegative integer. It is not too surprising that $n = 0$ gives $\alpha(s) = s$, $x(s) = \sin s$, $y(s) = -\cos s$, i.e., a circle of unit radius. For $n \geq 1$, we obtain $\alpha(s) = s^{n+1}/(n+1)$, but

$$x(s) = \int_0^s \cos \frac{u^{n+1}}{n+1}\,\mathrm{d}u, \quad y(s) = \int_0^s \sin \frac{u^{n+1}}{n+1}\,\mathrm{d}u$$

cannot be integrated in terms of elementary functions.

FIGURE 1 shows computer-generated plots of the curves corresponding to $n = 1, 2, 3$. Our plots were created in *Mathematica*, but any other software capable of numerical integration can serve the same purpose. Wolfram Research hosts a freely available interactive demonstration that shows plots like these for some other curvature funtions [**4**].

For $n = 1$, the curve is known as the Euler spiral, Cornu spiral, or clothoid. It has a long history, which can be traced back to Jacob Bernoulli's 1694 treatise *Curvatura Laminae Elasticae*. Besides the theory of elasticity, clothoids are useful in the construction of railroads and freeways (since they enable a smooth transition between straight and circular sections), and also show up in diffraction theory. The history and applications are described by Levien [**7**].

Is there anything else we can say about these spirals? One obvious fact is their symmetry: Each spiral consists of two parts, which are centrally symmetric with respect to the origin for odd values of n; for even values of n, we have two parts that are symmetric with respect to the vertical axis.

When $s \to \infty$, each spiral seems to approach a certain point; let us call it the center of the spiral (the other center corresponds to $s \to -\infty$). The coordinates of the center are

$$x_\infty = \lim_{s\to\infty} x(s) = \int_0^\infty \cos \frac{u^{n+1}}{n+1}\,\mathrm{d}u,$$

$$y_\infty = \lim_{s\to\infty} y(s) = \int_0^\infty \sin \frac{u^{n+1}}{n+1}\,\mathrm{d}u.$$

When we ask *Mathematica* to calculate these two integrals, we learn that

$$x_\infty = \Gamma\left(1 + \frac{1}{n+1}\right) \sqrt[n+1]{n+1}\, \cos \frac{\pi}{2(n+1)}, \tag{1}$$

$$y_\infty = \Gamma\left(1 + \frac{1}{n+1}\right) \sqrt[n+1]{n+1}\, \sin \frac{\pi}{2(n+1)}, \tag{2}$$

where Γ is the gamma function, which is defined by $\Gamma(w) = \int_0^\infty t^{w-1}e^{-t}\,\mathrm{d}t$ and satisfies the recurrence $\Gamma(w+1) = w\,\Gamma(w)$ when $w > 0$. In particular, when $n = 1$, we have $x_\infty = y_\infty = \Gamma(3/2) = 1/2\,\Gamma(1/2) = \sqrt{\pi}/2$. Where did the values in (1) and (2) come from and how can we verify their correctness?

Most complex analysis textbooks show how to derive the formulas

$$\int_0^\infty \cos t^2\,\mathrm{d}t = \int_0^\infty \sin t^2\,\mathrm{d}t = \sqrt{\frac{\pi}{8}}$$

by means of Cauchy's integral theorem. These integrals are known as the Fresnel integrals [**11**]. A linear change of variables then gives

$$\int_0^\infty \cos\frac{u^2}{2}\,\mathrm{d}u = \int_0^\infty \sin\frac{u^2}{2}\,\mathrm{d}u = \frac{\sqrt{\pi}}{2},$$

which agrees with the above-mentioned values of x_∞ and y_∞. The coordinates of the clothoid's center were first obtained by Euler in 1781. (See [**5**]; according to Levien [**7**], it took Euler 38 years to discover a method of calculating these two improper integrals.)

The situation is slightly more complicated when n is a general positive integer. By applying the change of variables $t = u^{n+1}/(n+1)$, or $u = \sqrt[n+1]{n+1}\;t^{\frac{1}{n+1}}$, we get

$$x_\infty = \int_0^\infty \cos\frac{u^{n+1}}{n+1}\,\mathrm{d}u = \frac{\sqrt[n+1]{n+1}}{n+1}\int_0^\infty t^{\frac{1}{n+1}-1}\cos t\,\mathrm{d}t, \tag{3}$$

$$y_\infty = \int_0^\infty \sin\frac{u^{n+1}}{n+1}\,\mathrm{d}u = \frac{\sqrt[n+1]{n+1}}{n+1}\int_0^\infty t^{\frac{1}{n+1}-1}\sin t\,\mathrm{d}t. \tag{4}$$

These improper integrals represent real and imaginary parts of $\int_0^\infty t^{w-1}e^{-it}\,\mathrm{d}t$, where $w = \frac{1}{n+1}$, and it is known that

$$\int_0^\infty t^{w-1}e^{-it}\,\mathrm{d}t = \Gamma(w)\,e^{-\pi i w/2}, \quad w \in (0,1). \tag{5}$$

Let us pause for a moment to explain why the last formula is true. Complex analysis comes to the rescue again: We integrate the function $g(z) = z^{w-1}e^{-z}$ along the two paths shown in FIGURE 2; by Cauchy's integral theorem, we have

$$\int_{c_1+c_2} g(z)\,\mathrm{d}z = \int_{c_3+c_4} g(z)\,\mathrm{d}z.$$

What happens if $r \to 0$ and $R \to \infty$? We see that

$$\lim_{r\to 0,\,R\to\infty}\int_{c_1} g(z)\,\mathrm{d}z = \int_0^\infty t^{w-1}e^{-t}\,\mathrm{d}t = \Gamma(w),$$

$$\lim_{r\to 0,\,R\to\infty}\int_{c_4} g(z)\,\mathrm{d}z = \int_0^\infty (it)^{w-1}e^{-it}i\,\mathrm{d}t = i^w\int_0^\infty t^{w-1}e^{-it}\,\mathrm{d}t.$$

Further, it can be shown that both $\int_{c_3} g(z)\,\mathrm{d}z$ and $\int_{c_2} g(z)\,\mathrm{d}z$ approach zero. (In the first case, note that $|g(re^{i\varphi})| < r^{w-1}$, $\varphi \in [0, \pi/2]$. In the second case, use the estimates $|g(Re^{i\varphi})| < R^{w-1}e^{-R\cos\varphi}$ and $\cos\varphi \geq 1 - 2\varphi/\pi$, $\varphi \in [0, \pi/2]$; for more details, see [**10**, p. 52]). Equation (5) then follows by writing i^w as $(e^{i\pi/2})^w$.

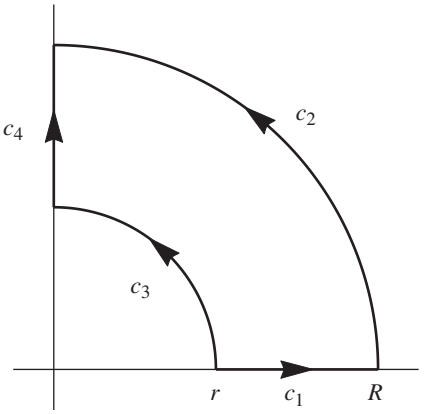

Figure 2 Quarter of an annulus in the complex plane

Now, back to our original problem. Decomposition of (5) into real and imaginary parts leads to

$$\int_0^\infty t^{w-1} \cos t \, \mathrm{d}t = \Gamma(w) \cos \frac{\pi w}{2},$$
$$\int_0^\infty t^{w-1} \sin t \, \mathrm{d}t = \Gamma(w) \sin \frac{\pi w}{2}.$$

We now substitute $w = \frac{1}{n+1}$ and use (3) and (4) to obtain the final result:

$$\begin{aligned} x_\infty &= \Gamma\left(\frac{1}{n+1}\right) \frac{\sqrt[n+1]{n+1}}{n+1} \cos \frac{\pi}{2(n+1)} \\ &= \Gamma\left(1 + \frac{1}{n+1}\right) \sqrt[n+1]{n+1} \cos \frac{\pi}{2(n+1)}, \\ y_\infty &= \Gamma\left(\frac{1}{n+1}\right) \frac{\sqrt[n+1]{n+1}}{n+1} \sin \frac{\pi}{2(n+1)} \\ &= \Gamma\left(1 + \frac{1}{n+1}\right) \sqrt[n+1]{n+1} \sin \frac{\pi}{2(n+1)}. \end{aligned}$$

Sine function

After $\kappa(s) = s^n$, it is natural to try other elementary functions. A particularly nice family of curves is obtained by letting $\kappa(s) = a \sin s$, where $a > 0$ is a parameter. Then

$$\alpha(s) = \int_0^s a \sin u \, \mathrm{d}u = a - a \cos s,$$

which leads to the parametrization

$$x(s) = \int_0^s \cos(a - a \cos u) \, \mathrm{d}u,$$
$$y(s) = \int_0^s \sin(a - a \cos u) \, \mathrm{d}u.$$

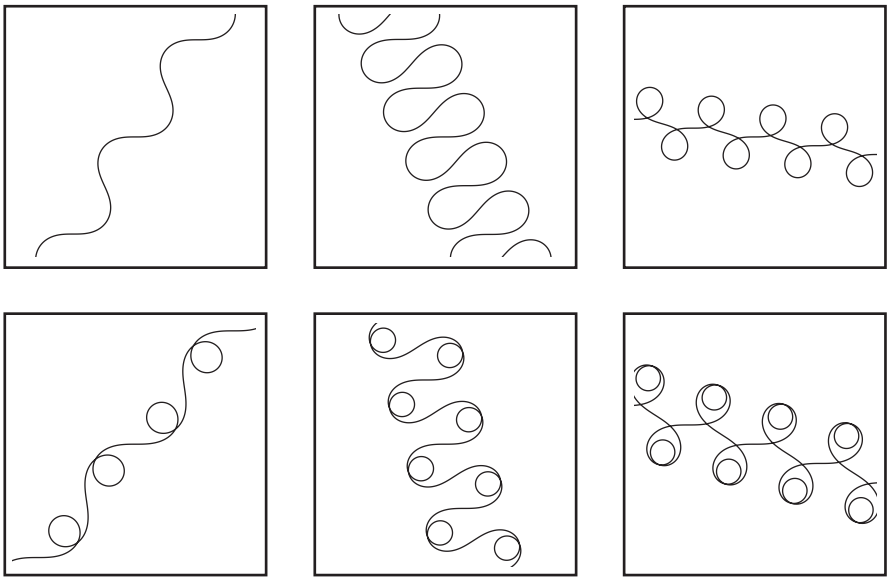

Figure 3 Curves with curvature $\kappa(s) = a \sin s$, $a \in \{1, 2, 3, 4, 5, 6\}$

We are unable to express these integrals in terms of elementary functions, and have to resort to numerical integration again.

FIGURE 3 shows the curves corresponding to $\kappa(s) = a \sin s$, where a is an integer. (The plots do not have the same scale.) More experimentation with various choices of a (perhaps with the interactive demonstration [**4**]) reveals that a value near to 2.4 leads to a closed figure-eight shaped curve (the first plot in FIGURE 4). Other values of a which give closed curves can be found near 5.52, 8.65 (second and third plots in FIGURE 4), 11.79, and 14.93.

This raises some natural questions:

- Can we prove rigorously that these curves are indeed closed?
- What are the magical values of a that produce these closed curves, and are there infinitely many of them? If yes, how fast do they grow?

For $s \in [0, \pi]$, the curvature is nonnegative and the tangent vector turns counterclockwise. This corresponds to the loops on the right sides of the curves in FIGURE 4. The left loops must be symmetric because $\kappa(s + \pi) = -\kappa(s)$. Consequently, the curve $\boldsymbol{c}$ is closed if and only if $\boldsymbol{c}(\pi) = \boldsymbol{c}(0) = 0$, and our task is to find the values of a such

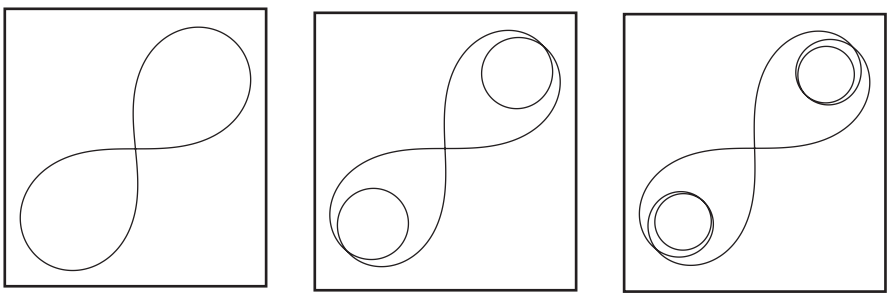

Figure 4 Closed curves with $\kappa(s) = a \sin s$, for a close to 2.40, 5.52, and 8.65

that

$$0 = x(\pi) = \int_0^\pi \cos(a - a\cos u)\,\mathrm{d}u,$$

$$0 = y(\pi) = \int_0^\pi \sin(a - a\cos u)\,\mathrm{d}u.$$

Applying the difference identities for the sine and cosine, we see that we need

$$0 = \cos a \int_0^\pi \cos(a\cos u)\,\mathrm{d}u + \sin a \int_0^\pi \sin(a\cos u)\,\mathrm{d}u,$$

$$0 = \sin a \int_0^\pi \cos(a\cos u)\,\mathrm{d}u - \cos a \int_0^\pi \sin(a\cos u)\,\mathrm{d}u.$$

However, by making the change of variables $u = \pi - v$, we obtain

$$\int_{\pi/2}^\pi \sin(a\cos u)\,\mathrm{d}u = \int_0^{\pi/2} \sin(a\cos(\pi - v))\,\mathrm{d}v = -\int_0^{\pi/2} \sin(a\cos v)\,\mathrm{d}v,$$

so that $\int_0^\pi \sin(a\cos u)\,\mathrm{d}u = 0$ for all $a \in \mathbb{R}$. Consequently,

$$x(\pi) = \cos a \int_0^\pi \cos(a\cos u)\,\mathrm{d}u,$$

$$y(\pi) = \sin a \int_0^\pi \cos(a\cos u)\,\mathrm{d}u.$$

Thus, the function

$$F(a) = \int_0^\pi \cos(a\cos u)\,\mathrm{d}u$$

plays a key role in the solution of our problem: the curve is periodic if and only if $F(a) = 0$.

When we ask *Mathematica* to calculate $F(a)$, we learn that

$$F(a) = \pi J_0(a),$$

where J_0 is the zeroth-order Bessel function. The history of Bessel functions goes back to Daniel Bernoulli [**13**]; before Bessel, these functions were usually defined as the sums of infinite series. The definition used by Bessel in his 1824 paper [**3**] is

$$J_n(a) = \frac{1}{\pi} \int_0^\pi \cos(nu - a\sin u)\,\mathrm{d}u, \tag{6}$$

where J_n is the nth-order Bessel function. Although modern textbooks usually define Bessel functions in a different way (we will return to this topic shortly), the formula (6) can be found in various compendia devoted to special functions [**1, 6, 8, 13**]. For $n = 0$, we have

$$J_0(a) = \frac{1}{\pi} \int_0^\pi \cos(a\sin u)\,\mathrm{d}u,$$

which looks slightly different from $\frac{1}{\pi}F(a)$. However,

$$F(a) = \int_0^\pi \cos(a\cos u)\,\mathrm{d}u = \int_0^{\pi/2} \cos(a\cos u)\,\mathrm{d}u + \int_{\pi/2}^\pi \cos(a\cos u)\,\mathrm{d}u$$

$$= \int_{\pi/2}^{\pi} \cos(a\cos(v-\pi/2))\,\mathrm{d}v + \int_{0}^{\pi/2} \cos(a\cos(v+\pi/2))\,\mathrm{d}v$$

$$= \int_{\pi/2}^{\pi} \cos(a\sin v)\,\mathrm{d}v + \int_{0}^{\pi/2} \cos(a\sin v)\,\mathrm{d}v = \int_{0}^{\pi} \cos(a\sin v)\,\mathrm{d}v = \pi J_0(a),$$

which proves that $F(a) = \pi J_0(a)$. Indeed, the graph of J_0 (FIGURE 5) confirms that the zeros of this function are exactly those values of a that we found experimentally. The calculation of these zeros is a delicate problem; the basic idea is to isolate each zero in a suitable interval and then use a numerical root-finding algorithm. Fortunately, modern software packages such as *Mathematica* have built-in commands to calculate the zeros to any prescribed degree of accuracy.

How can we be sure that the zeroth-order Bessel function has an infinite number of zeros? This fact was already conjectured by Daniel Bernoulli and Fourier [**13**], but the proof had to wait for Bessel. He showed [**3**] that J_0 is positive in the interval $[m\pi, (m+1/2)\pi]$ when m is even, and negative when m is odd. Watson's treatise has a proof that is accessible to the modern reader [**13**, pp. 478–9]. Since J_0 is continuous, it must have an odd number of zeros in each of the intervals $[(m+1/2)\pi, (m+1)\pi]$, $m \in \mathbb{N}_0$.

Nowadays, the proof of the fact that J_0 has infinitely many zeros is usually based on the oscillation theory of differential equations. We need to recall that the nth-order Bessel function is a solution of the second-order linear differential equation

$$a^2 J_n''(a) + a J_n(a) + (a^2 - n^2) J_n(a) = 0.$$

In fact, this property (together with a suitable initial condition) often serves as the definition of Bessel functions; the differential equation arises from various problems in physics [**12**]. For $n = 0$, this implies

$$aF''(a) + F'(a) + aF(a) = 0. \tag{7}$$

(As an exercise, the reader can try to verify this fact by using the definition of F and differentiating under the integral sign.) Performing the change of variables $F(a) = G(a)a^{-1/2}$, the differential equation (7) is transformed to

$$G''(a) + \left(1 + \frac{1}{4a^2}\right) G(a) = 0, \quad a > 0. \tag{8}$$

Note that for $a \in (0, \infty)$, the zeros of F and G coincide. It is now sufficient to apply the following theorem: If $q : [t_0, \infty) \to \mathbb{R}$ is a nonnegative function such that

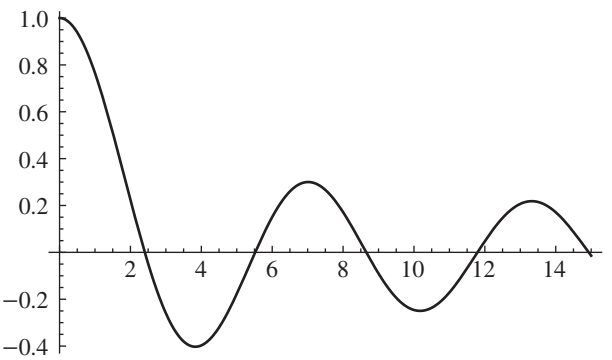

Figure 5 Graph of the zeroth-order Bessel function J_0

$\int_{t_0}^{\infty} q(t)\,\mathrm{d}t = \infty$, then every nontrivial solution of $x''(t) + q(t)x(t) = 0$ on $[t_0, \infty)$ is oscillatory, i.e., has an infinite number of zeros (see [**12**, p. 120] for a short elementary proof).

Finally, let us note that if a_n is the nth zero of F in $[0, \infty)$, then

$$\lim_{n\to\infty} (a_{n+1} - a_n) = \pi. \tag{9}$$

Intuitively, this follows from the fact that when $a \to \infty$, the term $(1 + 1/4a^2)$ in the differential equation (8) approaches 1, and all solutions of $G''(a) + G(a) = 0$ have distance π between their successive zeros. A rigorous proof of (9) can be based on the use of Sturm's comparison theorem [**2**, Theorem 31.1 and Problems 31.3, 31.4].

Conclusion

One aim of this paper has been to show that problems in differential geometry can serve as a motivation for the study of more advanced mathematics. We started by experimenting with intrinsically defined curves, and this simple geometrical problem has led us to a number of interesting topics in advanced analysis, such as the gamma and Bessel functions, evaluation of integrals by complex analytic methods, or the oscillation theory of second-order differential equations. The computer played a significant role in our initial investigation of intrinsically defined curves, and also in performing the subsequent calculations. Computer experiments often lead to the discovery of surprising phenomena, which are then proved by formal arguments.

An interested reader might enjoy learning more about the two families of curves studied in this paper, as well as exploring other types of intrinsically defined curves. Finally, let us mention the article by Zahn and Roskies [**14**], where the problem of closed curves is discussed from a different perspective. The authors establish a relation between simple closed plane curves and their Fourier descriptors, roughly corresponding to the Fourier series coefficients of the primitive function to κ. Conversely, they characterize closed curves as those where one of the Fourier descriptors is a zero of the first-order Bessel function.

REFERENCES

1. M. Abramowitz and I. Stegun, eds., *Handbook of Mathematical Functions, with Formulas, Graphs and Tables,* Applied Mathematics Series 55, National Bureau of Standards, Washington, DC, 1964.
2. R. P. Agarwal and D. O'Regan, *An Introduction to Ordinary Differential Equations,* Springer-Verlag, New York, 2008. http://dx.doi.org/10.1007/978-0-387-71276-5
3. F. Bessel, *Untersuchung des Theils der planetarischen Störungen welcher aus der Bewegung der Sonne ensteht*, Abh. d. K. Akad. Wiss. Berlin 1824, 1–52 (published 1826).
4. K. Boguta and F. Meinberg, *Intrinsically Defined Curves,* Wolfram Demonstrations Project, http://demonstrations.wolfram.com/IntrinsicallyDefinedCurves/.
5. L. Euler, *De valoribus integralium a termino variabilis $x = 0$ usque ad $x = \infty$ extensorum*, Institutiones calculi integralis 4 (1794) 337–345. English translation by Jordan Bell is available online at http://arxiv.org/abs/arXiv:0705.4640.
6. I. S. Gradshteyn and I. M. Ryzhik, *Table of Integrals, Series, and Products*, 7th ed., Academic Press, New York, 2007.
7. R. L. Levien, *From Spiral to Spline: Optimal Techniques in Interactive Curve Design*, Ph.D. dissertation, University of California, Berkeley, 2009. Online version at http://www.levien.com/phd/thesis.pdf.
8. F. W. J. Olver, D. W. Lozier, R. F. Boisvert, and C. W. Clark, eds., *NIST Handbook of Mathematical Functions*, Cambridge University Press, New York, 2010. Online version at http://dlmf.nist.gov/.
9. A. Pressley, *Elementary Differential Geometry*, 2nd ed., Springer-Verlag, New York, 2010. http://dx.doi.org/10.1007/978-1-84882-891-9

10. R. Remmert, *Classical Topics in Complex Function Theory,* Springer-Verlag, New York, 1998. http://dx.doi.org/10.1007/978-1-4757-2956-6
11. R. Remmert, *Theory of Complex Functions*, Springer-Verlag, New York, 1991. http://dx.doi.org/10.1007/978-1-4612-0939-3
12. G. F. Simmons, *Differential Equations with Applications and Historical Notes,* McGraw-Hill, New York, 1972.
13. G. N. Watson, *A Treatise on the Theory of Bessel Functions*, 2nd ed., Cambridge University Press, Cambridge, 1995.
14. C. T. Zahn and R. Z. Roskies, Fourier descriptors for plane closed curves, *IEEE Trans. Computers C-21* (1972) 269–281. http://dx.doi.org/10.1109/TC.1972.5008949

Summary We study two classes of plane curves with prescribed curvature. First, we investigate spirals whose curvature is a power function, and express coordinates of the spirals' centers in terms of the gamma function. For curves in the second family, the curvature is a multiple of the sine function. We show that this family contains infinitely many closed curves and provide their characterization in terms of the zeroth-order Bessel function.

Algebra Made Difficult

Anonymous graffiti found on a blackboard one late afternoon in April 2012 at the Mathematical Sciences Research Institute in Berkeley, California:

"Problem: Solve $x = ax + b$ for x.

Solution:

$$\begin{aligned} x &= a(ax+b)+b \;=\; a^2x+ab+b \\ &= a(a(ax+b)+b)+b \;=\; a^3x+a^2b+ab+b \\ &\;\;\vdots \\ &= (\text{assuming } |a|<1)\ \lim_{n\to\infty} a^n x + b\sum_{i=0}^{\infty} a^i \\ &= 0 + b/(1-a). \end{aligned}$$

This also holds by analytic continuation for all $a \neq 1$."

(submitted by James Propp, University of Massachusetts Lowell)

The Integrating Factors of an Exact Differential Equation

MOWAFFAQ HAJJA
Yarmouk University
Irbid, Jordan
mowhajja@yahoo.com, mhajja@yu.edu.jo

An integrating factor is a function that we multiply a differential equation by, in order to make it exact. Thus, it must sound ridiculous to ask about the integrating factors of an exact differential equation. Such a question can only be motivated by a playful human curiosity, which, in this case, has led to interesting questions in elementary real analysis.

Throughout this note, we fix an open connected set $\mathcal{D}$ in $\mathbb{R}^2$. The functions M, N, F, μ are real-valued functions defined on $\mathcal{D}$ and belong to class $\mathcal{C}^1$ on $\mathcal{D}$, which means that they have continuous first partial derivatives on $\mathcal{D}$.

A point $P \in \mathcal{D}$ is said to be a *singular point* of F if both partial derivatives of F at P are zero. We use the notation F_x and F_y for the partial derivatives of F with respect to the coordinates x and y.

The differential equation

$$M\,dx + N\,dy = 0 \tag{1}$$

is *exact* if one of the following two equivalent conditions is satisfied (on $\mathcal{D}$):

(a) $M_y = N_x$, or

(b) there is a function F such that $F_x = M$ and $F_y = N$.

The equivalence is shown by Boyce and DiPrima [**4**, Theorem 2.8.1, p. 76]. The function F is unique up to an additive constant, and is called a *potential* of (1) (or of the pair (M, N)). The general solution of (1) is then given by $F(x, y) = C$, where C is an arbitrary constant.

If μ is such that the differential equation

$$\mu M\,dx + \mu N\,dy = 0$$

is exact, then μ is called an *integrating factor* of (1).

Obviously, an exact differential equation remains exact when multiplied by a constant. In other words, all constants are integrating factors of an exact differential equation. In fact, we may for a while entertain the feeling that constants are the only integrating factors. But we soon discover that if an exact differential equation has potential F, then it can be written as

$$F_x\,dx + F_y\,dy = 0. \tag{2}$$

Then multiplying it by F results in another exact differential equation

$$F\,F_x\,dx + F\,F_y\,dy = 0,$$

which has potential $F^2/2$. Thus F, and similarly F^n, are integrating factors of (2). The same holds for any function $g(F)$ of F, where g is a real-valued function that is continuously differentiable on the range of F.

Math. Mag. **86** (2013) 220–226. doi:10.4169/math.mag.86.3.220.

This raises the possibility that all of the integrating factors of (2) are of the form $g(F)$. This is closer to the truth. In the next section, we give an example showing that this is not unconditionally true, but point to conditions on F that can be imposed in order to make it true. These conditions will become a theorem in the section that follows.

An example

We start with an example of an exact differential equation that has potential F, and an integrating factor that is not of the form $g(F)$.

EXAMPLE. The equation

$$4x\left(x^2+y^2-1\right)\,dx+4y\left(x^2+y^2-1\right)\,dy=0 \tag{3}$$

is exact, with $M=4x(x^2+y^2-1)$ and $N=4y(x^2+y^2-1)$, and potential

$$F(x,y)=\left(x^2+y^2\right)\left(x^2+y^2-2\right).$$

It is easy to check that the function

$$\mu(x,y)=x^2+y^2$$

is an integrating factor of (3). However, μ is not a function of F. To see this quickly, calculate $F(1,1/3)=F(2/3,2/3)=-80/81$, but $\mu(1,1/3)\neq\mu(2/3,2/3)$.

To understand this example better, we examine the level curves of F. For any k,

$$\begin{aligned}F(x,y)=k &\iff \left(x^2+y^2\right)^2-2\left(x^2+y^2\right)-k=0\\ &\iff x^2+y^2=1\pm\sqrt{k+1}.\end{aligned}$$

Therefore, we have:

- When $k=-1$, the level curve $F=k$ of F consists of the single circle $x^2+y^2=1$;
- when $-1<k\leq 0$, the level curve $F=k$ of F consists of the two circles

$$x^2+y^2=1-\sqrt{k+1},\ x^2+y^2=1+\sqrt{k+1};$$

- when $k>0$, the level curve $F=k$ of F consists of the single circle $x^2+y^2=1+\sqrt{k+1}$.

In the second case above, the function F is constant on the union of the two circles, while μ is constant on each of these circles separately but not on their union. This shows that μ is not a function of F.

A positive result

Note that the function F, in the example above, has disconnected level curves, and also has a lot of singular points, namely the point $(0,0)$ and all the points on the circle $x^2+y^2=1$. The next theorem shows that if F has connected level curves and not too many singular points, then μ would indeed be a function of F.

Its proof uses the implicit function theorem for real-valued functions of two variables. That theorem states that if $G(x,y)$ is of class $\mathcal{C}^1$ on a neighborhood of $P=$

$(x_0, y_0) \in \mathbb{R}^2$, and if $G(P) = 0$ and $G_y(P) \neq 0$, then there exists an open rectangle $I \times J$ centered at P, and a unique continuously differentiable function $f(x)$ from I to J such that $y_0 = f(x_0)$ and such that for every $x \in I$,

$$G(x, f(x)) = 0, \ G_y(x, f(x)) \neq 0;$$

see [**5**, p. 221] and [**11**, Theorem 14, p. 56, §12.1]. See [**2**] for a higher-dimensional version.

The proof also uses the rather sophisticated fact that *every subset of the plane* $\mathbb{R}^2$ *has a countable dense subset*. This follows from the facts that

(i) $\mathbb{R}$ is second countable (i.e., has a countable base),

(ii) the product of two second countable spaces is second countable,

(iii) any subset of a second countable space is second countable, and

(iv) a second countable space has a countable dense subset.

These are precisely Theorems 5.4, 5.12, 5.5, and 5.7 in Long [**9**, pp. 158–161], respectively, and they can also be found in Munkres [**10**, pp. 190–193]. As mentioned in the proof, this seemingly heavy machinery can be avoided if F is assumed to have no singular points at all.

THEOREM 1. *Suppose that the differential equation* (1) *is exact on* $\mathcal{D}$ *with potential* F*, and that* μ *is an integrating factor of* (1)*.*

(i) *If* Γ *is a connected component of a level curve* $F(x, y) = c$ *of* F*, and if the set of singular points of* F *on* Γ *is countable, then* μ *is constant on* Γ*.*

(ii) *In particular, if all level curves of* F *are connected, and if the set of singular points of* F *on each of these level curves is countable, then* μ *is a function of* F*; that is, there exists a real-valued function* g *such that* $\mu(x, y) = g(F(x, y))$ *for all* $(x, y) \in \mathcal{D}$*.*

Proof. (i) Suppose that Γ is a connected component of the level curve $F(x, y) = c$ of F, and suppose that the set S of singular points of F on Γ is countable. Let $\Gamma_0 = \Gamma \setminus S$. We will show that μ is constant on Γ.

Take $P = (x_0, y_0) \in \Gamma_0$. Since P is not a singular point of F, we may assume that $F_y(P) \neq 0$, the case $F_x(P) \neq 0$ being similar. By the implicit function theorem, there is an open rectangle $I \times J$ centered at P and a function $h : I \to J$ such that $h(x_0) = y_0$ and such that $F(x, h(x)) = c$ and $F_y(x, h(x)) \neq 0$ for all $x \in I$. From the exactness of the differential equations

$$M\,dx + N\,dy = 0 \quad \text{and} \quad \mu M\,dx + \mu N\,dy = 0$$

on $\mathcal{D}$, we conclude that

$$M_y = N_x \quad \text{and} \quad \mu\ M_y + M\ \mu_y = \mu\ N_x + N\ \mu_x \quad (\text{on } \mathcal{D}).$$

Hence $M\mu_y = N\mu_x$, or equivalently

$$F_x\,\mu_y = F_y\,\mu_x \quad (\text{on } \mathcal{D}). \tag{4}$$

Differentiating the relation $F(x, h(x)) = c$ on I, we obtain

$$F_x(x, h(x)) + F_y(x, h(x))\ h'(x) = 0 \quad (\text{for } x \in I).$$

Multiplying by $\mu_y(x, h(x))$, we obtain

$$\mu_y(x, h(x))F_x(x, h(x)) + \mu_y(x, h(x))F_y(x, h(x))\ h'(x) = 0 \quad (\text{for } x \in I).$$

Using (4), this reduces to

$$\mu_x(x, h(x))F_y(x, h(x)) + \mu_y(x, h(x))F_y(x, h(x))\, h'(x) = 0 \quad (\text{for } x \in I).$$

Since F_y is never 0 on I, it follows that

$$\mu_x(x, h(x)) + \mu_y(x, h(x))h'(x) = 0 \quad (\text{for } x \in I).$$

In other words, we have

$$\frac{d(\mu(x, h(x))}{dx} = 0 \quad (\text{for } x \in I),$$

and therefore $\mu(x, h(x))$ is constant on I.

We have proved that if $P \in \Gamma_0$, then there exists an open neighborhood $\mathcal{N}$ of P (namely the rectangle $I \times J$) such that μ is constant on $\mathcal{N} \cap \Gamma_0$. We let $\mathcal{O}_P$ denote the union of all such neighborhoods. Thus, $\mathcal{O}_P$ is the largest open neighborhood of P such that μ is constant on $\mathcal{O}_P \cap \Gamma_0$.

If $Q \in \Gamma_0$ is another point, then it is clear that $\mathcal{O}_P \cap \Gamma_0$ and $\mathcal{O}_Q \cap \Gamma_0$ are either equal or disjoint. Let $\Gamma_{00} \subseteq \Gamma_0$ be a set of representatives of the points of Γ_0 in the sense that for every $P \in \Gamma_0$, there is a unique $Q \in \Gamma_{00}$ such that $\mathcal{O}_P \cap \Gamma_0 = \mathcal{O}_Q \cap \Gamma_0$. We shall show that Γ_{00} is a singleton.

We digress here to consider the case where F has no singular points on Γ, i.e., S is empty and $\Gamma_0 = \Gamma$. In this case, $\{\mathcal{O}_P : P \in \Gamma_{00}\}$ is a family of pairwise disjoint open sets that cover Γ. Since Γ is connected, it follows that Γ_{00} consists of one element only, and thus μ is constant on Γ.

We now turn to the general case. Since Γ_0, being a subset of $\mathbb{R}^2$, has a countable dense subset T, and since each $\mathcal{O}_P \cap \Gamma_0$, $P \in \Gamma_{00}$, must intersect T, it follows that Γ_{00} is countable. Therefore $\mu(\Gamma_0)$, being equal to $\mu(\Gamma_{00})$, is countable. But $\mu(S)$ is countable, since S is. Hence, $\mu(\Gamma) = \mu(\Gamma_0) \cup \mu(S)$ is countable. Also, Γ is connected and μ is continuous. Therefore $\mu(\Gamma)$ is an interval. Since the only countable intervals are the singletons, it follows that $\mu(\Gamma)$ is a singleton. Thus μ is constant on Γ, as claimed.

(ii) By (i), μ is constant on every level curve of F. For any c in the range $F(\mathcal{D})$ of F, we define $g(c)$ to be $\mu(P)$, where P is any point on the level curve $F = c$. It then follows that $\mu = g(F)$, as desired. ∎

We illustrate Theorem 1 with an example. In this example, some level curves of F do indeed contain infinitely many singular points of F.

EXAMPLE. Let $\mathcal{D} = \mathbb{R}^2$ and let $F : \mathcal{D} \to \mathbb{R}$ be defined by $F(x, y) = y^3 - \cos x$. Consider the associated exact differential equation $\sin x\, dx + 3y^2\, dy = 0$. The level curve $F = c$, $c \in \mathbb{R}$, is the set $\{(x, y) \in \mathbb{R}^2 : y^3 - \cos x = c\}$. This is the image of $\mathbb{R}$ under the continuous function $f_c : \mathbb{R} \to \mathbb{R}^2$ defined by $f_c(x) = \left(x, \sqrt[3]{c + \cos x}\right)$. Thus it is connected. Therefore all the level curves of F are connected.

Also, the set of singular points of F consists of the solutions of $\sin x = 3y^2 = 0$, i.e., of the countable set $\{(n\pi, 0) : n \in \mathbb{Z}\}$. Note that the singular points $(n\pi, 0)$, n even, lie on the level curve $F(x, y) = -1$, and that the singular points $(n\pi, 0)$, n odd, lie on the level curve $F(x, y) = 1$. There are no singular points of F on the remaining level curves.

Thus Theorem 1 applies and shows that all of the integrating factors of the differential equation $\sin x\, dx + 3y^2\, dy = 0$ are functions of $y^3 - \cos x$.

Equations that are not exact

The question above is a special case of the question about how two integrating factors μ and ν of the same differential equation are related. In fact, the two questions are essentially equivalent. In the case when the differential equation is exact, the question is about μ, since one can take ν to be the constant function 1. In the general case, the question is about the function μ/ν, which is an integrating factor of the exact differential equation $\nu M\,dx + \nu N\,dy = 0$. In this case, the general solution is obtained from $\mu/\nu = C$, where C is an arbitrary constant; see the last lines of [**7**, § 1.1]. Of course, dividing μ by ν as done above cannot be performed without care, and several steps in our proofs are designed to avoid pitfalls of this nature.

The question regarding how two integrating factors of the same differential equation are related is, in essence, a question of how unique an integrating factor is. Stating it in this manner, we may feel amazed that such a question is not addressed in textbooks of differential equations where questions of uniqueness are fundamental. The only mention of such an issue that we know of are two passing statements made in the 1906 paper [**12**], a reference that was kindly pointed out to us by an anonymous referee. Those statements appear on lines 16–18 of page 156 and on lines 14–15 of page 158, and, when combined, they state that if ν is an integrating factor of a differential equation with potential F, then μ is an integrating factor if and only if $\mu = \nu g(F)$. A similar statement appears in Ince [**8**, §8, p. 15].

What sets can be the singular points of a level curve?

Theorem 1 also raises the question of what the set of singular points of a class $\mathcal{C}^1$ function may look like. Since a singular point of F is simply a solution of the equations $F_x = F_y = 0$, we are also led to seek a characterization of sets that can serve as the zero-sets of continuous (or class $\mathcal{C}^1$) functions of one or more variables. The next theorem gives some answers. Part (i) must be public knowledge (as suggested by the last two lines of an article by Gillman and Jerison [**6**, § 1.10, pp. 14–15]). Its strength lies in the fact that a closed subset of $\mathbb{R}$ can be quite wild. A popular illustration is supplied by the total Cantor set $\mathcal{K}$ (the union of the Cantor sets in $[n, n+1]$, $n \in \mathbb{Z}$) as described, for example, by Munkres [**10**, Exercise 6, p. 177]. This is a closed set that is uncountable, totally disconnected, and has zero Lebesgue measure. In particular, it contains no intervals (a, b), $a < b$.

The zero-set of a real-valued function f is defined to be the set of all points p in the domain of f for which $f(p) = 0$. It will be denoted by $\mathcal{Z}(f)$.

THEOREM 2.

(i) *Every closed subset of a metric space $\mathcal{M}$ is the zero-set of a continuous function f from $\mathcal{M}$ to $\mathbb{R}$.*

(ii) *Let A and B be any closed subsets of $\mathbb{R}$. Then there exists a class $\mathcal{C}^1$ function from $\mathbb{R}^2$ to $\mathbb{R}$, whose set of singular points is the Cartesian product $A \times B$.*

Proof. (i) Let d be the metric on $\mathcal{M}$ and let A be a closed subset of $\mathcal{M}$. If A is empty, take $f : \mathcal{M} \to \mathbb{R}$ to be a nonzero constant function. Otherwise, define f by

$$f(p) = d(p, A) = \inf\{d(p, q) : q \in A\}.$$

Clearly, f is continuous and the zero-set $\mathcal{Z}(f)$ of f is A.

(ii) Let A, B be closed subsets of $\mathbb{R}$. By (i) and its proof, there are continuous nonnegative functions g, h from $\mathbb{R}$ to $\mathbb{R}$ such that $\mathcal{Z}(g) = A$, $\mathcal{Z}(h) = B$. Take any points

$a \in A$ and $b \in B$, and set

$$G(x) = \int_a^x g(t)\,dt, \quad H(x) = \int_b^x h(t)\,dt.$$

Let $F : \mathbb{R}^2 \to \mathbb{R}$ be defined by

$$F(x, y) = G(x)H(y).$$

Then

$$F_x(x, y) = g(x)H(y), \quad F_y(x, y) = G(x)h(y).$$

Hence, F_x and F_y are continuous and thus F is of class $\mathcal{C}^1$ on $\mathbb{R}^2$. Also, the set S of singular points of F is the set of solutions of $g(x)H(y) = G(x)h(y) = 0$. If $H(y) = 0$, then $h(t) = 0$ for all t in $[b, y]$ (or $[y, b]$) and thus $y \in B$. Therefore, $\mathcal{Z}(H) \subseteq B$. Similarly, $\mathcal{Z}(G) \subseteq A$. Since $\mathcal{Z}(g) = A$ and $\mathcal{Z}(h) = B$, it follows that $S = A \times B$. Hence, F satisfies the desired properties. ∎

For more on the zero-sets of continuous functions from $\mathbb{R}$ to $\mathbb{R}$, the reader is referred to [**3**] and [**1**].

The next questions

Theorem 1 says that if the differential equation $M\,dx + N\,dy = 0$ is exact with potential F and an integrating factor μ, and also if

(i) the level curves of F are connected, and

(ii) the set of singular points of F on every level curve is countable, then

(iii) μ is a function of F.

Our opening example exhibits functions F and μ that do not satisfy any of (i), (ii), or (iii). It would be interesting to find examples satisfying (i) but not (iii) (and necessarily not (ii)), and examples satisfying (ii) but not (iii) (and necessarily not (i)). Of course, trivial examples satisfying (iii) but neither (i) nor (ii) can be constructed by taking μ to be the constant function. However, a referee kindly suggested that studying other examples that are less trivial may help us understand Theorem 1 better and may lead to stronger forms of that theorem.

Acknowledgment The author is thankful to Yarmouk University for the financial support.

REFERENCES

1. V. Baláž and T. Šalát, Zeros of continuous functions and the structure of two function spaces, *Math. Slovaca* **52** (2002) 397–408.
2. R. G. Bartle, *The Elements of Real Analysis*, 2nd ed., Wiley, New York, 1976.
3. T. D. Benavides, How many zeros does a continuous function have? *Amer. Math. Monthly* **93** (1986) 464–466. http://dx.doi.org/10.2307/2323473
4. W. E. Boyce and R. C. DiPrima, *Elementary Differential Equations and Boundary Value Problems*, 5th ed., Wiley, New York, 1992.
5. R. Courant and F. John, *Introduction to Calculus and Analysis*, vol. 2, Springer-Verlag, New York, 1989. http://dx.doi.org/10.1007/978-1-4613-8958-3
6. L. Gillman and M. Jerison, *Rings of Continuous Functions*, Van Nostrand, Princeton, NJ, 1960.
7. N. H. Ibragimov, Integrating factors, adjoint equations and Lagrangians, *J. Math. Anal. Appl.* **318** (2006) 742–757. http://dx.doi.org/10.1016/j.jmaa.2005.11.012

8. E. L. Ince, *Integration of Ordinary Differential Equations*, Oliver and Boyd, Edinburgh and London, 1952.
9. P. E. Long, *An Introduction to General Topology*, Charles E. Merrill, Columbus, OH, 1971.
10. J. R. Munkres, *Topology: A First Course*, Prentice-Hall, Englewood Cliffs, NJ, 1975.
11. D. V. Widder, *Advanced Calculus*, 2nd ed., Prentice Hall, Englewood Cliffs, NJ, 1961.
12. E. B. Wilson, Note on integrating factors, *Annals Math.* **7** (1906) 155–160. http://dx.doi.org/10.2307/1967240

Summary This note investigates the integrating factors μ of an exact differential equation $M\,dx + N\,dy = 0$ and finds conditions on the potential F under which μ is a function of F.

PROBLEMS

BERNARDO M. ÁBREGO, *Editor*
California State University, Northridge

Assistant Editors: SILVIA FERNÁNDEZ-MERCHANT, California State University, Northridge; JOSÉ A. GÓMEZ, Facultad de Ciencias, UNAM, México; EUGEN J. IONASCU, Columbus State University; ROGELIO VALDEZ, Facultad de Ciencias, UAEM, México; WILLIAM WATKINS, California State University, Northridge

PROPOSALS

To be considered for publication, solutions should be received by November 1, 2013.

1921. *Proposed by Enkel Hysnelaj, University of Technology, Sydney, Australia and Elton Bojaxhiu, Kriftel, Germany.*

Let $f : (0, \infty) \to \mathbb{R}$ be a function such that

$$\frac{1}{2}\left(f(\sqrt{x}) + f(\sqrt{y})\right) = f\left(\sqrt{\frac{x+y}{2}}\right)$$

for every $x, y \in (0, \infty)$. Prove that

$$\frac{1}{n}\left(f(\sqrt{x_1}) + f(\sqrt{x_2}) + \cdots + f(\sqrt{x_n})\right) = f\left(\sqrt{\frac{x_1 + x_2 + \cdots + x_n}{n}}\right)$$

for every positive integer n and for every $x_1, x_2, \ldots, x_n \in (0, \infty)$.

1922. *Proposed by Arkady Alt, San Jose, CA.*

Let m_a, m_b, and m_c be the lengths of the medians of a triangle with circumradius R and inradius r. Prove that

$$m_a m_b + m_b m_c + m_c m_a \leq 5R^2 + 2Rr + 3r^2.$$

Math. Mag. **86** (2013) 227–234. doi:10.4169/math.mag.86.3.227.

We invite readers to submit problems believed to be new and appealing to students and teachers of advanced undergraduate mathematics. Proposals must, in general, be accompanied by solutions and by any bibliographical information that will assist the editors and referees. A problem submitted as a Quickie should have an unexpected, succinct solution. Submitted problems should not be under consideration for publication elsewhere.

Solutions should be written in a style appropriate for this MAGAZINE.

Solutions and new proposals should be mailed to Bernardo M. Ábrego, Problems Editor, Department of Mathematics, California State University, Northridge, 18111 Nordhoff St, Northridge, CA 91330-8313, or mailed electronically (ideally as a LaTeX or pdf file) to mathmagproblems@csun.edu. All communications, written or electronic, should include **on each page** the reader's name, full address, and an e-mail address and/or FAX number.

1923. *Proposed by Leonid Menikhes and Valery Karachik, South Ural State University, Chelyabinsk, Russia.*

Let m and n be nonnegative integers. Find a closed-form expression for the sum

$$\sum_{k=0}^{2n}(-1)^k\binom{2n}{k}\binom{2m}{m-n+k}.$$

1924. *Proposed by Omran Kouba, Higher Institute for Applied Sciences and Technology, Damascus, Syria.*

Find a necessary and suffcient condition on (a_1, a_2, a_3, a_4) for the series

$$\sum_{n=0}^{\infty}\left(\frac{a_1}{4n+1}+\frac{a_2}{4n+2}+\frac{a_3}{4n+3}+\frac{a_4}{4n+4}\right)$$

to converge, and determine the sum of this series when that condition is satisfied.

1925. *Proposed by Tim Kröger and Rudolf Rupp, Georg Simon Ohm University of Applied Sciences, Nürnberg, Germany.*

Probably every mathematician teaching undergraduate mathematics has experienced the difficulty of persuading every student that the equation $(A + B)^{-1} = A^{-1} + B^{-1}$ is not true for arbitrary matrices A and B. However, the equation is true for *some* matrices A and B.

For every positive integer n, determine all pairs of $n \times n$ real matrices A and B such that $(A + B)^{-1} = A^{-1} + B^{-1}$.

Quickies

Answers to the Quickies are on page 233.

Q1031. *Proposed by Herman Roelants, Institute of Philosophy, University of Leuven, Belgium.*

For which positive integers n do there exist positive integer solutions x, y to the diophantine equation $4xy - x + y = n$?

Q1032. *Proposed by Michael W. Botsko, Saint Vincent College, Latrobe, PA.*

Suppose that f is a continuous real-valued function on $[a, b]$ and $c \in (a, b)$. In addition, suppose that f' exists and is decreasing on (a, b). Prove that

$$(b - c)f(a) + (c - a)f(b) \leq (b - a)f(c).$$

Solutions

A Fresnelian definite integral — June 2012

1896. *Proposed by Timothy Hall, PQI Consulting, Cambridge, MA.*

Find with proof the value of

$$\int_0^{\infty}\frac{\cos(\sqrt{x})}{\sqrt{x}}\cos x\,dx.$$

I. *Solution by Missouri State University Problem Solving Group, Missouri State University, Springfield, MO.*
Substituting $u = \sqrt{x}$ and noting that the integrand is an even function gives

$$\int_0^\infty \frac{\cos(\sqrt{x})}{\sqrt{x}} \cos x \, dx = 2\int_0^\infty \cos(u)\cos(u^2)du = \int_{-\infty}^\infty \cos(u)\cos(u^2)du.$$

Using the addition and subtraction formulas for cosine, completing the square, and using the substitutions $v = u + 1/2$ and $w = u - 1/2$, gives

$$\begin{aligned}
\int_{-\infty}^\infty \cos(u)\cos(u^2)du &= \frac{1}{2}\int_{-\infty}^\infty \left[\cos(u^2+u) + \cos(u^2-u)\right]du \\
&= \frac{1}{2}\int_{-\infty}^\infty \left[\cos\left(\left(u+\frac{1}{2}\right)^2 - \frac{1}{4}\right) + \cos\left(\left(u-\frac{1}{2}\right)^2 - \frac{1}{4}\right)\right]du \\
&= \frac{1}{2}\int_{-\infty}^\infty \cos\left(v^2 - \frac{1}{4}\right)dv + \frac{1}{2}\int_{-\infty}^\infty \cos\left(w^2 - \frac{1}{4}\right)dw \\
&= \int_{-\infty}^\infty \cos\left(v^2 - \frac{1}{4}\right)dv \\
&= \int_{-\infty}^\infty \left[\cos(v^2)\cos\left(\frac{1}{4}\right) + \sin(z^2)\sin\left(\frac{1}{4}\right)\right]dv \\
&= \cos\left(\frac{1}{4}\right)\int_{-\infty}^\infty \cos(v^2)dv + \sin\left(\frac{1}{4}\right)\int_{-\infty}^\infty \sin(v^2)dv.
\end{aligned}$$

Since the Fresnel integrals

$$\int_{-\infty}^\infty \cos(v^2)dv = \sqrt{\frac{\pi}{2}} = \int_{-\infty}^\infty \sin(v^2)dv$$

are well known, the integral in question equals $(\cos(1/4) + \sin(1/4))\sqrt{\pi/2}$.

II. *Solution by Khristo N. Boyadzhiev, Ohio Northern University, Ada, OH.*
As in the first solution, the requested integral is equal to $\int_{-\infty}^\infty \cos(u)\cos(u^2)du$. Consider the real-valued function

$$y(t) = \int_{-\infty}^\infty e^{-ax^2}\cos(xt)dx,$$

where a is a complex constant with $\Re(a) > 0$. Because the integral is absolutely convergent, it is possible to differentiate inside the integral to get

$$y'(t) = -\int_{-\infty}^\infty xe^{-ax^2}\sin(xt)dx.$$

Integrating $y(t)$ by parts gives

$$\begin{aligned}
y(t) &= \int_{-\infty}^\infty e^{-ax^2}\frac{d}{dx}\left(\frac{\sin(xt)}{t}\right)dx \\
&= \lim_{R\to\infty}\frac{1}{t}e^{-ax^2}\sin(xt)\Big|_{x=-R}^{x=R} + \int_{-\infty}^\infty \frac{2ax}{t}e^{-ax^2}\sin(xt)dx \\
&= 0 + \frac{2a}{t}\int_{-\infty}^\infty xe^{-ax^2}\sin(xt)dx = -\frac{2a}{t}y'(t).
\end{aligned}$$

The separable differential equation $dy/dt = (-t/2a)y$ in the variable t has the solution $y(t) = Me^{-t^2/4a}$. To evaluate the constant M, we set $t = 0$ and use the well-known value of the Gaussian integral,

$$y(0) = \int_{-\infty}^{\infty} e^{-ax^2} dx = \sqrt{\frac{\pi}{a}}.$$

Thus

$$\int_{-\infty}^{\infty} e^{-ax^2} \cos(xt) dx = \sqrt{\frac{\pi}{a}}\, e^{-t^2/4a}$$

holds for all $t \in \mathbb{R}$ and for all complex numbers a with $\Re(a) > 0$. By continuity, the equation also holds for $\Re(a) = 0$ as long as $a \neq 0$. Setting $t = 1$ and $a = i$ gives

$$\int_{-\infty}^{\infty} (\cos(x^2) - i \sin(x^2)) \cos(x) dx = \int_{-\infty}^{\infty} e^{-ix^2} \cos(x) dx = \sqrt{\frac{\pi}{i}}\, e^{-1/4i}$$
$$= \sqrt{\pi}\Big(\frac{\sqrt{2}}{2} - i\frac{\sqrt{2}}{2}\Big)\Big(\cos\Big(\frac{1}{4}\Big) + i \sin\Big(\frac{1}{4}\Big)\Big).$$

Comparing real parts gives

$$\int_{-\infty}^{\infty} \cos(x) \cos(x^2) dx = \sqrt{\frac{\pi}{2}}\Big(\cos\Big(\frac{1}{4}\Big) + \sin\Big(\frac{1}{4}\Big)\Big).$$

Also solved by M. Reza Akhlaghi; George Apostolopoulos (Greece); William C. Bauldry; M. Benito, Ó. Ciaurri, E. Fernández, and L. Roncal; Gerald E. Bilodeau; Robert Calcaterra; Hongwei Chen; Paul Deiermann; Eugene S. Eyeson; Fisher Problem Group; John N. Fitch; Ovidiu Furdui (Romania); J. A. Grzesik; Eugene A. Herman; Julio C. Herrera and Mariano Perez; Omran Kouba (Syria); Isaac Edward Leonard (Canada); Ryan Q. McCluskey; Matthew McMullen; Rituraj Nandan; José Heber Nieto (Venezuela); Northwestern University Math Problem Solving Group; Moubinool Omarjee (France); Tomas Persson and Mikael P. Sundqvist (Sweden); José M. Pacheco (Spain) and Ángel Plaza (Spain); Paolo Perfetti (Italy); Mohammad Riazi-Kermani; Kendall Richards and Therese Shelton; Nicholas C. Singer; Thomas Steinberger; Nora Thornber; Tiberiu Trif (Romania); Michael Vowe (Switzerland); Stan Wagon; Haohao Wang and Jerzy Woydylo; A. David Wunsch; Yanping Xia; Li Zhou; and the proposer.

Partitions with balanced sums **June 2012**

1897. *Proposed by H. A. ShahAli, Tehran, Iran.*

Let n and m be positive integers such that $m < n$. Determine necessary and sufficient conditions for a sequence $\{x_j\}_{j=1}^n$ of real numbers to satisfy that

$$\Big|\sum_{j\in S} x_j\Big| = \Big|\sum_{\substack{1\le j\le n\\ j\notin S}} x_j\Big|,$$

for every m-element subset S of $\{1, 2, \ldots, n\}$.

Solution by Eugene A. Herman, Grinnell College, Grinnell, IA.
When $m \neq n/2$, the condition is $\sum_{j=1}^n x_j = 0$; when $m = n/2$, the condition is $\sum_{j=1}^n x_j = 0$ or $x_1 = x_2 = \cdots = x_n$. The sufficiency of these conditions can be readily confirmed. Now suppose $\{x_j\}_{j=1}^n$ is a sequence of real numbers satisfying the condition given in the problem. If for some m-element subset S of $\{1, 2, \ldots, n\}$,

$$\sum_{j\in S} x_j = -\sum_{\substack{1\le j\le n\\ j\notin S}} x_j,$$

then $\sum_{j=1}^{n} x_j = 0$. Otherwise,

$$\sum_{j\in S} x_j = \sum_{\substack{1\le j\le n\\ j\notin S}} x_j$$

for every m-element subset S of $\{1, 2, \ldots, n\}$. If for some fixed S_1, there exist $i \in S_1$ and $j \notin S_1$ such that $x_i \neq x_j$, then for $S_2 = (S_1 \setminus \{i\}) \cup \{j\}$,

$$\sum_{j\in S_2} x_j \neq \sum_{\substack{1\le j\le n\\ j\notin S_2}} x_j.$$

Therefore, every element in S_1 equals every element in $\{1, 2, \ldots, n\} \setminus S_1$, and so $x_1 = x_2 = \cdots = x_n$ and $m = n/2$.

Also solved by George Apostolopoulos (Greece), Jeffrey Boerner and Natacha Fontes-Merz, Paul Budney, Bruce S. Burdick, Robert Calcaterra, Con Amore Problem Group (Denmark), Dmitry Fleischman, Michael Goldenberg and Mark Kaplan, Omran Kouba (Syria), Missouri State University Problem Solving Group, Jaeik Oh (Korea), Texas State University Problem Solvers Group, and the proposer. There were three incorrect solutions.

More on Kuratowski 14-sets **June 2012**

1898. *Proposed by Mark Bowron, Laughlin, NV.*

A subset E of a topological space X is called a *Kuratowski* 14*-set* if 14 distinct sets can be obtained by repeatedly applying closure and complement to E in some order. It is known that Kuratowski 14-sets E with $|E| = 3$ exist. Do any exist with $|E| < 3$?

Solution by Bruce S. Burdick, Roger Williams University, Bristol, RI.
The answer is no. Suppose we had such an E. Using c for closure and i for interior, the sets E, cE, icE, $cicE$, iE, ciE, and $iciE$ must all be distinct. (The other seven sets are the complements of these. Note that $iE = X \setminus c(X \setminus E)$.)

The set iE must not be E and it must not be empty, since that would imply that $ciE = iE$. So that rules out $|E| < 2$. Assume then that $E = \{x, y\}$ and $iE = \{x\}$. Note that if $icE \subseteq ciE$, then it would follow that $icE = iciE$. So there is some $z \in icE$ with $z \notin ciE = c\{x\}$. But $z \in cE$, so it must be that $z \in c\{y\}$. Therefore, $y \in icE$. Since x is isolated, we have $E \subseteq icE$, hence $cE \subseteq cicE$. Therefore, $cE = cicE$, a contradiction.

Also solved by Alex Aguado, George Apostolopoulos (Greece), Jeffrey Boerner, Robert Calcaterra, José H. Nieto (Venezuela), and the proposer. There was one incomplete submission.

Tangent points collinear with the centroid **June 2012**

1899. *Proposed by Michel Bataille, Rouen, France.*

Let $A_1A_2A_3$ be a triangle with centroid G. For $i \in \{1, 2, 3\}$, the circle $\mathcal{C}_i$ with center O_i and radius r_i is tangent to the two lines through A_i spanned by the sides of the triangle; moreover, the points of tangency and G are collinear. Prove that

$$\frac{r_1}{r_1 + GO_1} + \frac{r_2}{r_2 + GO_2} + \frac{r_3}{r_3 + GO_3} = 2.$$

Solution by Shohruh Ibragimov (student), Lyceum Nr2 under the SamIES, Samarkand, Uzbekistan.

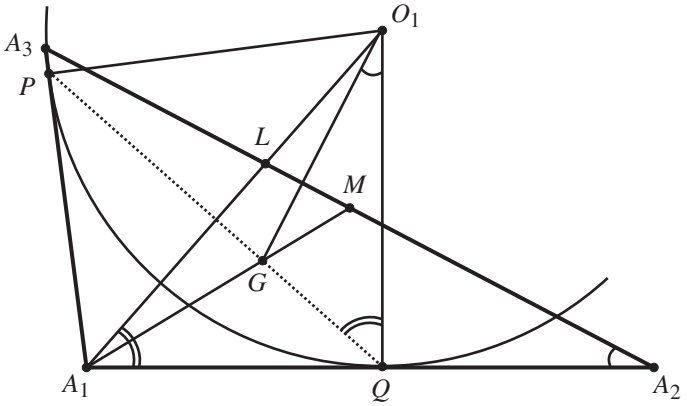

Denote by M the midpoint of $\overline{A_2A_3}$, and by P and Q the tangent points of the circle $\mathcal{C}_1$ with the lines A_1A_3 and A_1A_2, respectively. Denote by L the intersection of the bisector of the angle $\angle A_2A_1A_3$ and $\overline{A_2A_3}$. By the Generalized Angle Bisector Theorem applied to $\triangle A_1A_2A_3$ and M, and the Law of Sines applied to $\triangle A_1A_2A_3$, it follows that

$$1 = \frac{A_3M}{MA_2} = \frac{A_1A_3 \cdot \sin\angle MA_1A_3}{A_1A_2 \cdot \sin\angle A_2A_1M} = \frac{\sin\angle A_2}{\sin\angle A_3} \cdot \frac{\sin\angle MA_1A_3}{\sin\angle A_2A_1M}.$$

Again, the Generalized Angle Bisector Theorem applied to isosceles triangles QPA_1 and PQO_1 and point G implies that

$$\frac{\sin\angle MA_1A_3}{\sin\angle A_2A_1M} = \frac{\sin\angle GA_1P}{\sin\angle QA_1G} = \frac{PG}{GQ} = \frac{\sin\angle PO_1G}{\sin\angle GO_1Q}.$$

The last two equations imply that

$$\frac{\sin(\angle A_1 + \angle A_2)}{\sin\angle A_2} = \frac{\sin\angle A_3}{\sin\angle A_2} = \frac{\sin\angle PO_1G}{\sin\angle GO_1Q}.$$

Because $\angle QPO_1 = \angle O_1QP = \frac{1}{2}\angle A_1$, it follows that $\angle PO_1G = \pi - (\angle A_1 + \angle GO_1Q)$, and so

$$\frac{\sin(\angle A_1 + \angle A_2)}{\sin\angle A_2} = \frac{\sin(\angle A_1 + \angle GO_1Q)}{\sin\angle GO_1Q}.$$

Thus $\angle GO_1Q = \angle A_2$. In addition, $\angle O_1QG = \angle O_1QP = \frac{1}{2}\angle A_1 = \angle A_2A_1L$, therefore triangles A_1LA_2 and QGO_1 are similar. Hence

$$\frac{LA_2}{A_1A_2} = \frac{GO_1}{QO_1} = \frac{GO_1}{r_1}.$$

Once more, by the Angle Bisector Theorem applied to $\triangle A_1A_2A_3$, it follows that $(A_2A_3 - LA_2)/LA_2 = A_3L/LA_2 = A_1A_3/A_1A_2$, and so

$$LA_2 = \frac{A_1A_2 \cdot A_2A_3}{A_1A_2 + A_1A_3}.$$

Using this we obtain $GO_1/r_1 = A_2A_3/(A_1A_2 + A_1A_3)$, and thus

$$\frac{r_1}{r_1 + GO_1} = \frac{1}{1 + GO_1/r_1} = \frac{A_1A_2 + A_1A_3}{A_1A_2 + A_2A_3 + A_1A_3}.$$

Adding similar identities for the expressions $r_2/(r_2 + GO_2)$ and $r_3/(r_3 + GO_3)$, we get

$$\sum_{i=1}^{3} \frac{r_i}{r_i + GO_i} = \frac{\sum_{\text{cyc}}(A_1A_2 + A_1A_3)}{A_1A_2 + A_2A_3 + A_1A_3} = 2.$$

Also solved by George Apostolopoulos (Greece), Robert Calcaterra, Chip Curtis, Michael Goldenberg and Mark Kaplan, L. R. King, Omran Kouba (Syria), Kee-Wai Lau (China), Peter Nüesch (Switzerland), Traian Viteam (Uruguay), Michael Vowe (Switzerland), and the proposer. There was one incorrect submission.

Rings that are never isomorphic **June 2012**

1900. *Proposed by Greg Oman, University of Colorado at Colorado Springs, Colorado Springs, CO.*

Let X be a set, and let S_X denote the set of all functions $f : X \to \mathbb{Z}$. The set S_X becomes a ring via the operations $(f + g)(x) := f(x) + g(x)$ and $(f \cdot g)(x) := f(x)g(x)$. Let B_X be the subring of S_X consisting of the functions f whose images in $\mathbb{Z}$ are finite. Does there exist an infinite set X such that the rings B_X and S_X are isomorphic?

Solution by Paul Budney, Sunderland, MA.
The answer is no. Suppose X is infinite and $\phi : B_X \to S_X$ is a ring isomorphism. Let $h \in S_X \setminus B_X$ be a function whose range is the set of positive integers, and let $f = \phi^{-1}(h)$. If $f \cdot g = \mathbf{0}$ for some nonzero function $g \in S_X$, then $h \cdot \phi(g) = \phi(f) \cdot \phi(g) = \phi(f \cdot g) = \phi(\mathbf{0}) = \mathbf{0}$, which is a contradiction since $\phi(g)$ is not the zero function and $h(x)$ is never zero. It follows that $f(x)$ is never zero, otherwise if $f(x_0) = 0$, then g defined as $g(x_0) = 1$ and $g(x) = 0$ for $x \neq x_0$ verifies that $f \cdot g = \mathbf{0}$. Let $m \neq 0$ be the product of all the numbers in the range of f. Define $j \in B_X$ by $j(x) = m/f(x)$. Then $f \cdot j = \mathbf{m}$, the constant function $\mathbf{m}$. Note that the constant function $\mathbf{1}$ is the multiplicative identity, and thus $\phi(\mathbf{1}) = \mathbf{1}$ and $\phi(\mathbf{m}) = m\phi(\mathbf{1}) = m\mathbf{1} = \mathbf{m}$. It follows that $h \cdot \phi(j) = \phi(f) \cdot \phi(j) = \phi(f \cdot j) = \phi(\mathbf{m}) = \mathbf{m}$. But then every positive integer divides m, which is impossible. Thus B_X and S_X are not isomorphic for any infinite set X.

Also solved by George Apostolopoulos (Greece), Robert Calcaterra, Bruce S. Burdick, Eugene A. Herman, Reiner Martin (Germany), Peter McPolin (Northern Ireland), Texas State University Problem Solvers Group, and the proposer.

Answers

Solutions to the Quickies from page 228.

A1031. The answer is all positive integers n such that $4n - 1$ is a composite integer. Multiplying both sides of $4xy - x + y = n$ by 4 and adding -1 to both sides leads to $(4x + 1)(4y - 1) = 4n - 1$. This implies that $4n - 1$ is a positive odd integer. Conversely, any composite integer of the form $4n - 1$ is always the product in at least one way of an integer of the form $4x + 1$ and an integer of the form $4y - 1$ with $x, y > 0$.

A1032. By the Mean Value Theorem, there exist $d \in (a, c)$ and $e \in (c, b)$ such that

$$\frac{f(c) - f(a)}{c - a} = f'(d) \qquad \text{and} \qquad \frac{f(b) - f(c)}{b - c} = f'(e).$$

Because $d < e$ and f' is decreasing, it follows that

$$\frac{f(b) - f(c)}{b - c} \leq \frac{f(c) - f(a)}{c - a}.$$

Multiplying both sides by $(b - c)(c - a)$ and rearranging gives

$$(b - c) f(a) + (c - a) f(b) \leq (b - a) f(c).$$

REVIEWS

PAUL J. CAMPBELL, *Editor*
Beloit College

Assistant Editor: Eric S. Rosenthal, West Orange, NJ. Articles, books, and other materials are selected for this section to call attention to interesting mathematical exposition that occurs outside the mainstream of mathematics literature. Readers are invited to suggest items for review to the editors.

Fortnow, Lance, *The Golden Ticket: P, NP and the Search for the Impossible*, Princeton University Press, 2013; x + 176 pp, $26.95. ISBN 978-0-691-15649-1.

———, The status of the P versus NP problem, *Communications of the Association for Computing Machinery* 52 (9) (September 2009) 78–86.

The book is an elaboration and simplification of the most-downloaded article from the *Communications of the Association for Computing Machinery*, on the status of the P vs. NP problem. That article has been "translated" to a popular level through imaginative use of examples, such as frenemies, sudoku, map coloring, Minesweeper, the traveling sales problem, cryptography, and zero-knowledge proofs. All of this is accomplished with a reliance on intuitive notions of what it means to be in one or the other class of problem. There is even a visionary narrative of what life would be like, in terms of changes in society, if it were ever proved that P = NP. There are a few omissions: a diagram showing the relations of problems of varying difficulty; guidance to further references that would gently "ramp up" the understanding of a reader who becomes seriously interested (most references are to technical papers); and a lower price—at $26.95, rather than $9.95, vastly fewer high school students and general readers will buy the book and become inspired (they will have to wait for a hoped-for paperback edition). (The "golden ticket" of the title is a reference to Roald Dahl's *Charlie and the Chocolate Factory*.)

Schneps, Leila, and Coralie Colmez, *Math on Trial: How Numbers Get Used and Abused in the Courtroom*, Basic Books, 2013; xi + 256 pp, $26.99. ISBN 978-0-465-03974-0.

"[M]ath can be deadly." Well, some students may feel that way, but it's not what is meant here. This book details 10 court cases in which mathematics—really, in all but one case, probability—was misused. The focus is on the drama resulting from the errors committed: multiplying non-independent probabilities, bad estimation, Simpson's paradox, wrong probability model, and the birthday problem. The cases include some classics (Dreyfus affair, Berkeley sex bias, People v. Collins) and the suddenly-again-in-the-news case of Amanda Knox.

Barrett, Scott, Avoiding disastrous climate change is possible but not inevitable, *Proceedings of the National Academy of Sciences* 108 (no. 29) 11733–11734, http://www.pnas.org/content/108/29/11733.full .

Can countries live up to voluntary carbon reduction targets? This paper reports results of games that model countries' decisions. Experiments with the games, with their two pure-strategy Nash equilibria (cooperate or defect), favored cooperation in the face of a catastrophe known to be certain by a set date. However, with the problem's magnitude unknown, worsening being only gradual, and catastrophe uncertain, cooperation might not happen. Author Barrett suggests the importance of "communication" (negotiation of trustworthy pledges) and of fairness (already-wealthy countries used a lot of carbon in becoming wealthy, hence should contribute more to reduction).

Math. Mag. **86** (2013) 235–236. doi:10.4169/math.mag.86.3.235.

Roulstone, Ian, and John Norbury, *Invisible in the Storm: The Role of Mathematics in Understanding Weather*, Princeton University Press, 2013; ix + 325 pp + 15 color plates, $35. ISBN 978-0-691-15272-1.

Before the late twentieth century, there were no satellites, no weather maps on the nightly news, and no weather prediction in most of the world—certainly not for more than a day or so in advance. Most of the book by Roulstone and Norbury is devoted to the history before then, as scientists began to understand the movements of air currents. One or two page-long "Tech Boxes" in each chapter give mathematical accounts suitable for a mathematics major (logarithms, vector forces, partial derivatives, transformation of variable in differential equations). The last two chapters are devoted to the more recent topics of the Lorenz system of nonlinear differential equations for convection currents and to weather prediction in circumstances that can give rise to mathematical chaos.

Watkins, Matthew, *Secrets of Creation. Vol. 1: The Mystery of the Prime Numbers; Vol. 2: The Enigma of the Spiral Waves*; Inamorata Press, 2010, 2011; 353 pp, £17.50 (postpaid to anywhere); 237 pp, £15.00 (postpaid to anywhere). ISBN 978-0-9564879-0-2, -1-9.

The "Secrets of Creation" is a trilogy; vol. 3, *Prime Numbers, Quantum Physics, and a Journey to the Centre of Your Mind*, is to be released later this year. Fortunately, the subtitles give a more precise sense of the content, which is an elaborate and fascinating nontechnical introduction, explanation, and speculation about prime numbers and the Riemann Hypothesis. The exposition is handsomely accompanied by numerous entertaining cartoons by Matt Tweed. The first chapter, though, may derail some readers; it delves into the influence in our lives of the quantifiable at the expense of the unquantifiable. That chapter is followed by a gentle development of the integers via the Peano axioms and then an introduction to prime numbers. The distribution of primes is explained in terms of a spiral—which, as mention in the title of the second volume makes clear, is a fundamental touchstone for the author's explanations. The second volume concludes with several intriguing reformulations (new to me) of the Riemann Hypothesis, a discussion of its significance, and a claim that the zeros of the Riemann zeta function are "vibrations"—with the third volume promising to investigate the mystery of what is doing the vibrating. These books are remarkably readable by a general audience, with mathematical details isolated to appendices.

Hadlock, Charles R., *Six Sources of Collapse: A Mathematician's Perspective on How Things Can Fall Apart in the Blink of an Eye*, MAA, 2012; xiv + 207 pp, $50 (member: $40). ISBN 978-0-88385-579-9.

This book confronts catastrophes of all kinds (civilizations, species, products, companies, structures, markets, social orders, diseases, networks) and treats them in the light of the mathematics of the six sources of the title: chance, patterns, competition, instability, nonlinearity, and propagation through a network. Probability density functions plus bifurcation (in the logistic differential equation with harvesting) are the high-water marks for the sophistication of the mathematical formulations. Although the mechanisms of collapses are investigated, not emphasized are human causative influences, such as greed (the Great Recession), inadequate funding of infrastructure (network failures), and dedication and determination (elimination of smallpox).

Kainzinger, Albert, The mathematics in the structures of Stonehenge, *Archive for the History of Exact Sciences* 65 (2011) 67–97; online at doi:10.1007/s00407-010-0071-0 together with supplementary material.

"All measurements of the Stonehenge structures are based on a consistent metrology [the cubit] ... in line with practiced standards in Babylonia .... The major mathematical concept in the design ... is the application of Pythagorean triangles ... [S]pecific Pythagorean triangles were repeatedly applied ...: (5, 12, 13), (28, 45, 53), and (48, 55, 73)." Despite all the measurements and figures, the beauty of the theory, similar claims about other prehistoric sites, and maybe even wishing it were true, I'm just not inclined to believe that there was a Babylonian International Standards Organization, especially one that favored Pythagorean triangles with such large sides.

MAA MATHFEST

Jul 31-Aug 3, 2013

Join us in Hartford, CT for *the* summer celebration of mathematics.

Catch up with colleagues and friends, and expand your professional network:

- Kick off MAA MathFest 2013 at the Grand Opening Reception, Wednesday, July 31st, from 6:00-8:00 p.m.
- Mathematical sessions begin on Thursday, August 1st
- Math Jeopardy, banquets and awards ceremonies, 5k fun run, ice cream socials, and many more networking opportunities
- Graduate & undergraduate student activities

Hear from leading mathematicians and educators:

- **Olga Holtz**, University of California-Berkeley
- **Judy Walker**, University of Nebraska-Lincoln
- **Susan Loepp**, Williams College
- **Gordan Zitkovic**, University of Texas at Austin
- **Chris Danforth**, University of Vermont
- **Patricia Kenschaft**, Montclair University
- **Ann Watkins**, California State University Northridge
- **Frank Morgan**, Williams College
- **Jeremy Gray**, Open University
- **Gilbert Strang**, Massachusetts Institute of Technology
- **Karen Morgan Ivy**, New Jersey City University

Keep up with best practices in teaching, learning, and curriculum development:

- Contributed and invited paper sessions
- Minicourses and workshops
- Panel sessions on careers, assessment, summer programs, and teaching statistics

Register online at:
www.maa.org/mathfest

Participate • Investigate • Educate

MATHEMATICAL ASSOCIATION OF AMERICA
1529 Eighteenth St., NW • Washington, DC 20036

CONTENTS

ARTICLES

NOTES

PROBLEMS

REVIEWS